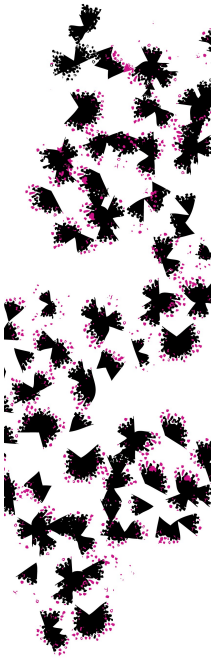

Autonomous Ultrasound Scanning for Breast Cancer Screening in the Presence of a Designed Breast Holder

P. (Patricia) Rodrigues

MSc Report

Committee:
Prof.dr.ir. S. Stramigioli
Dr. F.J. Siepel
M.K. Welleweer, MSc
Dr.ir. W.B.J. Hakvoort

November 2017

050RAM2017
Robotics and Mechatronics
EE-Math-CS
University of Twente
P.O. Box 217
7500 AE Enschede
The Netherlands

"Não sou nada.
Nunca serei nada.
Não posso querer ser nada.
À parte isso, tenho em mim todos os sonhos do mundo."

Fernando Pessoa in *"Tabacaria"*

SUMMARY

The MURAB project aims to provide an efficient and effective solution for the breast cancer screening in patients with high risk of developing breast cancer. In order to do so, MURAB combines the accuracy of the MRI with the real-time evaluation and reduced discomfort of an US-guided biopsy, turning this technique into an easily repeatable procedure with very little margin for error by automating the whole process with an KUKA LBR iiwa robotic arm.

The work developed in this master assignment focused on two topics within the MURAB project. On one hand, the thesis attempted to develop an autonomous ultrasound trajectory using the KUKA LBR iiwa 14 R820 that could be adaptable to surface of the breast (in this case a breast phantom) maintaining contact with it and conducting the motion through impedance control. On the other hand, so that the deformation induced on the breast by the US scan is reduced, it was also attempted to design a breast holding structure that could make the breast as whole stiffer in the response to the US transducer.

In terms of trajectory design and implementation, it was possible to generate a robot controlled motion that could react compliantly to its surroundings, though the adjustability to the breast surface is still to be attained in future work. The current situation uses an algorithm that can generate the trajectory points necessary to scan over the breast after an MRI scan provides its 3D model, which assures a high level of position and contact accuracy provided that the breast position is not changed during the scan.

From the second task, it was possible to design a breast holding structure made out of PVC that was able to fulfil all the pre-established requirements. In order to design the complete structure, some characteristics were established as optimal: the mesh structure should be about 35 mm thick, with squared holes with 4x4mm. In addition, through this design process, a thorough evaluation of other candidate materials was conducted though it was concluded that they were not US compatible. Despite being able to successfully reduce deformation in one of the experiments, this reduction was still not very pronounced.

Lastly, the design and the trajectory are brought together to evaluate how the response of one changes in function of the other. From this, it was observed that the two can coexist without compromising image quality but the trajectory is not entirely smooth if the forces applied by the transducer in the direction perpendicular to the surface suffer a significant increase. Though this effect can be counteracted if certain adjustments are made both to the trajectory program and/or the breast holder's setup.

PREFACE

A bit over two years ago I started my adventure at the University of Twente. In the beginning, I was just an Erasmus student from Lisbon. Little did I know what the future had in store for me back then.

The reason that encouraged me to prolong my stay in the Netherlands was indeed the quality of the research facilities that I encountered here and the possibility to be a part of interesting projects dealing with pertinent biomedical issues using state-of-the art technology. As a biomedical engineer (to-be), one of my main goals was always to be able to learn as much as possible in all the areas that bioengineering has to offer. These were the main motivations that lead me to the MURAB project.

In MURAB, I found the possibility to be a part of a creative and challenging project working towards the prevention of breast of cancer. For this opportunity I would very much like to thank Dr. Françoise Siepel and Vincent Groenhuis, MSc, in addition to Prof. Dr. Stefano Stramigioli, the chairman of the Robotics and Mechatronics lab, where all the magic happens. I would specially like to thank Dr. Françoise Siepel and Marcel Welleweerd, MSc, for the supervision and guidance throughout the project as well as the many fruitful discussions that allowed me to produce this report and to always see past the difficulties that arose. A warm thank you to my external supervisor, Dr. Wouter Hakvoort, for the availability to take part in this master project.

However, this path wouldn't have been possible for me take hadn't it been for the people in my life that allowed me to reach this far. For this, I would like to thank my grandparents, António and Ilda Almeida, and Valetim and Piedade Rodrigues, who invested in me and made it possible for me to believe that I would always be able to reach my goals, if I worked hard enough. I would also like to thank my parents, José Carlos Rodrigues and Anabela Almeida, who always encouraged me to follow my ambitions no matter how hard they may be. Thank you also for never restricting me from dreaming big and wanting to explore the world even if that means we have to be apart. In addition, I would like to thank my sister, Carolina Rodrigues, for the constant laughs and support even when the times are tougher.

The past two years have been one of the most exciting and eventful of my life, but this journey wouldn't have been so amazing, hadn't I shared it with the some of the greatest people a person can encounter, Aina, Christian, Daniel, Eric, Fitsum, Giovanni, Juanvi, Magali, Marc, Mattia, Paulina and many others. I would like to thank all of them for all the time we shared together, for all the parties, the dinners, the movies nights, the Saturdays in the market, the travels, the workouts but most of all for the companionship that made Enschede feel like home, where they were my family. I'm sure the bonds we made will last us a lifetime.

One of the things Portuguese people don't expect a lot when they go abroad is to find other fellow countrymen. However, this is not what happened when I arrived in the Netherlands: we somehow managed to quickly find each other. Thank you, Dani, Sousa, Paulo, Becas, Ivo, Gonçalo, Zé and Inês, for keeping the Portuguese spirit alive and for proving that the distance is never an obstacle to keep us apart, but a very special thank you to Rita, for always being there for me with her unconditional support. Without her all that I've accomplished would not have been possible. Many thanks also to my friends who stayed in Lisbon but managed not to forget me, even if I was away, and still make me feel as if I've never left every time that I return.

I would like to thank the friends that shared with me the crazy stressful thesis life, Jeroen, Carlos, Saskia, Adel, Dennis, Andrea, Reynaldo, Khaled and Emiddio, and made my choice to do my thesis in

RaM impossible to regret. A special thank you to Éamon for all the insight that he shared with me, particularly, how to properly explain myself in a clear manner (something that is still work in progress) and that age is just a number. Lastly, I would like to thank Shamel, for always believing in me even in times when I couldn't. Words cannot describe how grateful I am that he is my friend.

An enormous thank you to all the people that I crossed paths with from all the corners of the world, may that have been in Portugal, Australia, Norway or Enschede. This journey has made me into the person I wished to become.

Enschede, November 7th of 2017

Patrícia Rodrigues

CONTENTS

1. INTRODUCTION

1.1 PROBLEM DESCRIPTION

Alongside with skin cancer, breast cancer is the most frequent cancer type that can be encountered in women in the United States. The prevalence of breast cancer amongst women does vary considering several of factors such as age, race/ethnicity or family history of breast cancer. But there are also other aspects that can lead to breast cancer, mostly associated with a women's hormonal changes throughout life and associated experiences such as giving birth. Nevertheless, men can also be affected by breast cancer though the incidence is much smaller [1]. In 2013, the American Cancer Society [2] estimated 296980 new cases of breast cancer (including both in situ and invasive cases), giving American women a 12.3% chance of developing breast cancer . Later, in 2015, 292130 [3] was the estimated number of new cases for the United States of America. The most recent data encountered for worldwide values was from 2012, in the World Cancer Research Fund International[4], which revealed that about 1.7 million new cases where diagnosed that year and that this was the most prevalent type of cancer in women. It accounts for 12% of all new cases of cancer and 25% of all cancer cases in women. It showed also that Belgium was the country with the highest rate of breast cancer incidence, but also the country with highest proportion of breast cancer survivors.

The diagnosis of breast cancer follows a certain amount of steps depending on the size of the lesion, its location, age of the patient and his/hers family history. When the doctor asks for an MR examination, it means that the patient has already been through the other types of exams that are less accurate but easier to obtain, or that the patient is part of the group with high risk of developing breast cancer. It will generally start with a regular palpation exam, then moving on to a mammogram (X-ray), which can then lead to an ultrasound (US) scan and from this point, if the scans are still not sufficiently informative, the physician can request an magnetic resonance imaging (MRI), which is the most accurate form of diagnostic and can detect lesions that might have been missed by the previous examinations. Generally, the patient moves from exam to exam if either the results are inconclusive regarding tumour location and/or there is a high risk of breast cancer given the patient's particular characteristics (a more thorough analysis of the diagnostics procedure can be found in [5]) or even to make sure the previous exam was not a false-positive. Biopsy surgery can be performed at any stage in between these exams if the clinician is confident enough on the tumour location to remove the identified mass. However, the biopsy procedure is prone to quite an amount of error depending on the imaging procedure that supports it and the experience of the practitioner conducting the exam. Usually, all of these steps take the patient days or even weeks of multiple consults until the diagnosis is actually complete and a course of treatment can be decided upon.

1.2 MURAB PROJECT

In order to provide a method that helps early detection and analysis of breast cancer, particularly for the patient group with a more challenging diagnosis, the MURAB project was created. MURAB stands for MRI and US Robot Assisted Biopsy and it sets its goal as having a fully automated robotic arm performing an US scan of the breast and needle positioning for biopsy, while encompassing information from the MRI scan conducted. All of these techniques are part of MURAB as they aim to tackle the

problems existent with the current diagnostic procedure: MRI is able to detect even the smallest lesions, yet it does not provide real time feedback for the biopsy, which is why US is added. However, the US scan can encompass a large range of variability depending on the skill of the clinician conducting the exam, which is also the current problem with needle biopsy. For this reason, it is considered rather advantageous to be able to develop a standardized way to conduct the scan and biopsy and, thus, the robot is added to create an automated process. This way it is possible to join the best features of all the available techniques and it is also possible to combine them all into one daily procedure instead of several separate examinations. Apart from breast cancer, this technique also has the potential to help with muscle biopsy.

The MURAB project involves the usage of a medical robotic arm controlled in such a way that it can perform an US scanning trajectory and needle positioning given the tumour location. Ultimately, it should be possible to scan only the region where the mass is thought to be. To assure that it is possible to actually perform an ultrasound scan and do a needle biopsy, the robotic arm is equipped with a specialized end-effector. This is constituted by two cameras that allow position detection and adjustment, an ultrasound probe that will collect the US image and a motor that positions and moves the needle guide for the biopsy (with the help of the clinician). The procedure will be divided into two phases: a scanning-phase and an intervention phase. The scanning phase includes all the steps that lead to the collection of a complete ultrasound scan and its combination with the MRI image, finalizing when the exact tumour location is known. In addition, elastographic data is also collected during the breast scan to be able to predict how the breast should deform as well as to help with the location of the lesion and, if possible, provide information regarding the nature of the lesion before the biopsy. At this point, starts the intervention phase, where the end-effector moves the needle towards the expected position and enables needle insertion.

As a European project, MURAB counts with the participation of several entities, namely, three universities, the University of Twente, the University of Verona and the Medical University of Vienna, two companies, KUKA and Siemens, the university medical centre of Nijmegen, RadboudUMC, and one hospital, ZGT.

1.3 THESIS PURPOSE

The current master thesis fits within the scope of the MURAB project. It will follow the progress already achieved by previous master students and also introduce new research on a part of the project that has not been developed yet.

This assignment will include two topics. It will focus on the recently developed strategies that optimize the trajectory conducted by the KUKA LBR IIWA 14 R820 robotic arm to fulfil the US scan, while incorporating an analysis of internal and external force sensors. Additionally, this thesis will include the design of a breast holder structure attending to all the specifications necessary to reduce breast motion and deformation during the scanning and intervention phases.

With the first task, the aim is to implement an adaptable scanning trajectory of the breast surface that can act upon the environment with interaction control, provided that it does not compromise imaging quality, whilst the second task aims explore the possible designs for a breast holding structure that helps reducing breast deformation during the motion, being compatible with the robotic trajectory

without losing image acquisition quality. As the MURAB project is a European project with a 4-year duration and this thesis falls on the second year of this project, it is expected to provide recommendations and future analysis for the steps still to come.

1.4 THESIS OUTLINE

The report is organized as follows:

- Chapter 2: Provides a thorough description of the MURAB project, the techniques used and why are they part of the procedure, exposing some of the challenges still to be tackled.
- Chapter 3: Focuses on the analysis of the topics that will be the subjects of the research conducted and what kind of requirements are involved for each one of them
- Chapter 4: Describes the initial plan for the design of the US scan trajectory, the difficulties encountered and how it was implemented
- Chapter 5: Describes possible solutions for the problem in question while motivating the choice for one of them and then explains the design process that lead to the final design concept.
- Chapter 6: Explains all the testing conducted and the results obtained at each stage, starting from the experiments that allowed for the design of chapter 5 to be developed and culminating in the analysis of the results that bring together the two topics investigated.
- Chapter 7: Concludes about the work that was performed during this project and provides recommendations for future projects.

The final part of the report includes an appendix section to which the reader is referred to for additional information about experimental data.

2. BACKGROUND

The following section describes in more detail the necessary concepts for a better understanding of the methods used in this thesis, also helping in providing motivation for the course of research decided upon. There are several techniques than can and will be used throughout the MURAB project and by understanding their strengths but also limitations it is possible to comprehend the research direction presented by MURAB and what are the challenges that still need to be tackled.

2.1 BREAST CANCER

Despite affecting so many women worldwide, breast cancer has a high survival rate, ranging from 80 to 93%, 5-years after diagnosis [1]. The case is such due to the screening programmes included in the majority of the developed countries leading women to do at least one mammogram to check if there any unusual masses around the stage of their lives where cancer is thought to develop. This helps in the early detection of breast cancer, thus facilitating treatment before the cancer reaches higher stages of development. In the Netherlands, the "mandatory" screening starts at age 50 and should be repeated every two-years until the age of 75 [6]. Though people at a higher risk should start these frequent examinations earlier in life.

As mentioned in the introduction, the first step for breast cancer diagnosis is palpation and the first scanning step is mammogram. This is the exam that is regularly conducted when a patient starts being part of the screening programme. For women with higher risk of breast cancer, the screening also involves an MRI scan[1]. According to www.breastcancer.org, there is a group of patients who is most likely to benefit from a MRI scan. This includes patients that had palpation masses which could not be found through mammogram or US, younger women with breast tissue denser than normal complicating the visualization through other techniques or patients with lesions on the underarm lymph node. In addition, if a mass is found on one breast only, it could be because the diagnostics technique was limiting, thus MRI is used for analysis of the patient's other breast. This is the target group of patients that would benefit from a diagnostic procedure such as the one being developed by MURAB.

After a positive identification of the mass's location with the MRI, the next step is to biopsy the tissue to confirm its nature (benign or malignant) through a pathological analysis.

2.2 BREAST PROPERTIES

The breast is a type of body structure composed by different types of tissue. On the outside it has a skin layer, which has skin-like properties, and on the inside it has both adipose tissue and glandular tissue, which have very different mechanical behaviours. For this reason, the breast does not respond linearly to mechanical stimuli and its behaviour has been defined as hyperelastic [7], [8]. Moreover, studies have shown that tumorous breast tissue is stiffer than normal breast tissue and this is what actually allows tumour identification through diagnostic techniques like US as well as elastography [8], [9].

Anatomically speaking, on average, an adult woman breast's diameter falls between 10-12 cm and is 5-7 cm thick at the centre, having a conic shape. The volume of this structure can fluctuate between 21-2000 ml though being on average around 400 ml [10]. In terms of mass, the interval is from an average

of 0.43kg to 1.9kg, depending on the breast cup size[11]. Though these values have a lot variance since, in addition to patient-to-patient variability, even among the same individual the breast size can differ reasonably. Results indicate that there is no correlation between the breast size and the development of breast cancer[12].

In terms of elastic properties of a material there are 3 main moduli that help describe its response to the application of external forces, the Young's Modulus (E) – material's capacity to stretch and deform once under stress (compression or extension), i.e., longitudinal strain –, the Shear Modulus (G) – material's shear stress over the displacement when it is being deformed – and the Bulk Modulus (K) – material's capacity to resist compression. In addition, the Poisson's ration (υ), which is the ratio of transversal strain versus axial strain is generally also associated to these 3 moduli. These quantities are all related to one another and by knowing any two of them it is possible to derive all the rest, as can be seen by the equations 2.1, 2.2 and 2.3. Given the usage of the Hooke's law in the field of elasticity, which relates the Poisson's ration to the Young's modulus, makes E one of the quantities of higher interest [13].

$$\boldsymbol{G = \frac{E}{2(1+\upsilon)}\ [kPa]} \quad \textbf{(2.1)}$$

$$\boldsymbol{\upsilon = \frac{E}{2G} - 1} \quad \textbf{(2.2)}$$

$$\boldsymbol{K = \frac{E}{3(1-2\upsilon)}\ [kPa]} \quad \textbf{(2.3)}$$

For the breast tissue and for each type of structure found inside it, there are some discrepancies in the E values encountered, as it can be seen in Table I. Researchers report that there are wide variations for the encountered values [8], [14]. The tissue's elasticity follows a non-linear behaviour, which justifies why it is complex to define a range of values for E [8]. It is important to add into this analysis the effect of ageing into the breast properties given the changes introduced by the alterations to the body's hormonal behaviour. A younger woman will have a higher content of fibrous tissue, which is rich in collagen and thus stiffer, implicating a higher E, and as the time goes by this composition starts changing. Furthermore, less adipose tissue seems to also be related to a higher attenuation of sound waves[15]. This could be associated to a harder diagnosis under US for younger patients scanning given the signal attenuation and also the largest amount of high density healthy tissue.

Understanding the properties of the breast is important to be able to underline which kind of techniques can or not be useful to reach the ultimate goal of the project and to be able to properly design a solution that will take into account the aspects described above.

Table I - Different values for the Young's Modulus in breast. For some tissue types, more than one value are referred in [14] .

Type of Breast Tissue	E (kPa)
Unspecified	21-23; 29 [14];
Adipose	1.9; 19 [14]; 18.8 [16]
Ductal Carcinoma	25 [14]; 29 [16]
Invasive Carcinoma	93 [14]; 34.5 [16]
Glandular	33 [14]; 31.3 [16]
Fibrous	1.8; 110 [14]

2.3 MAGNETIC RESONANCE IMAGING

MRI is a highly accurate medical imaging technique based on the presence of strong magnetic field and how it influences the environment being imaged. MRI detects the signal produced by the hydrogen atoms present in the molecules of whatever is being imaged once exposed to an external magnetic field, since the hydrogen protons have magnetic momentum. The energy transported by the electromagnetic waves will influence the spin of the protons and they will rotate and align with the field turning into a transverse direction instead of the longitudinal initial direction. By doing this, they emit an alternating voltage which allows for the detection of the MR signal[17]. To comply with this imaging technique, so that the results are not affected, nothing in the MRI room can be made out of metal. Otherwise, they too will produce a magnetic response that will be detected by the MR scanner and influence the final image.

MRI started being incorporated in the breast cancer diagnosis process in order to reduce the number of false-positives (that lead to biopsies) resulting from mammograms given its high sensitivity. In addition, the usage of contrast agents such as Gadolinium allow for the distinction of structures such as silicone implants or cyst from the actual carcinoma which facilitates the diagnostic[18]. MRI is also advantageous since it does not use any kind of radiation that is harmful to the body (such as the mammogram or the computed tomography (CT) scan). MRI's superior image quality also becomes clear through Figure 2.1 and why it is the "go-to" technique for diagnosis of smaller lesions that would not otherwise be detected for risk patients. Nevertheless, this high quality imaging comes with a few setbacks. MRI is a very expensive technique, it takes a longer period of time than US and does not provide immediate feedback of the generated image. Once paired with a biopsy procedure, the latter aspect may mean the necessity for needle re-insertion caused by wrong positioning which will increase patient discomfort and the overall duration of the procedure.

The MRI procedure is normally conducted in prone position, which will also be done in this project. Prone position is selected as it reduces deformation of the breast in comparison to supine position, reduce the influence of motion due to breathing as well as making it easier to eliminate other body structures from the image collected (such as the lungs and the heart). In general, studies have showed prone position to be advantageous as it seems to reduce the dosimetry the tissue is exposed to, though one setback is that chest wall lesions become much harder to reach, especially in patients with larger breasts [19]–[21]. Nevertheless, the breast stays in a floating position suffering the effects of gravity, so the current solution is to compress it between two plates, though it will alter the shape of the breast. This can become a problem of misalignment when a biopsy is required, since the exact tumour location is not well-known, and it is even more problematic if the biopsy is conducted in supine position. For this reason, it is quite important that the breast position remains as similar as possible during the whole intervention and that is one of the aspects that MURAB wants to incorporate.

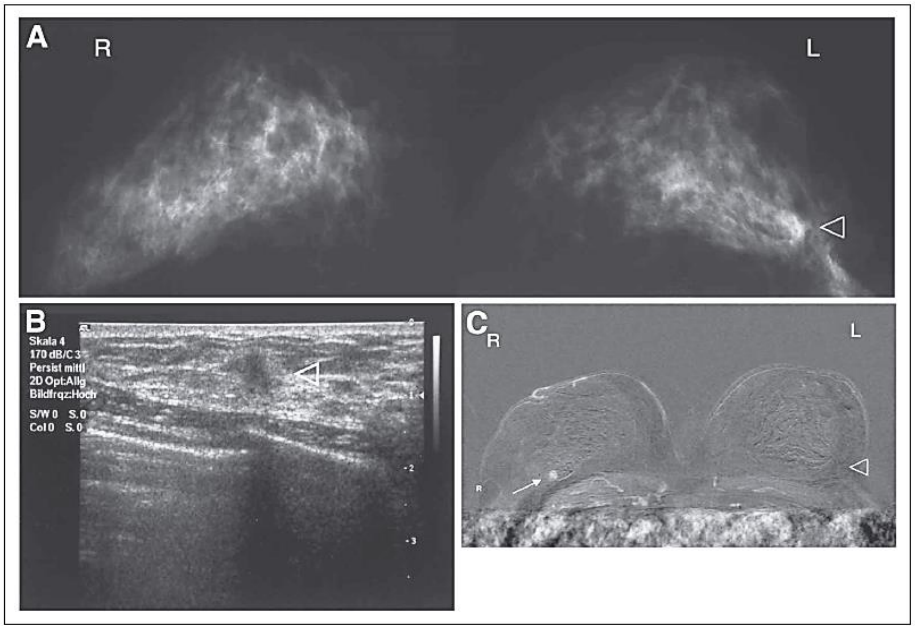

Figure 2.1 - Images of a 53-year-old patient with family history of breast cancer and a benign tumour already detected in the left breast. (A) is the mammogram taken initially, (B) is the Ultrasound scan and (C) is the MRI result. The open arrowhead was an area identified in A and B as possible tumour, though C revealed it to be only scar tissue (open arrow) and actually indicated a lesion in the opposite breast (white small arrow) which would have been missed otherwise. Adapted from [6].

2.4 ULTRASOUND

Ultrasound is one of the main imaging techniques used in the MURAB project as well as the MRI, but is introduced here to be able to replace the MR in the biopsy step of the diagnostics procedure. In addition, US is one of the main techniques being used during the research conducted in this assignment, therefore it will be explored in detail. Smaller lesions are generally undetectable to the US, yet a US biopsy offers a less invasive and painful alternative. US is a very useful tool for the imaging of soft tissues given their lower density and acoustic attenuation, which is one reason to use this technique for breast diagnostic purposes[14].

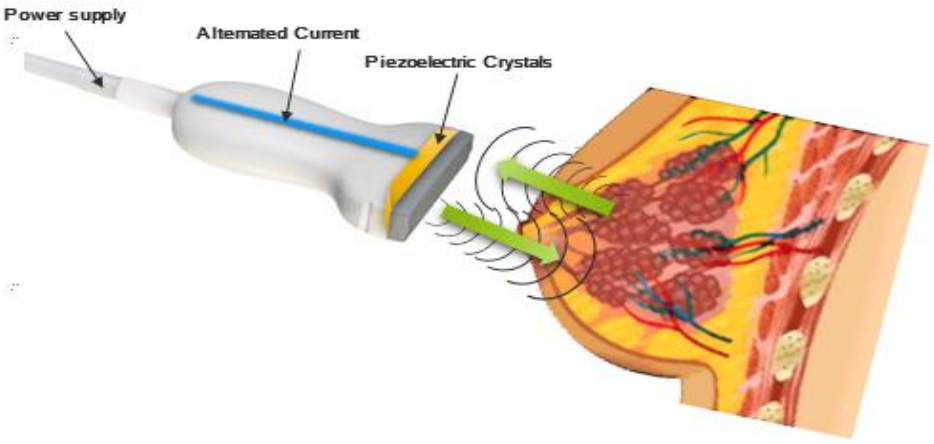

Figure 2.2 – Ultrasound transducer's simplified mechanism of action according to the Piezoelectric Effect. The transducer and the breast tissue are not to scale. It is possible to observe the probe acting as both an emitter and a receiver of the ultrasonic waves.

According to the "*Basics of Biomedical Ultrasound for Engineers"*, the definition for an ultrasound is "acoustic waves (sound or pressure waves) propagating within a medium at frequencies exceeding the auditory band"[22] that is, frequencies exceeding 20 MHz. Indeed, medical devices use frequencies from 1 to 20 KHz, depending on what type of tissue and how much skin penetration is necessary for the experimental setup. The signal's frequency can be a determinant factor for adequate image acquisition, as low frequencies cause less signal attenuation (allowing deeper tissue penetration) and high frequencies attenuate much faster (lesser imaging depth). The ultrasound transducer is responsible for both emitting and receiving the reflected signal, as illustrated in Figure 2.2, and so construct a cross-sectional image of the tissue being imaged [23].

Despite there being several possibilities for the functioning of the ultrasound transducer, the most common one is through the usage of piezoelectric materials. Piezoelectric materials can be crystals, ceramics or polymers, though the most frequently encountered format is a group of crystals. The transducer is able to operate given the existence of the piezoelectric effect. This phenomena actually describes application of pressure onto the material being able to generate electric current, though the reverse was also verified, i.e., the possibility to induce material vibration by exposing it to a certain voltage. It is based on this latter principle that US generates a signal that reaches the tissue and receives the output result from the tissue, which it then receives as input to the piezoelectric crystals, as seen in Figure 2.2. Essentially, an electric alternated current will be supplied to the transducer so that the piezoelectric crystal will vibrate and generate pressure waves (through the form of sound waves). Once the signal reaches the tissue it can be transmitted, reflected or scattered, and the reflected portion will be detected again by the transducer causing its crystals to vibrate again, now with the waves carrying tissue specific information, i.e., the changes in frequency, wavelength and/or amplitude [22]–[24]. Furthermore, the quantity that is more determinant for understanding the wave behaviour once it encounters a boundary (i.e., a new medium) is acoustic impedance (Z). This is a property of each medium and it is mathematically described through equation 2.4. It is defined as the resistance the medium/material offers to acoustic flow travelling through it as a result of a pressure stimulus and it is an important measure since it is intimately related to how much of the wave will be reflected and how much will be transmitted [25]. One could assume that it is desirable to have as much transmission as possible to make sure we access deeper into the tissue, thus being able to reach a broader area. Nevertheless, the reflected portion is the actual part that allows for the image reconstruction and so, per each type of tissue the wave travels through, it is important to assure that there are both transmitted and reflected portions in such a way that it both possible to keep travelling and also receive the material's input. This is accomplished by having different Z values in between the mediums but within a small range, as a big difference will cause the wave to be only reflected or scattered and it will not be possible to actually reconstruct an image of anything but the outer layer. This is illustrated by Figure 2.3.

$$\boldsymbol{Z} = \boldsymbol{\rho} \times \boldsymbol{c} \quad \left[\frac{\boldsymbol{kg}}{\boldsymbol{s \cdot m^2}}\right] \tag{2.4}$$

Where ρ is the density of the medium and c is the speed of sound. The velocity of sound in a medium is also highly dependent on the medium's compressibility (inverse of K). The less a material needs to be compressed by a sound wave (i.e. its particles are already close to each other), the easier it

will be to quickly transfer energy through it. Thus, a lower compressibility (higher K) will result in a higher speed of sound and, hence, a higher Z [26]. This means that the acoustic velocity of a wave changes considerably depending on the medium it is travelling through due to new characteristics it encounters that translate into a new speed of sound. For the types of tissue encountered in the breast the ultrasound velocity values described in the literature can be found in Table II.

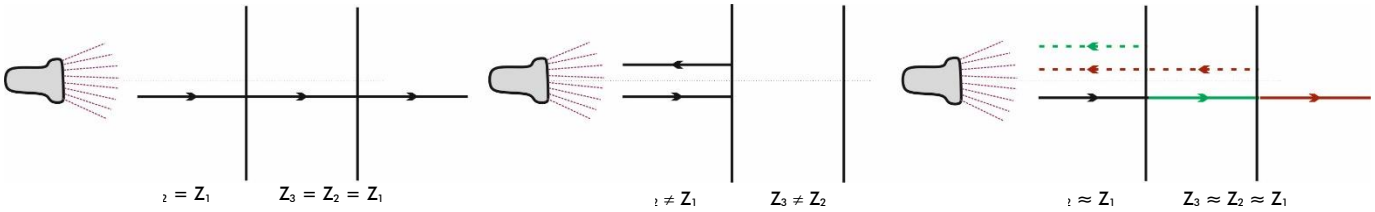

Figure 2.3 - Three possible scenarios for each possible acoustic impedance a wave can encounter when it reaches a different medium. The figure to the left shows the case when there is only transmission of the wave and little to no reflection. The middle case show exactly the opposite, when there is only reflection since the medium properties are too different. The case on the right shows the ideal scenario where the impedance throughout the medium is similar enough to allow for both transmission and reflection when crossing the two mediums.

It is important to note that, though the acoustic impedance is one of the most relevant quantities to encounter acoustic transparency, even with the desired value for Z, it might not be possible to penetrate as much as desired through the tissue. This is because of the attenuation suffered by the waves when travelling through the media. As mentioned, the attenuation is influenced by the frequency of the wave but it also depends on the absorption coefficient of the material, which designates the amount of wave energy converted into thermal energy. The less the absorption, the smaller will be the attenuation. For the breast tissue, attenuation is 0.75 dB cm^{-1} MHz^{-1} [27].

In Figure 2.3, it may seem as though there is only two possible phenomena for a wave to suffer, reflexion and transmission, as it illustrates only what happens to signal that is not lost. However, there is a portion of the wave that is scattered, due to angle of incidence on the surface, and due to generation of shear waves that travel perpendicularly to the original wave direction once a different medium is reached.

Nevertheless, it has been observed that there is a significant decrease in breast attenuation and speed of sound with age, though not linearly, it is most pronounced from 20 to 35 years old, after when it stabilizes, and then after 60 years of age it decreases again [15].

In order to generate an image there are several possibilities. The most commonly used is the brightness-mode (B-mode) display. This mode produces changes in the brightness of the image being detected (which creates the contrast) associated to the voltage of the signal generated by the crystals (a higher voltage is related to higher brightness). The voltage intensity will change considering the wave mechanical properties produced by the tissue that stimulate the crystals [22], [23].

The usage of ultrasounds as an imaging procedure for medical purposes has many of advantages in comparison to other methods, namely [22], [23]:

- Not hazardous - The type of radiation being used is not harmful and ultrasounds cannot be heard by humans which does not cause discomfort during the procedure;

- Real-time - It provides immediate visual feedback ("real-time") imaging since the time it takes to send the signal, for the signal to go through to the body and for the output signal to be received is quite short and allows for the image to be generated almost immediately;
- Compact - It is space and cost effective since it does not require a lot of machinery to be conducted (portable US machines are also available) plus the signal input is sent by the same probe that receives the output;
- Economic - It does not need a lot of expensive hardware to be used and maintained.

Though caution is still recommended as there can be some local tissue side effects in response to ultrasonically induced heating.

Table II – Ultrasound velocity in different components that can be found in the breast and ultrasound velocity on the breast with and without specific conditions [28]. The values obtained *in-vitro* differ slightly from the ones presented in this table. It is important to note that most of these values are within very similar ranges, which might cause difficulties upon attempting to distinction.

Breast Tissue	Ultrasound Velocity [m s^{1}]
General	1553 ± 35
Fat	1436 ± 18.4
Lymph node	1513.8
• With Carcinoma	$1437 - 1547$
• With Fibroadenoma	$1502 - 1556$
• With Fibroadenosis	$1482 - 1566$
• With Fibrocystic Disease	$1482 - 1551$
Cancer	1550 ± 35
Cyst	1568 ± 40
Benign Lump	1561 ± 32

Despite all the advantages of the ultrasound, one of its drawbacks is the scanning variability introduced by the expert conducting the procedure. The way to hold the probe against the surface of the skin, the amount of pressure necessary to generate an adequate image and the trajectory followed with the probe are not entirely standardized, which allows for different outcomes in the obtained results [29]. Normally, this procedure is conducted independently of any other imaging techniques and its only goal is to locate a lesion. However, if this method needs to be paired with others, then having a pre-established manner of conducting the procedure while minimizing these inconsistencies is of the utmost importance.

2.5 NEEDLE BIOPSY

Biopsy is a term that describes the technique where there is identification of a lesion (through palpation or with the guidance of an imaging method) followed by tissue collection of the recognised mass (with microscopically identifiable margins). The next step, in order to finalize the diagnostics, is taking the collected sample to histology and learn the nature of the tumour (benign or malignant). After knowing the location of the lesion, in the case of needle biopsy, the intervention will involve an incision

followed by the introduction of a biopsy needle to remove the necessary amount of tissue, which can implicate the introduction of the needle several times to fulfil the previous condition [30], [31].

Prior to the development of needle biopsy, the alternative procedure was surgical biopsy, which was a very invasive, much more expensive and psychologically more devastating for the patient. Its biggest advantage is the high success rate in completely removing the mass. Needle biopsy is a cost-effective solution, causing little discomfort and little cosmetic side-effects, thus being considered one of the best tools for the diagnostics of cancer [30]–[33]. Nevertheless, there are some limitations to this technique in terms of being able to always successfully reach the lesion accurately. These limitations are generally not because of the actual needle biopsy itself but can arise from complementary factors such as the chosen setup (prone positioning or supine), the image modality chosen that can have a limited field of view or low image quality that can be misleading, or the location of the mass can be indeed in an intricate place, such as the axilla or the chest wall [32]. Additionally, its success can also be dependent on the physician's ability to accurately insert the needle.

Within needle biopsy there are a lot of types of procedure that can be chosen which mostly differ by the type of needle used or the type of mechanism in the needle that collects the tissue. For MRI, there are a few types of needle biopsy that can be performed (which are also compatible with the US machine): fine needle aspiration (FNA); core needle or vacuum-assisted device. It goes without saying that these needles need to be MRI compatible[34]. These three types mostly differ on the amount of tissue they can collect (implicating less need for multiple insertions), the need for a small amount of local anaesthesia and the cost of the procedure. Nonetheless, once paired with MRI, even vacuum-assisted device might require a second insertion, despite the amount of tissue it can remove, since the image feedback is not present at the time when the procedure takes place.

In the MURAB project, needle biopsy is one of the last steps of the intervention phase and it decided to use a core needle biopsy as it is less invasive and the positioning will be quite accurately guided by the robot. This procedure is illustrated in Figure 2.4. In addition, the presence of the two imaging modalities will also ensure that the lesion can be appropriately localised.

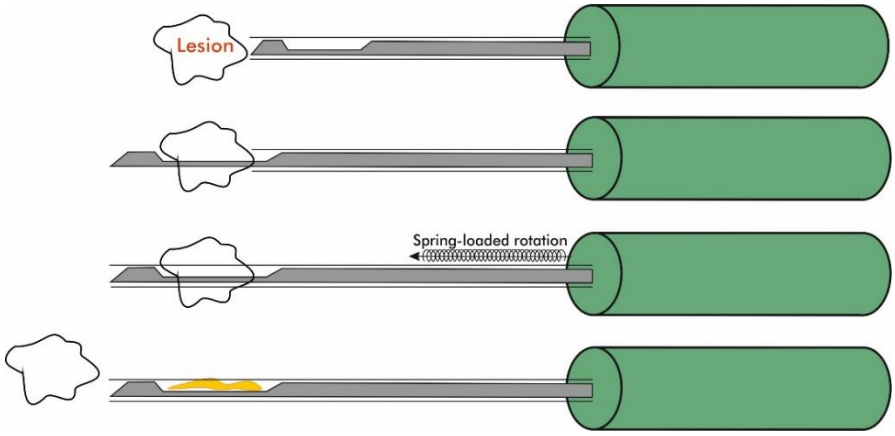

Figure 2.4 – Example of core needle biopsy to obtain small part of the identified lesion. The procedure occurs chronologically from top to bottom: first, the needle plus its outer shaft are inserted inside the tissue; once the lesion location is reached, the needle will be pushed through the lesion followed by the released of the outer shaft over the needle through a spring loaded mechanism which cuts through the lesion; afterwards, the collected portion can be removed safely from the region of interest for histological analysis.

2.6 ELASTOGRAPHY

Elastography is another one of the key imaging techniques that will be used during the MURAB procedure to help in the location of the lesion, hence being a part of the scanning phase of the project.

The principle of elastography lies on the fact that elasticity properties vary within tissues and different components will have a different stiffness thus, they will respond differently upon a mechanical stimulus that will alter the pressure (compression and decompression). So the goal is to measure the strain generated by each element, which will be higher or lower considering its ability to deform [35]–[38]. The elastogram is obtained with an ultrasonic transducer that collects the data in two different times (during the stimulus and after the stimulus) and cross-correlation is applied to each pair in order to create the image [38]. The elastogram can be in a greyscale or in colour [36]. This technique has been already applied to a few kinds of tissue, like the breast, prostate, pancreas, skin and seems to be very promising for liver [36], [37]. Additionally, there are three types of methodologies that can be used for elastography: one based on quasi-static compression of the tissue that could be applied globally or locally (which is generally used by Acoustic Radiation Force Impulse – ARFI); another one based on monochromatic low frequency vibration where it can use Doppler signals for the estimation; and lastly, one based on the changes caused by the propagation of the shear waves in the tissue, commonly referred to as transient elastography [36]. But, most of the times, elastography is conducted under B-mode ultrasound scanning, so following the first method.

Furthermore, elastography can be an advantage to ultrasound imaging as it can contribute to identify the nature of the lesion without the need for a biopsy, since the response of certain benign components can be observed from this type of scan [37]. Hence, it can be used to complement the technique that is incorporated in the clinical practice and help reducing the number of unnecessary biopsies that would otherwise take place. For this reason, it definitely adds value to the MURAB procedure to incorporate an elastography analysis of the tissue.

2.7 MURAB PROCEDURE

The MURAB project is looking to implement a new procedure for the special cases of patients who need MRI-guided biopsy, in order to tackle the current challenges it faces. With MURAB, the whole procedure will be more automated, more accurate (increasing efficacy in diagnostic), have fewer costs and reduce patient discomfort, not only by providing a less invasive procedure, but also by assuring that the whole set of exams is conducted during the same day.

The project will follow the steps described by Figure 2.5, consisting of two separate phases. The procedure starts with an MRI scan in prone position and this gives the initial information regarding where the lesion is located (and if there is any lesion). The patient is then moved to another room (not MRI compatible) where the robot can conduct an ultrasound scan over the breast (still in prone position) where it gathers information on the location of the mass by producing a sonogram and an elastogram. All the image information is compiled into a 3D image of the breast with the position of the lesion. If no benign lesion is clearly identified, then the intervention phase will begin and the robot will guide the needle to the exact position.

Using a robotic arm for conducting the US of the breast is a great advantage for MURAB since one of the problems of a manual US is the variability introduced by the practitioner conducting the

examination, as described in [39]. By using a robot, it is possible to assure the repeatability of the procedure with a much smaller margin for error. It not only ensures that the trajectory is always the same as well as the exerted forces. Plus, the robot is able to conduct the procedure in a shorter time than the clinician. This seems to be the line of current research in the medical field: automation of most of the procedures. Similar investigations can be found here [29], [40]–[42].

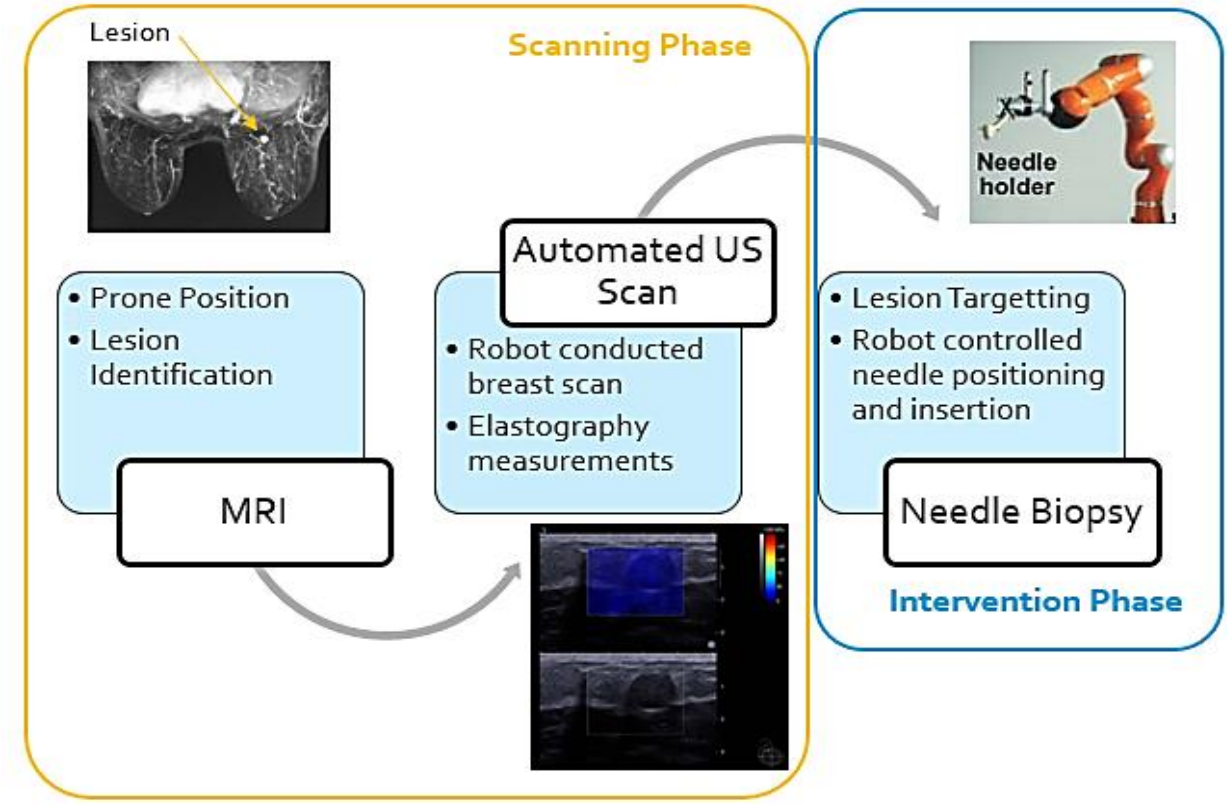

Figure 2.5 – Summary of the MURAB workflow. It is divided into two phases, a first one responsible for all the image acquisition, and a second one responsible for receiving the lesion's location, guide the needle towards the exact location and allow insertion by the physician. The top left image illustrates an MRI scan of a breast with a visible lesion (from [43]). The bottom image illustrates a US scan with elastography data from an identified mass (from [44]). The robot conducting the procedure will be similar to the one represented on the top right corner (from [41]).

It is important to note that, despite the majority of the process being conducted with a robotic arm, the needle insertion step will still be done by the clinician, to comply with ethical standards. The depth of the insertion is, nevertheless, also established by the end-effector of the robot to prevent that the mass is missed.

Given the combination of different imaging modalities, it is imperative to fulfil some conditions so that the procedure can be compatible with all the methods and the image quality will not be compromised. Also, the procedure needs to be optimized for minimal motion during the entire scan (though taking into account possible movements like the respiratory cycle or sporadic patient motion) since the acquired images need to be assemble into a final 3D image, task that will be difficult if there is little position correspondence between MRI and US.

With that in mind, the procedure will take place in two different rooms, one that is MR compatible (i.e. no metals or anything that can interfere with the magnetic field), and another where the ultrasound and needle biopsy can be performed. In order to reduce changes on the environment, the patient will always be laying down on the same table, in prone position. This table is specially designed for this project, so that the removal and transport are facilitated. It will always have two holes where the patient should place hers/his breasts. However, with this setup, there will still be room for breast oscillation due to the motion of the patient in between rooms, so ideally, an external structure should be used to help maintain the breast position.

It is clear that the robot conducts the majority of the functions and so another challenge is to be able to encompass all these tasks in one end-effector and work around the spatial constraints it might cause. This end-effector will have the US probe, a motor that will move the biopsy needle and will have a set of two cameras that will detect specific markers as well as adjust the trajectory when necessary. Additionally, the motion of the end-effector needs to assure that there is always contact with the surface being imaged, the probe maintains an angle close to 90º to the surface and that the force is optimal for imaging so that the image quality is not affected during the trajectory.

Nevertheless, the choice to perform an US-guided biopsy comes with a lot of advantages for the patient, as indicated in table III, especially if it is still possible to achieve the same accuracy in lesion detection with the combination of all these imaging techniques.

Table III – Comparison between the two most common biopsy procedures for breast cancer screening

	Advantages	**Disadvantages**
MRI-Guided Biopsy	Image Quality (Higher Accuracy)	• No Immediate Image Generation • Setup Constraints • Expensive • Moderate Patient Discomfort
Ultrasound-Guided Biopsy	• Immediate Image Generation • No Setup Constraints • Cheap • Reduced Patient Discomfort	Image Quality (Lower Accuracy)

If the overall procedure is successfully achieved for breast, the next step is to incorporate this strategy also for muscle biopsy, where similar challenges can also be encountered. In this case, the problem is simplified since the trajectory will be easier to execute, but it is necessary to investigate whether or not the trajectory requirements will still be met for accurate imaging.

In sum, it is possible to observe that MURAB is quite an ambitious project bringing together many areas of research. Nonetheless, it seems quite reasonable to admit that, once successful, it will help in reducing the amount of misdiagnosis in risk patients and, thus, prevent the development of more cases of breast cancer while contributing to reduce the mortality rate associated.

3. ANALYSIS

The previous chapter addressed the overall status of the methodology to be used in MURAB project, mentioning some of the challenges that it still faces. The following chapter will focus on the specific issue that is to be tackled by the current thesis, what has already been accomplished in this area of the project, what are the next steps developed here and how it is planned to be done.

3.1 PROBLEM ANALYSIS

The goals of MURAB were made clear during the previous section, but the research to fulfil them is still ongoing, though a lot of progress has already been accomplished. Following what is described in section 1.3, for the current master thesis, the focus will be on the difficulties surrounding the current trajectory and tackling oscillations in the shape of the breast throughout the procedure due to motion or breast deformation.

Great part of the diagnostic procedure needs to be performed by a robotic arm in an automated way, thus the trajectory followed by the robot must satisfy certain conditions, whether those may be in terms of safety, quality assurance, adjustability or overall efficiency. Hence, in order to generate the most adequate trajectory it is necessary to have an appropriate type of trajectory. It should be able to execute a pathway that can cover all the breast surface ensuring that the probe is always in contact with it (to reduce air in the medium between transducer and surface) but is still able to assure that there is no danger for the patient. Also, it needs to be able to implement the motion in prone position as this was the setup decided upon for the project. In addition, following the contact condition, the probe's angle during the scanning can also influence the imaging obtained, so it is necessary to take that into account.

One of the biggest challenges that arises from the trajectory planning is being able to make it adjustable to each breast shape and size. From work in previous projects, [35] and [36], or from literature studies, some of the characteristics that the trajectory should feature have already set a research direction. This brings us to 3 main areas of action.

1. **Trajectory type**

From Kelly et al [47], the medical description suggest 3 possibilities that can fully cover the breast's surface during an ultrasound scan: a linear trajectory, a radial trajectory and a circular trajectory that are illustrated by the figure 3.1.

Figure 3.1 - The three types of scanning trajectories with the breast in supine position. For the linear trajectory, the start is more common at the collarbone. The circular trajectory can start from the chest side of the breast and move its way to the nipple or vice-versa. The radial trajectory starts always from the nipple and every iteration goes back to the nipple to re-start the next step.

The linear trajectory is immediately discarded as its feasibility in prone position is quite low – it causes too much deformation of the breast. In an initial project [46], the radial trajectory was attempted though it revealed some inaccuracies in terms of positioning and orientation so the author suggested

trying another scanning pathway. The following attempt, described here [45], implemented a circular trajectory that was rather successful and was able to scan the breast in a shorter amount of time than the previous one, though it lacked a few of the requirements, such as a compliant response to the environment and being able to assure contact with the surface at all times of the procedure. Thus, the present work will follow the progress accomplished with the circular trajectory, as it had promising results. However, this is the first master project where ultrasound feedback will be introduced to have visual feedback of the scanned phantom, which can actually help pointing towards the most efficient option.

2. Surface contact and Probe Orientation

As mentioned in chapter 2, ultrasound imaging is highly dependent on the acoustic impedance of the medium it encounters. If Z is much lower than the Z from the piezoelectric crystals, then energy transmission is quite difficult. Even though the Z of the chosen US material (crystal, polymers or composites) can vary, they are generally approximately 1.5 Mrayl, which is rather close to the Z of water (~1.48 Mrayl) but quite further away from the Z of air (~0.0004 Mrayl) [24]. This will logically implicate that once in contact with air, the image quality will dramatically drop and this is the reason why contact between the probe surface and the breast surface ($Z_{\text{fat tissue}}$=1.39 Mrayl and $Z_{\text{fibrous muscle}}$=1.65 Mrayl [22]) is so crucial. In order to assure that most of the air is removed, the ultrasound probe is generally covered with a specific gel (whose properties are similar to those of water), which allows for a continuum of medium that is acoustically compatible.

There are essentially two ways to scan the breast surface while keeping the whole probe in contact with it, but from figure 3.2, it becomes clear that having the probe always perpendicular to surface causes less discomfort (less opposition to the motion, thus less force and reduced counterforce from the breast) and provides a smoother motion over the surface (reduced friction). Accordingly, this is what the programmed trajectory will try to encompass – conducting the scan with the probe always in contact with surface and in an orientation that is always perpendicular to the surface plane.

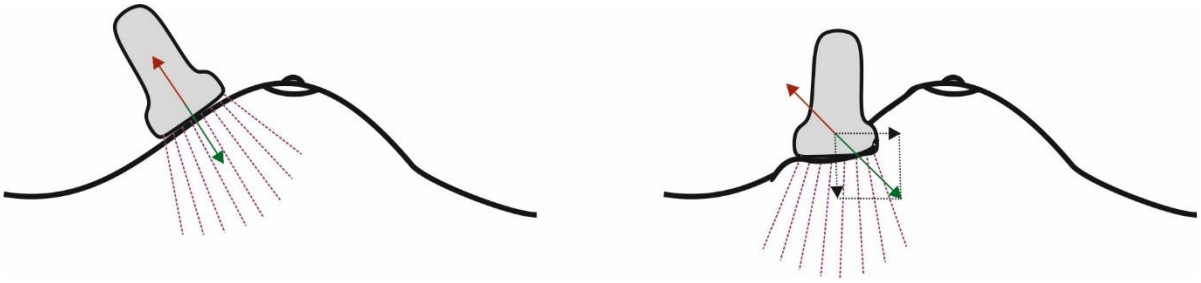

Figure 3.2 – Two possible configurations to keep contact with the surface: perpendicular to the surface or always in the same vertical direction. The red arrows indicate the counterforce generated by the breast surface given the pressure it receives from the probe, while the green arrows indicates the force applied by the probe.

In order to assure contact to the surface and that this contact is sufficient to produce an accurate visualization of the structure being imaged, the transducer needs to apply a minimal force on the breast surface. However, this value is not very well known. Depending on the studies found in the literature, the ideal range seems to vary, as it can be observed in Table IV.

A previous master thesis defined an interval between 2 to 7 N, allowing a maximum force of 14 N but referencing at 5 N [46], while another shortened the range to 5 to 7 N [45]. For the current project it

was decided to have as start point 5 N and evaluate the behaviour of the robot while performing the trajectory.

Table IV - Registered compressional forces with difference ultrasound transducers and setups

Tissue Type	Testing Setup	Reported Force [N]	
Uterus Phantom	Handheld Probe; Robot Assisted with Freehand Scan	20 11-18	[29]
Gelatine Phantom	Robotic System	7	[48]
Not Specified	Robotic System	7	[49]
Breast (with and without lesion)	Handheld Probe	4.4 (max); 1-2	[50]
Breast (with and without lesion)	Handheld Probe	2-15	[51]

3. Safety

During an automated scan it is always necessary to ensure that the patient's safety is guaranteed. So, it is first important to understand what the scenarios that can occur are:

- Sudden patient movements
- Too much force exerted on the breast surface or too much friction, causing pain and discomfort
- Counterforce response of the breast once a force is applied on its opposite side, generating a clamping situation between the breast and probe, in the case of prone position

Some of these situations are easier to tackle than others. For example, too much friction is solved by the usage of the ultrasound gel, which not only improves the image quality but it allows for a much smoother motion of the probe over the breast surface, reducing the damage that could be caused by dragging the probe directly through the skin.

To tackle sudden patient movements it is important to have a way to adjust the trajectory performed by the robot, which suggests the necessity for a closed-loop control mechanisms that can bring the robot back to its route if for any reason there are deviations. For the purposes of human-robot interaction, always with safety considerations in mind, a control based purely on position should not be used as it will not be able to flexibly respond to changes in the environment. A much better alternative is to use impedance control, as it can mimic better the interaction dynamics between the two compliant bodies, by allowing the robot to behave as a spring. Generally, the robot behaves as the rigid structure that it is with a very high stiffness. However, by using impedance control, the robot is modelled as a spring, whose stiffness can be adjusted, being now capable of producing a compliant reaction to the environment [52]. This means that the forces at the surface of contact will be reduced, thus, the safety of the motion control is increased. For this reason, impedance control seems to be a good strategy for the trajectory to be developed.

Using impedance control makes it possible regulate the forces/torques of the desired motion based on the position or velocity required to achieve said objective [53]. For the current task, it is necessary that the forces stay within a certain range. On one side, there is the safety issue that is

associate to high forces so the force needs to be low enough that it will not hurt the patient but a certain pressure still needs to be exerted so that the image quality will not be compromised, remembering that contact with the surface needs to be a constant factor during the whole scan, as it was already mentioned in the previous section.

Adding to these 3 subtopics of the trajectory design, the trajectory has another requirement: it needs to be conducted using a specific robotic arm, KUKA LBR iiwa 14 R820, using the software provided by the robot's manufacturer (KUKA), *Sunrise.OS*. The reasoning behind this decision is motivated by the existent partnership with KUKA inside the MURAB project, allowing for all tasks that are robot related to be conducted within the same framework and, thus, facilitate the interchanging of information. This condition was only introduced in the scope of the current master project.

4. **Breast Motion and Deformation**

Nevertheless, regardless of the developed trajectory, the transducer will always exert pressure against the breast surface, which will locally change the shape of the breast, a problem described shortly in the section 2.3. Since an accurate tumour localization is of the utmost importance for MURAB, being able to properly fit all the images collected to generate a 3D image will be essential. For this reason, breast motion and deformation should be reduced as much as possible to establish a direct correspondence with the MR image acquired initially. Thus, a structure that can hold the breast in place, while in prone position, provides significant benefit to the procedure.

However, designing such a structure is no easy task. This structure will be present during the whole procedure, both scanning and intervention phases, which means that there is a lot to be taken into account. It needs to be a combination of something that provides rigidity while still being flexible and adaptable to the breast shape and size while not compromising image acquisition. A material that can fulfil these requests should have the following properties:

- Flexible / Adjustable shape to fit different breast types
- Open design to allow needle insertion during the biopsy (enabling contact)
- Strong enough to provide support of the breast in prone position
- No metallic components to assure MR compatibility
- Adequate acoustical properties to assure US compatibility
- No air in between the breast holder and the skin and between the probe and the breast holder
- As thin as possible so that the US penetrability will still be able to cover all the possible tumours
- Compatible with the planned trajectory being developed
- Easy (affordable and repeatable) fabrication method
- Comfortable for the patient

The requirements related to US acoustics follow from the problems regarding image quality that were already described for the trajectory. Also here it is important to take into account properties like acoustic impedance that will make sure the image reconstruction is possible and the signal will not be compromised. Logically, air within the structure and the breast surface cannot be permitted. Additionally,

this structure needs to be able to support the breast weight and dimensions described above, though the possibility of creating such a structure for a few breast sizes.

How to immobilize the breast during a prone position scanning, with the advantages of prone versus supine positioning in imaging, is not an unknown question, though it is frequently solved with the usage of compression plates. Nevertheless, two "bra-like" structures, seen in Figure 3.3, were described in the literature, though none of them would completely fulfil the target goal. In [54], the objective is to reduce the deformation of the breast caused by skin distension, so the solution provided is simply a commercial bra without the cup and an adjustable strap to help the breast immobilization. Despite successful for the purpose it was meant for, it does not help in preventing lateral deformation caused by a US transducer (Figure 3.3, left). The other possibility encountered is described in detail in [55]. It consists on a breast cup that aims to reduce deformation and to immobilize the breast for radiotherapy techniques such as MRI, CT and positron emission tomography (PET). This means that the structure can be simply a rigid cup that is put over the breast, nevertheless, it does have a few openings to allow tissue biopsy, even if not everywhere. The most interesting feature of this cup is that is built by two different layers and while the outer layer is rigid, the inner layer is a mesh wall. The top of the cup has a vacuum source assembly, which removes the air in between the two surfaces of the cup and makes the mesh wall fit perfectly around the breast surface given the suction. Additionally, the cup has locking pins that allow for its fixation to any imaging table (Figure 3.3, right). The downsides of this solution are essentially the necessity of more than one size necessary to fit all the breasts, but mainly the fact that it's not possible to collect elastography data as well as probable incompatibility with US scanning (rigid materials have a tendency to be acoustically opaque).

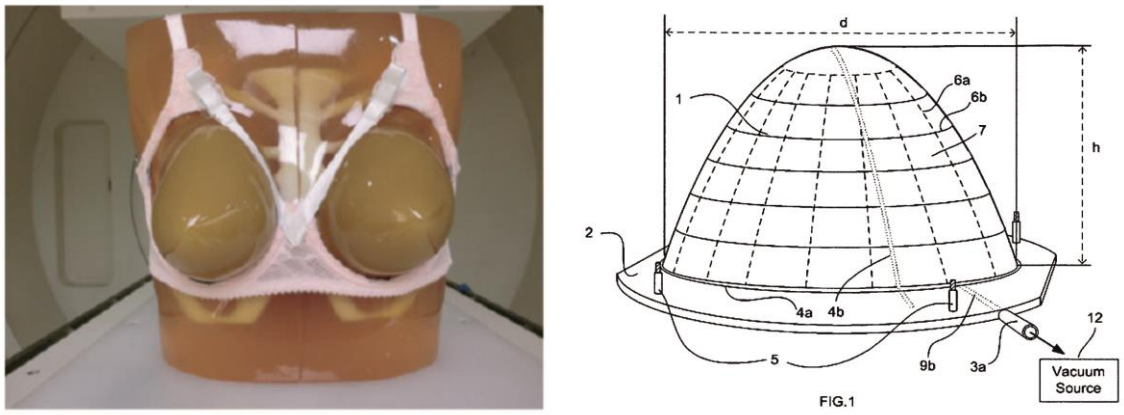

Figure 3.3 - Already available breast immobilization structures.

The concept that was initially developed was a rigid structure placed all over the breast with an opening to fit the ultrasound probe and designed in such a way that the probe would be large enough so that it would only need to travel one time around the breast. The disadvantages of this design were the inability to fit different types of breasts, preventing the execution of the needle biopsy step and not allowing appropriate elastography measurements since the motion of the probe is more restricted. Logically, this was not the adequate solution for the problem. Hence, taking into account the current set of requirements, the design of a new structure that can effectively fulfil the requirements is in need.

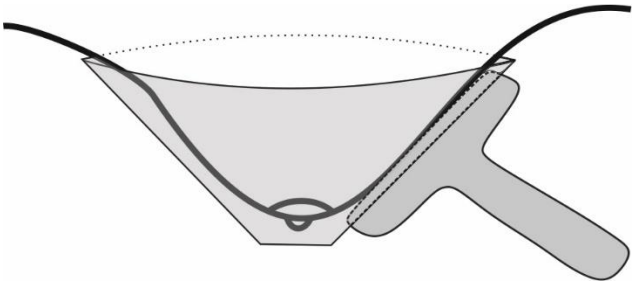

Figure 3.4 - Rigid breast cover with oversized probe represented schematically

3.2 PLAN OF APPROACH

Following the problem analysis, after a better understanding of the current status, it is possible to plan a strategy in order to reach a solution for the obstacles described.

To start the trajectory planning, a strategy to tackle the problem is outlined. Then, as an implementation problem, the first step is understanding the software and its possibilities. With this knowledge, the trajectory planning can be divided into pathway design and integration of impedance control fulfilling the conditions described in the analysis, i.e., a circular trajectory with a probe that always keeps contact with the surface while perpendicular to it, ensuring the safety of the patient.

For the design of the breast holder, the procedure will be different as the nature of the problem is not similar. Here, it is first necessary to envision a concept to create. Following the idealization, the next step is attempt to manufacture it, which involves deciding on a production methodology and a material choice. To complete the design, it has to be tested, evaluated and re-adjusted (if needed). On this project specifically, the testing will essentially come down to simulating the conditions an actual breast would have to face during the procedure and make sure that the breast holder can withstand them based on the pre-defined requirements.

In order to assure that the two projects are in tune and can work with each other, one of the biggest parts of the project will include an evaluation of how the trajectory behaves in the presence of the breast holder thus validating (or not) the design for the purpose it was generated.

4. TRAJECTORY DESIGN AND IMPLEMENTATION

Given the different nature of the two subtopics, the strategy used for each of them was rather distinct and, therefore, they will be addressed separately. Initially, there is an introduction to the system and robot used, followed by the initial plan of what will be attempted to execute for the trajectory design. Furthermore, with the knowledge built regarding the software to be used, the design is adapted to the possibilities and a thorough description of the final trajectory implemented is provided taking into account the challenges that were encountered.

4.1 KUKA LBR IIWA 14 R820

The robot system that was used during this master project, as part of the project requirements, was the KUKA LBR iiwa 14 R820, visible in Figure 4.1. This is a seven degrees of freedom (DOF) robot on a 6-dimension framework (3 translations and 3 rotations) which means that one of these DOF introduces redundancy to the system. Each joint of the lightweight robot has force/torque sensors as well as position sensors that allow for the implementation of different types of control and temperature sensors. This type of robot is manufactured for handling and assembly tasks, though the model use here is compatible with Human-Robot Collaboration tasks.

The robot system is constituted by a manipulator that executes the programmed motions, a KUKA control panel (KCP) that allows for real-time interaction with the robot and monitoring of the tasks – the KUKA smartPAD – and the KUKA Sunrise cabinet robot controller, where all the hardware and the software to directly communicate with manipulator can be found. In order to design specific algorithms that execute desired motions it is necessary to have a computer that will send the commands to the KUKA Sunrise cabinet controller via Ethernet connection. The communication between the two independent systems is only accomplished with compatible software available in the computer. Commonly, this is done using the Robot Operating System (ROS) but in the current master thesis, the Sunrise Workbench was the selected interface and this is shown in Figure 4.1.

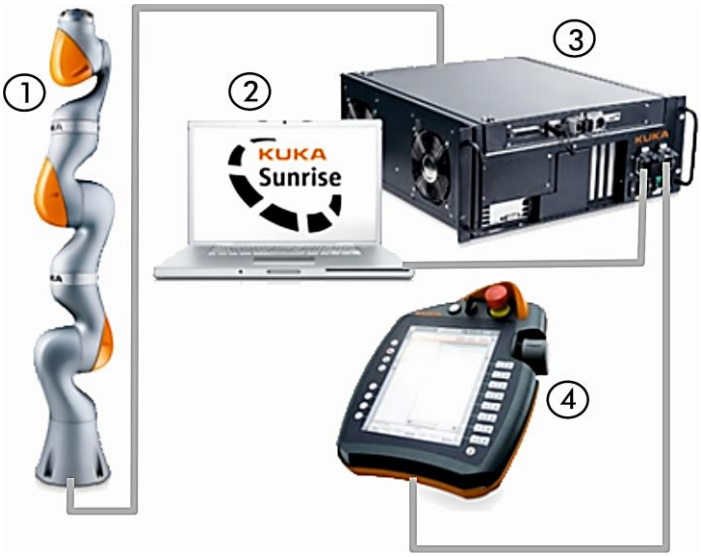

Figure 4.1 - Robot Communication Overview. In this figure, 1 represents the manipulator, 2 represents de computer with Sunrise Workbench, 3 represents the KUKA Sunrise Cabinet Robot Controller and 4 represents the KCP. Adapted from [56].

The smartPAD has 3 different modes for motion performance: T1, T2 and AUT. With T1 the motion is limited to a velocity of 250mm/s and it reduces the programmed velocity. T2 allows the user to set a maximum velocity above 250mm/s and keeps the programmed velocity. AUT mode keeps the programmed velocity and does not have velocity restrictions apart from the mechanical limitations of the robot. It is generally used for industrial applications as it executes the tasks automatically [57].

It is advantageous for the robotic system to have an extra DOF because it will allow for the existence of several solutions to reach the same end. With the robot, the goal is to execute a motion, though certain configurations might be restrictive and by adding the amount of ways to reach one point, a motion that might not be able to be executed can be done with alternative joint configuration. Nevertheless, this can cause a problem if the positions to reach are known but the joint configurations are unknown. Here, the fact there are many solutions available will make this an undetermined problem. Luckily, the KUKA LBR iiwa 14 R820 has an internal way of solving this issue, though not completely infallible.

It is possible to move the robot in both Joint space and Cartesian space, though the Cartesian coordinates are bound to the position of an initial frame, the base frame. For the KUKA LBR iiwa 14 R820, this frame is set at the base of the robot as illustrated in black by Figure 4.2.

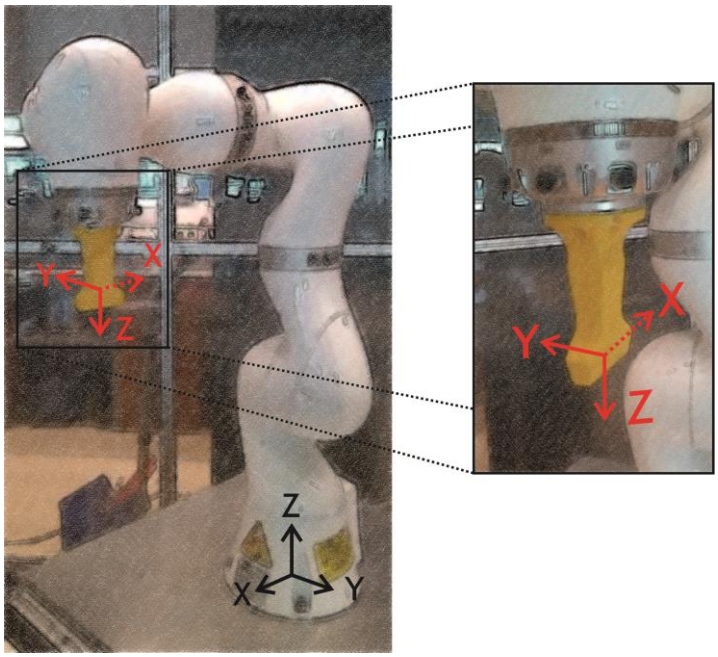

Figure 4.2 - KUKA LBR iiwa 14 R820 used during this project with the corresponding end-effector close up. The base frame is identified in black while the end-effector frame (at the tip) is identified in red.

4.2 SUNRISE WORKBENCH

The Sunrise Workbench is an integrated development environment (IDE) developed by KUKA similar to the open-source software Eclipse, extending the already existent workspace to be adapted for the implementation of robot applications. Within the application development it is possible to not only program robot applications in Java, but also to manage projects and programmes, edit and manage runtime data, project synchronization with the smartPAD and remote debugging [57]. One of the

advantages of using software that uses Java as a programming language is the fact that it allows object-oriented implementations and it is easy to import external libraries on a broad range of topics that may be required. Each overall task that the robot will perform is an application in the Sunrise environment. In order to generate a fully functioning application, the user needs to create a Java project where there is the possibility to create a Robot Application or a Background Task (in addition to all the types of files possible to create in Eclipse) and program them using the KUKA-specific libraries for robot specific commands such as movements, force conditions, control, etc. These are the only two types of scripts that generate an application that will be able to directly "interact" with the robot, done through what is called project synchronization. This way information is transferred from the computer to the smartPAD, updating them so they both have the same version. Transferring information from the smartPAD to the computer is also possible. However, caution is required when synchronizing a project because it will overwrite the current version present in either of the environments, thus any unsynchronized changes will be lost.

Furthermore, the Workbench also allows for the generation of tools and frames correspondent to what can be found in the actual physical workspace. For the tool this is particularly advantageous since this is generally an external part added to the robot that needs to be calibrated and Sunrise offers an easy way to accomplish it.

Sunrise.OS admits three possible motion types: Point-to-Point (PTP), linear (LIN) and circular (CIRC) [57].

- PTP: Chooses the fastest way to move from one point to another, which does not mean that this will be the shortest way but the easiest manner for the joints to reach the point
- LIN: Generates a straight trajectory between the two points
- CIRC: Defines a circular trajectory between two points with the help of an auxiliary third point that sets the inflection point of the curve.

Figure 4.3 - Different types of motion possible to execute with the robot. From left to right – PTP, LIN and CIRC. Adapted from [57].

For a more complex motion it is possible to add several instances of the same motion type into a spline. It is possible to create a spline with a mix between LIN and CIRC motions, but when using PTP the motion is restricted to this type. Nevertheless, when using a spline the pathway planned may suffer approximate positioning that will make the motion smoother and easier for the robot to execute.

The Sunrise Workbench also provides several controllers that are implemented at a lower-level as types of objects. Essentially, the robot can be controlled using position control or impedance control commands. The position controller, as the name would indicate, executes a motion with the highest position accuracy in terms of the planned path but it is not capable of evaluating the external

environment. When it comes to impedance control, there are three types of controllers: a cartesian impedance controller (1), a cartesian impedance controller with overlaid force oscillation (2) and an axis-specific impedance controller (3). Controller (1) is modelled as a virtual spring-damper system where the values for stiffness and damping are adjustable by the user. Controller (2) has the same compliant reaction as (1) but makes it possible to overlay constant or sinusoidal forces causing the robot move with an oscillating motion. Controller (3) is similar to (1) but at the joint level in each joint. The advantage of these controllers is that they are very simple to implement in the IDE, but since they are part of the internal libraries of Sunrise to which the user does not have access to, the extent of the control is rather limited. Nevertheless, the compliant behaviour explained in the manual is such that the manipulator should follow Hooke's law, as shown in equation 4.1, where F stands for force, K stands for stiffness and Δx stands for position displacement [57].

$$\boldsymbol{F = K \cdot \Delta x} \ [\boldsymbol{N}] \tag{4.1}$$

Even though Sunrise allows the user to execute parallel threads and asynchronous tasks, the robot can only execute one application at a time. In order to have tasks running at the same time as the main application running that can interact and retrieve information about the motion (for example, read sensor data real-time) it is possible to implement Background Tasks, which will run in the background simultaneously as the Robotic Application.

Using Sunrise.OS instead of ROS allows a more direct communication between the whole system, especially when it comes to accessing sensor data. This is one of the advantages of the choice to program in this environment.

4.3 TRAJECTORY PLANNING: INITIAL CONCEPT

Given the setup available in the lab at the beginning of this thesis, the trajectory was planned to be performed in supine position and not yet in prone position.

The automated breast scan is divided into two separate steps: the initialization step, which designates the phase where the robot is not yet in contact with the breast and needs to locate the start point, and the scanning step, where the robot has encountered the breast and starts the scanning trajectory. There are two possible approaches for the initialization step:

- With markers on the breast surface: this alternative assumes that there is no knowledge about the breast position and in order to find the breast it is necessary to use identifiable markers on its surface. To carry out this task, a camera must be attached to the end-effector and it is necessary to design markers that are US and MRI compatible. The camera will then detect the markers and send the position information to the robot.
- With prior information about the breast: since the scanning part assumes that the MRI scan of the breast has already been conducted, it is possible to extract information about the breast location. Like this, the robot can be commanded to a specific position without any visual input.

The camera option's success is dependent on how good the detection algorithm is while the MRI scan option is dependent on how accurate is the 3D scan of the breast and how the breast maintains its position throughout the procedure.

Previous work featured the camera option in the design of the trajectory and for this reason, the initial concept includes this approach to locate the breast and initialize the motion.

For the scanning step, from section 3.1, the decision was to continue with the circular trajectory and initially position the transducer on the nipple of the breast and from then start a trajectory that would describe circumferential paths over the breast surface, adjusting to the size of the breast as the transducer moves closer to the chest wall. The number of movements around the breast is dependent on the transducer's size and on the size of the breast. A trajectory example is indicated in Figure 4.4.

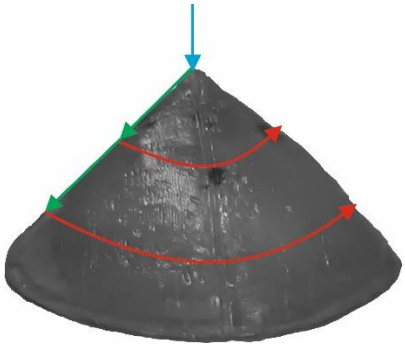

Figure 4.4 - Trajectory scheme over a breast phantom. The blue arrow indicates the initialization step using the nipple as identification point while the green arrows indicates the translational motion after the completion of one round over the breast which is represented by the red arrows.

In the past, this trajectory was developed using position control to move the robot around the designed trajectory, which meant that the positions were previously set and if the manipulator would move away from this pathway the controller would compute the error and redirect it. However, this on its own will not assure that the transducer will be in contact with the breast surface. In order to tackle this, a force feedback loop was also incorporated, with the assumption that contact is achieved when a certain force is reached (in that case, 5 N) and it would then correct deviations from this value. The results showed that this did not assure contact at all stages of the movement so this control strategy was insufficient. Additionally, the end-effector was not kept perpendicular to the breast surface but always perpendicular to the base of the setup, thus, this was one of the aspects to still be incorporated.

The "dummy" transducer visible in Figure 4.2 was introduced only in the current master project as it was considered more advantageous to use it since its shape is much similar to the actual US probe used in this type of procedure. Moreover, the amount of times the robot will have to move around the breast will be determined by how much length is covered by the surface of the probe on each round and this will help with the planning of the overall motion.

One of the main challenges of the design of a trajectory as the one in Figure 4.4 is keeping the trajectory adjustable to the shape it is encountering during the motion, as every breast will be different and the circular shape does not accurately describe the breast shape at all points. Hence, completely planning the trajectory of the manipulator beforehand based on a pre-set mathematical function seems to leave room for error. Plus, the force condition used previously allowed for a certain margin of error which added to why the contact condition was not fulfilled.

The strategy to control the robot that was attempted in this master thesis had the goal to implement a trajectory based on the contact force with the breast surface building the motion pathway

setting a small force along direction of motion, while allowing the robot to respond in a compliant manner based on the contact force. If nothing else would be measured, this would not assure that the robot would follow the breast shape. However, the contact with the surface is maintained with force feedback. The trajectory should be generated based solely on a small constant force applied in the direction perpendicular to the transducer on the same plane as the red arrows in Figure 4.4. This way the trajectory does not need to be described using position control and the robot will move only when in contact with the surface.

To keep the probe perpendicular to the surface a similar approach as in previous work is used [46]. The concept used before was based on the principle that the point where the transducer is perpendicular to the surface is the point where the forces should be applied if the end-effector position is to be kept normal to the surface. For the end-effector used, the Z direction is the perpendicular one, thus, it is expected that Z will move with the contact force encountered and the other two directions will have force = 0 N (within a certain error). Nevertheless, given the shape of the transducer, the initial positioning of the transducer needs to be set prior to motion start or else there is more than one configuration of the probe that could generate such a solution for zero forces in X and Y. In addition, the Sunrise Workbench offers an option to set the orientation of the end-effector (through the manipulator joints) according to the path being described, so this option can also be explored.

This approach is based on the assumption though there is a way to detect the initial start point so that not only the transducer's orientation can be set accordingly but also because the necessary force for contact is at first not known. With this first position information, an impedance controller would be used to produce a force for the robot to move with in order to reach that point compliantly. The idea behind this controller is better described in top scheme of Figure 4.5. Since the impedance controller introduces a displacement, the first point actually needs to be a point inside the phantom's surface to compensate. It is also imperative to ensure that there is a maximum force condition to stop the robot's motion in case the values are getting high enough that it would endanger the patient's safety.

Then, once the first point is reached and contact has been made with the surface, the force of contact will be measured and used to assure contact with the surface further on and a perpendicular force will be introduced into the system to start the actual trajectory around the breast. For this step, an impedance controller is used since the contact between the two surfaces should continue to be compliant and for this reason it handles a position change (a twist) and not just a position. This would correspond to the middle controller of Figure 4.5.

The second step is to measure whether or not there are forces in the other directions and if yes, they will be controlled so that they can be minimized. In addition, it should be possible to know on which direction the motion will be conducted and to which side (positive or negative) so that the correction to adjust the transducer will result in a rotation in the appropriate direction. Therefore, this is a control that receives a force and compares it to the expected and the resultant action is to rotate the end-effector to the expected direction and re-measure if this position already provides a force equal to zero. The correspondent controller is the last one of Figure 4.5 and should also be last one to be executed.

Once one full cycle around the breast is completed, which is done by saving the initial position and comparing it to the current position along the motion, the transducer will break the contact with the surface and move upwards (or downwards, depending on the breast positioning) half the amount of the transducer's surface length, the second cycle is ready to be repeated as the contact force is now known.

In the event that the transducer would miss the breast phantom completely, a time constraint should also be introduced for the execution of the first controller.

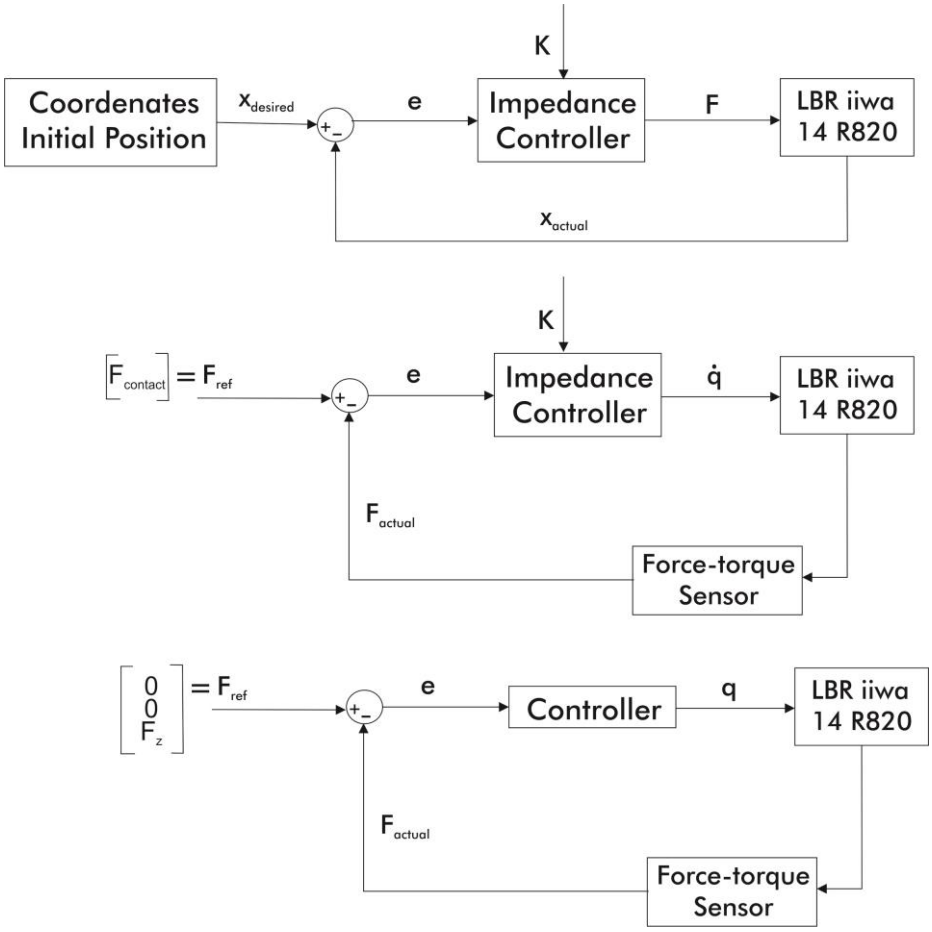

Figure 4.5 - Block diagram of the three controllers planned for this trajectory. The reference force for the second comes from the initial controller when it finishes. During the last control loop, the manipulator also does a position check to see whether or not the cycle has been completed. The last controller only needs the force in Z to be different from zero.

4.4 TRAJECTORY IMPLEMENTATION

Given the novelty of the software used for programming applications, the way to design fully functioning applications had to be unravelled step-by-step. This was a challenging task because the limitations were not well-known, which made the whole process more time consuming and required an initial set of simpler trajectories to be developed to build up the required knowledge to execute the desired strategy. The architecture of programming used in Sunrise Workbench is quite different from ROS, as mentioned in section 4.2, which meant that most of the work developed before this master thesis could not be directly used as it was not only developed in a different programming language but also since the implementation had to be done in a different manner.

Before implementing the concept described in section 4.3, the following steps were performed:

- A simple scanning trajectory with manually set frames to understand the basics of motion

- The same trajectory but with the pathway built from one initial set point and the mathematical function that describes the rest of the trajectory, to test the inverse kinematics on changes occurring in the same plane
- Same trajectory but adding the impedance controller provided by Sunrise[1]
- Introduction of more challenging trajectories including the impedance controller and attempting to understand the robustness of the inverse kinematics of the robot in different planes and orientations

Setting frames manually is a task that can only be done with the help of the smartPAD since there was not an alternative way of finding the initial position, at least the start point of each motion had to be manually defined. The advantage is that the user can decide on the configuration of the manipulator setting the end effector in the wanted orientation and in contact with the surface of the obstacle. The disadvantage is logically the fact that there is a big margin for error when setting these definitions manually.

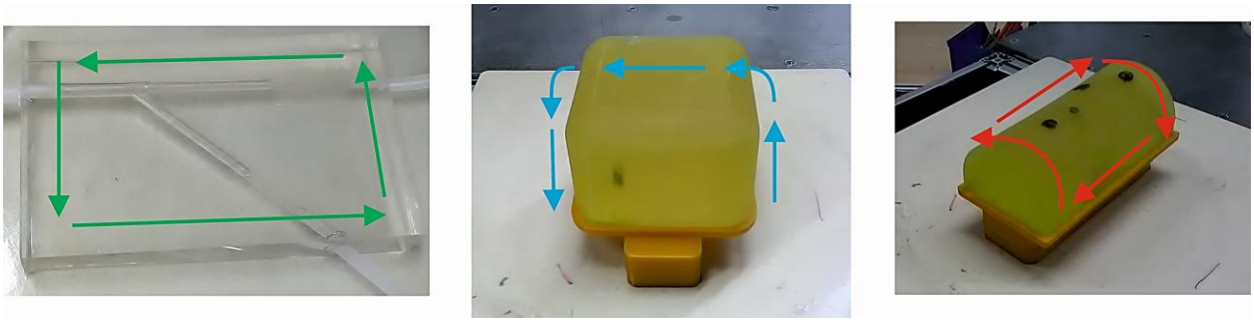

Figure 4.6 - Different phantoms used to test simpler trajectories

The trajectories implemented initially were designed based on 3 different phantoms with different shapes, not as complex as the breast phantom, and the concept is shown in Figure 4.6. By studying these diverse situations it was possible to understand which situation would fit better with a certain motion type. As it would be expected, LIN is most useful for the pathway for straight movements where there is only one specific direction for motion. PTP can be used for the previous case as well, as it is a more versatile type of motion, though it's not possible to predict exactly what movement will be generated beforehand. CIRC motion is by far the more specific type of the three. All throughout these initial steps, the objective of conducting a scan over a phantom was always present, thus keeping contact with the surface was always taken into account. However, with a CIRC motion this was hard to always assure since it generates a "perfect" circle with the 3 frames involved, which may not be able to describe exactly the wanted shape. Additionally, there is a minimal distance between two frames, so for smaller trajectories is a very hard task to set an auxiliary frame. For this reason, whenever the direction of the movement is not singular it is easier to use PTP which will be able to generate a smoother desired motion as it takes into account the joints preferential way to execute action.

[1] The position controller already present in the Sunrise libraries was not tested because its implementation method is similar to the impedance controller and so it did not add significant value in terms of software comprehension

A Robot Applications in Sunrise always follows a similar structure – declaration of variables; initialization of variables and executable section (run), as it can be seen in Figure 4.7. In order to implement the steps described above there is essentially 3 types of constructions that need to be understood:

1. Generating a motion with manually set frames

If the user chooses to set the frames with the smartPAD, they need to be taught before running the code. The alternative is to be familiar with the coordinate workspace and set the frames through specific commands. These choices both assume that the user knows where the phantom is located. To move the manipulator with the Workbench, the following command is used:

`Tool.move(motion_type(frame))` or `Robot.move(motion_type(frame))`

This is the simplest iteration that can be done to obtain a movement. To move to more points this command just needs to be repeated while changing the desired frame. To obtain a smoother motion, the motions can be grouped into a spline.

2. Generating a motion based the mathematical description of the pathway

With the assumption that the phantom's shape is well known and possible to describe mathematically, it is possible to develop a motion through code. The idea here is to generate a step motion changing the parameters of the initially defined start frame for the amount of steps it takes to complete the trajectory. There is some variability on how to implement such a cycle but in terms of pseudo code, it would look like this:

```
Move robot to start frame;
Define a step;
While (final position is not reached) {
Move robot one step according to the mathematical description;
(Example:robot.move(LIN(startframe.setX(startframe.getX()+step))))
Update the start frame;
}
Initiate next motion similarly or do nothing and end motion;
```

It is advantageous to plan the motion with this approach if one of the 3 motion types is not accurate enough to describe the function and by doing it over small steps it is possible to obtain a better approximation of the desired result.

3. Creating a controller and adding it to the motion

Each controller is defined inside of Sunrise in a class that creates the specific type of object. The controller is initiated similarly to any variable with its associated constructors. The impedance controller allows the introduction of a compliant behaviour in all possible combinations of rotation and translation. In order to introduce the impedance controller into the motion, the program would be something as presented below:

```
Initialization: ctrlmode = new CartesianImpedanceControllerMode();
ctrlmode.parametrise(CartDOF.X,CartDOF.Y).setstiffness(500.0);
Run: robot.move(motion_type(frame).setmode(ctrlmode));
```

With this knowledge, the previous two examples can be repeated adding the impedance controller. Logically, the control mode can have more properties added to it, such as damping, maximum control force, maximum path deviation, additional force control, among others. These commands are helpful to add for example a force control in addition to the impedance control, though this appeared to be the only way to actually implement some kind of force control.

After these implementations were tested for the different phantoms, some limitations were encountered:

1. **Inverse kinematics**

When the motion was planned without manually set frames through the smartPAD but using a description of the pathway compiled in Sunrise based on its mathematical description and this motion would require a reasonable change in the redundancy configuration in order to accompany the changes in direction of the surface of the phantom (which are present in the middle and left phantoms of Figure 4.6), the motion would become impossible to plan and the robot would not move further. However, if the frames are set manually, the robot is able to perform the whole trajectory. The only apparent difference between the two situations is the fact that by setting the positions manually, the redundancy is also set, something that is not given to the robot in the code. The only way the robot has to convert 6 cartesian positions into 7 joint positions is through the inverse kinematics, which is a task the manipulator generally does automatically and for these specific trajectories, this mechanism failed to perform the adequate transformation. Since the information on how the iiwa calculates the inverse kinematics is very limited and the only command existent in the software is poorly explained, this problem remained unsolved. This was rather limiting when it came to trajectory planning as it constrained the setting to manual when the trajectory is more complex.

2. **Workspace constraints**

For the breast phantom, the attempt to manually define the frames did not allow to set a pathway that would cover the full breast surface with one smooth motion that could keep contact with the surface. Given the phantom's shape, it was not possible to set all the frames without having to drastically change the manipulator's configuration, which meant that reaching that frame would be a complicated task that would alter the type of trajectory generated.

Given the limitations encountered, the initial plan had to be redesigned, but the situation was used to build more knowledge about what is not yet understood and another trajectory was developed with input from the partners from KUKA that are also involved in MURAB. This trajectory will be explained in detail in section 4.5.

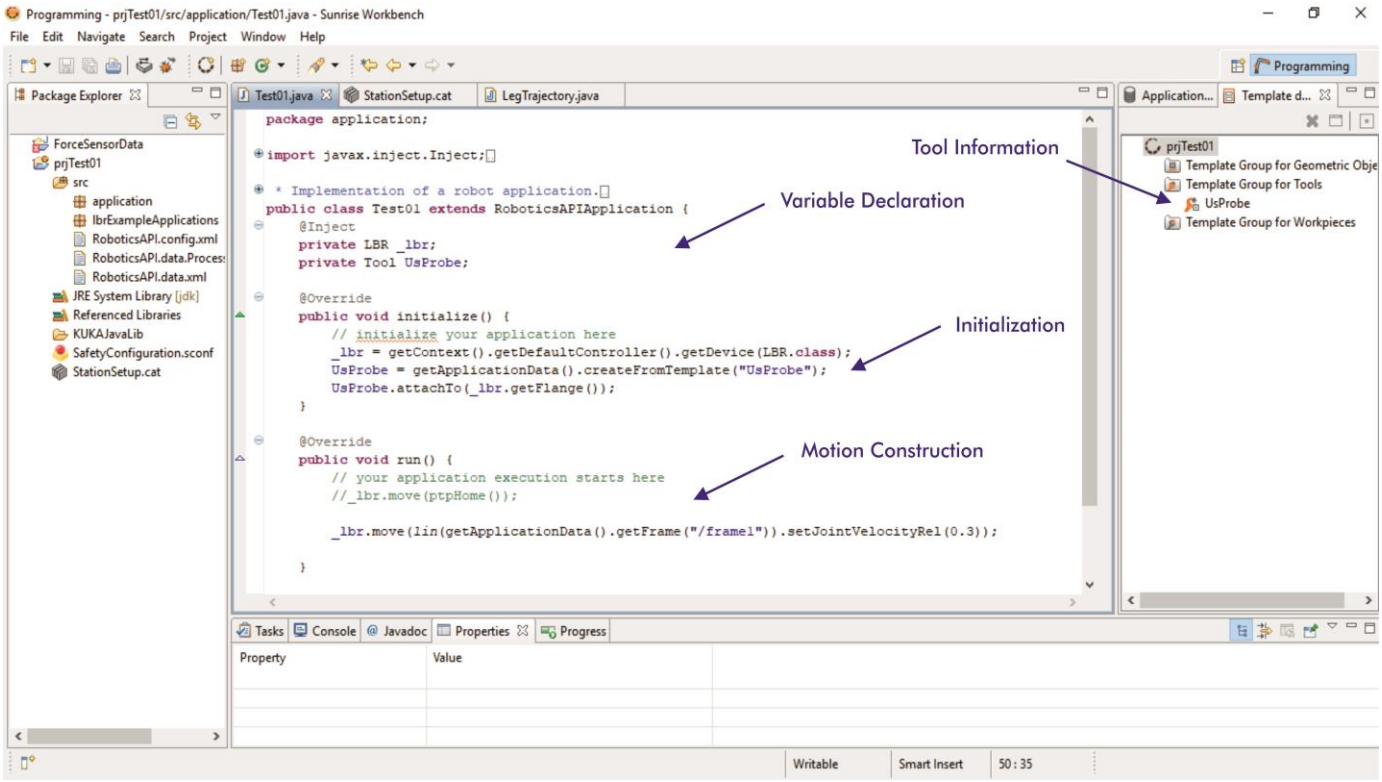

Figure 4.7 - Example of a basic application in the Sunrise Workbench environment and how the environment is organized.

4.5 FINAL TRAJECTORY: OFFLINE PLANNING

One of the challenges encountered in the trajectory was the fact that the autonomous mechanism for the inverse kinematics was not always dependable. It would be possible to work around this setback if all the joint positions could be planned before the motion is conducted or if the conversion step could be done alongside the planning (if the planning was done in cartesian positions).

There is an algorithm in MATLAB, currently being developed, that is able to receive a CAD file of the breast phantom and obtain the joint positions of the LBR iiwa 14 R820 that will be assumed by the robot to execute the desired scanning trajectory. It is essentially a simulator of the manipulator that is able to predict the positions needed for a certain pathway that are executable. It functions as follows: import a model of the structure to be scanned; define mathematically the trajectory that should be performed, in this case it was an ellipse; project it onto the surface of the imported model; generate a trajectory; compute the joint positions required to perform the projection trajectory with the robot.

This means that the whole trajectory will be conducted based on this offline planning algorithm. For the purposes of MURAB, since the MRI scan is conducted prior to the trajectory, it is possible to generate a model of the actual breast and apply the same concept. Nevertheless, this does not allow for online repositioning of the transducer in the case of sudden patient movements.

In terms of implementation in Sunrise, this simplifies the task of the main application, though it is necessary to develop a way to properly import, read and structure the data to make it usable by the Workbench. To accomplish this, two classes were created: one responsible for reading the text file with

the joint positions provided by the MATLAB algorithm and building the data into a [Nx7] array ("ReadFile") and another that transforms this array into an array list of PTP motions in order to create a group of splines that will represent the trajectory ("SpiralTrajectory"). A group of splines is necessary because there is a maximum amount of motions that can be compiled into one spline and there is an amount of points that is much superior to that value.

The actual robot application is not very complex and thus it will be described in pseudo code. To see the entire code of the application the reader is referred to the Appendix A.

```
Declaration of variables
Initialization {
Attach tool to robot;
Generate empty file reader with "ReadFile";
Import txt file;
Set control mode (Impedance Controller - CartD0F.Z, K=450.0);
Generate empty group of splines with "SpiralTrajectory";
}
Create filtering function; // secure minimal distance in between
points inside each spline
Run {
Read imported file;
Turn into a group of splines of PTP;
Filter the array list;
Create a MotionBatch with the group of splines;
Move robot to a predefined initial frame away from the phantom;
Move the robot through the MotionBatch;
Move the robot to a predefined end frame away from the phantom;
}
```

This program is capable of executing the planned motion while keeping contact with the surface, since the planning already takes that into account, as well as the position that maintains the end-effector perpendicular to the surface. Since the impedance controller is used, the manipulator reacts compliantly in the direction that puts pressure on the phantom's surface (in this case Z of the end-effector, as shown in Figure 4.2). However, this solution does not completely fulfil all the requirements, as it can be seen in Table V. Additionally, even though the robot moves in a compliant manner, which creates a safer environment for the patient, this algorithm only implements an impedance control feedback loop at a low-level with which the user cannot interact once the motion has been started . Thus, effectively, there is an open loop system for the position since the next position will not be influenced by the past positions of the end-effector, as illustrated in Figure 4.8.

On the other hand, given the inexistence of a mechanism that allows for real-time re-positioning of the breast in case contact is broken, the necessity of a force feedback in the direction of the pathway becomes evident.

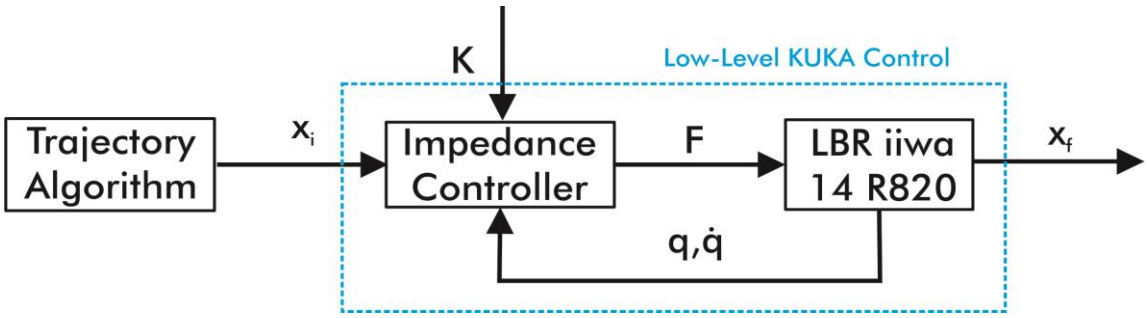

Figure 4.8 - Block diagram of the control loop implemented. The parameters outside the blue box are introduced by the user. In addition, if it is desired to add a force to the system, the force is introduced by the user and it will be sent directly to the impedance controller block.

With the help of the MATLAB algorithm, it was also possible to confirm the limitations encountered with the workspace. With the breast in supine position, the manipulator cannot fully complete one complete circle around the breast as part of the same continuous motion as the existent workspace is restrictive.

Table V - Requirements of the scanning trajectory

Requirements	Achieved	Not Achieved
Circular Trajectory	X	
Surface Contact	X	
Perpendicular Orientation	X	
Impedance Control	~~	
Online Adjustment		X

This trajectory was quite useful to perform some of the experiments that are explained in Chapter 6. Since the controller present in this chapter is internally embedded in the software, there are virtually no parameters that can be changed to test its performance. The stiffness that was used was pre-defined to fit the purpose it was designed, that is, it provide a motion that was compliant enough and did not compromise the positions that needed to be reached as this was also incorporated into the MATLAB algorithm before generating the positions. In addition, the position generation algorithm has a very accurate model of the robot, so has very little error. For this reason, the trajectory itself is not tested but it is used to ensure that the next part of the project can work with the trajectory developed.

5. BREAST HOLDER DESIGN

This chapter aims to depict all the steps that lead to the final design of the breast holder structure described as the second challenge in the analysis. From the possible initial concepts to the end version it was necessary to decide upon a manufacturing method and an appropriate material, as well as overall adequateness to the purpose. Bellow, several designs contemplated as possible solutions can be found as well as the reasons that lead to the selection one of them. Further, possible materials are investigated as well as the possible ways to fabricate them. Before explaining the final design, the intermediate steps that lead to this final structure are explored.

5.1 CONCEPTS

From the analysis chapter, the overall concept of the type of structure looking to be developed can be understood. Three different possible approaches were conceived. They are described below and illustrated in Figure 5.1:

In previous work [45], [46], having only a partial US scan after the tumour location was known from the MRI was discussed as possibility to be incorporated in future work. Some of designs are thought taking into account this option.

1. Open Concept

Allowing direct contact with the skin avoids deteriorated image quality. The open concept is constituted by an even number of pillars (depending on the size of the scanning probe as this will be the minimum distance between two consecutive columns) connected to one small ring on the bottom and larger ring on top. The amount of pillars should be even so that the forces are equally distributed on all the directions (each pillar will have an opposing one on the other end). To maximize the open space the numbers of columns should be minimized. To assure the adaptability of the holder to the breast, the material should not be completely rigid. It should be a material capable to stretch while also providing structure to be able to hold the breast.

Since the problem of US compatibility here is neglected, the choices for possible materials are much wider. However, a complete circular trajectory would not be executable but it could be replaced by a partial trajectory or a radial trajectory instead. Even though this concept would facilitate the needle biopsy step and will not compromise the image quality, it could cause difficulties in the image reconstruction step. While adequate support would provide a reduction of changes in the breast shape during the procedure, its capacity to reduce deformation is not very clear.

2. Mesh-like Structure

Optimizing the support structure while allowing needle biopsy is the main idea behind this concept. The material has to be quite flexible to adjust and adhere to breast surface, which it will cover completely, while still strong enough to keep the breast in place. It is thought to have the transducer scan over it and for this reason, both MRI and US compatibilities have to be taken into account, thus there is a risk of compromising image quality and acquisition. To reduce the deformation and breast motion, the holder needs to push the breast in the opposite direction as gravity. A way to do this is assuring that the material

is being stretched. Finding a material that can have all these characteristics can be a difficult task. Nevertheless, any kind of trajectory can still be executed.

3. Partial Mesh with Rigid Combination

Assuming that only a partial trajectory is sufficient, with this design, it is possible to combine two material characteristics that could otherwise not be found together: the adequate support and immobilization from a rigid material with the adaptability from a flexible material. Both materials would need to be MRI compatible, but only the mesh like structure would need to be US compatible as the scan would be conducted only in that side. The possibility for needle insertion is still assured but again the image obtained might be affected if the material is not suitable enough. The plan incorporates a transition material if necessary, though the possibility to add small springs in this transition area (in light grey in Figure 5.1) to make the whole structure more adjustable to different breast sizes was also contemplated. In terms of execution, this is the most intricate solution. The rigidity introduced in this concept would reduce the overall adaptability of the breast holder to many different shapes and sizes.

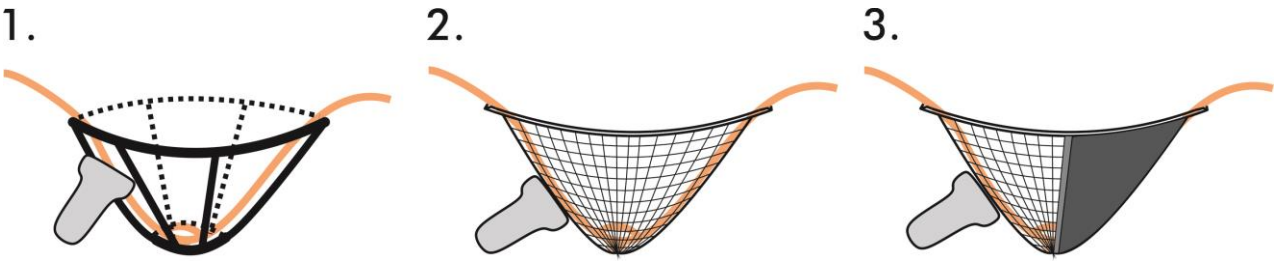

Figure 5.1 - Three concepts idealized for the current problem. The numbering is correspondent to numbering encountered in the text. The thickness of the structure columns is reduced from 1 to 2 and 3 because the pillars need to be stronger to provide the same structural support.

Given the lack of restrictions in terms of trajectory and the versatility of the solution for several breast shapes and sizes, without compromising needle insertion, the decision was to investigate concept 2. The biggest challenge that arises from this choice is the encountering a viable material able to comply with the structural requirements while being both MRI and US compatible. An investigation on the candidate materials will be conducted in the next section.

5.2 MATERIAL ANALYSIS

To evaluate if a material is MR Safe or not, it is necessary to bear in mind its magnetic properties. Materials that are made from the more commonly used metals such as iron, copper and nickel, among other ferromagnetic metals, cannot be used in a MRI environment as they will both endanger the patients' safety as well as interfere with the generated image.

The initial material that was looked into was nitinol (material used for medical stents) which is biocompatible, very flexible and causes minimal MR interference despite being an alloy made out of nickel [58].However, it is quite expensive for fabrication which lead to its disregard as a viable option. It could also be extrapolated that this option could cause patient discomfort as its elastic modulus is rather elevated in comparison to the one of the breast.

As it seemed an easier principle to stay away from metals regardless of the existent exceptions, the focus was mainly redirected to investigate ultrasound compatible materials.

In line with what was said in section 2.4, to find whether a material has the ideal acoustic properties, the goal is to find a material with similar properties as the soft tissue, such as its speed of sound, and acoustic [27]. Other acoustic properties should be minimized as much as possible so that the signal transmission and reflection are optimal, such as attenuation coefficient, the backscattering coefficient and the nonlinearity parameter. However, these last two are rarely reported in the literature and are difficult to measure accurately so they won't be evaluated.

The easiest way to discover materials that are known US compatible is to look into the materials that are generally used to mimic tissue properties in a laboratory environment – the phantoms. Literature separates the existent phantoms into several different material types for soft tissues [27], [59] :

- Water and water based gels
- Gelatine based
- Agars
- Magnesium-silicate based
- Oil based
- Silicones
- Polyacrylamide (PAA) gels
- Polyurethanes (PU)
- Polyvinil-alchohols (PVA)
- Polyvinil-chloride (PVC)

For some of these materials, the acoustic properties are described in Table VI.

Water and water based gels are generally used for mimicking more fluid like tissue such as blood or marrow but their major disadvantage is their lack of properties stability with temperature changes around room temperature [27]. Gelatine, agar can to some extent be also considered water based materials [60], though the way to fabricate them allows for the addition of complementary materials that build up the necessary properties to achieve acoustically compatibility [27], [59]. Their disadvantage is their longevity as they degrade easily as well as dehydrate and can suffer microbial invasion [59]. Magnesium-silicate has good acoustic properties but lacks support capability and cannot be fabricated into different shapes. Oil based materials have good acoustics properties and durability, so they seem quite good candidates. Amongst them it's possible to find paraffin gel and PVC(P). Silicones have good stability and durability though low speed of sound and high attenuation. PAA is rather toxic, so it was immediately discarded. The acoustic properties seem to be dependent on the type of polyurethane and the attenuation rate is quite variable, though specific types could be investigated. PVA seems to be a good candidate, though with some range of variability within the type and its fabrication time is very long and it needs the addition of an external component to avoid microbial infection [59]. PVC has the stability and durability required, though PVCP has a lower speed of sound and a higher attenuation rate [59], [61].

In addition, there are also some US compatible materials that are already commercialized, such as Zerdine, a condensed-milk gel and a urethane rubber[27], [62], [63]. The downside is that it is generally not possible to alter their composition and mould them to the specifications of the problem.

This information mentioned above is relative to the the available phantom types for all soft tissues. However, for breast phantoms, the available examples mention the usage of PVA, PVC, safflower oil gel in solid gelatine (anthropomorphic) [63] and a paraffin gel [62].

Table VI - Acoustic properties of phantom materials. Adapted from [27], except PVC(P) which can be found in [64].

Material	Velocity [m s^{1}]	Density [kg m^{-3}]	Attenuation [dB cm^{-1} MHz^{-1}]	Impedance (MRayl)
Agar based	1498-1600+	1016-1100	0.04-1.40	1.52-1.76+
Gelatine based	1520-1650	1050	0.12-1.5	1.60-1.73
Magnesium-Silicate based	1458-1520	-	0.85	-
Oil-gel based	1480-1580	1040-1060	0.4-1.8	1.54-1.67
PAA based	1540	1103	0.7 (5MHz)	1.7
PU	1468	1130	0.13	1.66
PVA based	1520-1610	-	0.07-0.35	1.60-1.77
PVC(P) (20ºC)	1501.5	953	0.46	-
Water based	1518-1574	1000+	-	1.48-1.60
Condensed-Milk based	1540	-	0.5	-
Urethane Rubber	1460	900	0.5-0.7	1.31
Zerdine	1540	-	0.5-0.7	-

At this stage there is enough information to make a pre-selection of what materials could be possible candidates for this design based on the literature described above and the materials available in the laboratory (or that are easy to obtain). The materials that had little longevity (agar and gelatine) were immediately excluded. From the list above, it was decided to test PVC (P), PU and urethane rubber. PVC is a widely used polymer whose applications are most of the time related with its harder version but given its versatility as a vinyl, it is also capable of originating very flexible structures with long durability, especially when combined with plasticisers, which is why it can be useful in several medical applications such as blood bags and the majority of fluid transporting tubing for the patient, thus it seems like this materials could be able to mimic the desired properties for the purpose of this research.

Additionally, since 3D printed materials are generally not the usual choice for soft tissue phantoms, the available data on acoustic properties is rather scarce. However, 3D printing is an incredible tool to use when it comes to design, so if there was a possible way to incorporate this technique into the fabrication of the concept, it would definitely be beneficial. For this reason, in addition to the materials picked above, it was also decided to investigate 3D printing materials that would have mechanical properties suitable for to support the breast and run experiments to test whether or not they would be US compatible. Three promising options were considered:

1. Strong and Flexible Plastic, PA 2200 (Shapeways Inc. NL, Eindhoven, The Netherlands)
2. Rubber-like Polymer, TangoBlackPlus FLX980 (and VeroWhitePlus RGD835 and VeroClearPlus RGD810) (Stratasys Ltd., Eden Prairie, MN, United States)
3. Flexible Thermoplastic PU (TPU), NinjaFlex 85A (NinjaFlex®, Manheim, PA, United States)

TPU is the version of PU (found in Table VI) that will be used for testing, so there are actually 5 material types being considered.

Even if it is possible to find flexible printing materials, which is essential for adjusting to the breast shape, it is a more intricate task encountering materials that in addition have adequate stretch, which is required for adjusting to several breast sizes. Nevertheless, it is possible to look into some properties of these materials that can provide some insight on whether or not the materials might be US compatible and this information can be found in Table VII. It is important to note that second printable option, this polymer is generally obtained from the combining two materials (generally one is very flexible and the other very rigid) that allow the user to adjust the flexibility of the design, thus the properties can be altered.

Table VII - Properties of the 3D Printed materials

Material	**PA 2200** [65]	**NinjaFlex 85A** [66]	**TangoBlackPlus FLX980 + VeroWhitePlus RGD835**[2] [67]	**VeroClearPlus RGD810 + TangoBlackPlus FLX980**[3] [67]
Young's Modulus [MPa]	1700	4	1.3-10	1400-2000
Elongation at break [%]	24	660	35-130	15-30

The (healthy) breast tissue has values for E ranging from 2 to 29 KPa, thus observing Table VII, all the values seem too large by comparison given the order of magnitude, pointing to the ones with lowest E to be more likely to be acoustically compatible are NinjaFlex 85A and TangoBlackPlus FLX980 (combined with VeroWhitePlus RGD835), since their elasticity is closer to tissue properties.

Since the majority of the materials used for breast phantoms want to mimic the breast as much as possible, they may lack the required strength to hold and pull the breast against the forces of gravity. With 3D printed materials, despite being flexible their stiffness is expected to be larger than tissue, which can be more ideal to provide the necessary support and reduce the deformation caused by transducer. This is one of the properties that will be investigated during the experimental tests.

An ideal material is US and MRI compatible, while being flexible but not plastically deformed as this would allow for position displacement during the procedure due to the effect of gravity.

5.3 DESIGN CHOICES

Even though a concept to execute has already been selected, the detailing of how exactly it will be done has not been explored yet. It is necessary to contemplate fabrication options and specific requirements the design should attempt to incorporate such as the hole size for the mesh, for example.

Given the advantages of 3D printing when it comes to manufacturing – low cost, highly customizable, relatively fast production for a small amount of samples –, it was one of the main options contemplated for fabrication of this design. However, using 3D printing as fabrication technique assumes

[2] This will be further referred as simply TangoBlack, unless specified otherwise

[3] This will be further referred as simply VeroWhite, unless specified otherwise

that the material chosen can be 3D printed, which might not be possible. It could also be possible to use techniques like laser cutting, though these are slightly more restrictive in what it can create and it is not guaranteed that the materials can handle this technique.

A common way to make phantoms for soft tissue seems to be through pouring the substance over a mould with the desired shape [61]–[63], which was also the fabrication method for the breast phantom seen in Figure 4.4, and thus this technique could also be considered. In addition, the mould could also be 3D printed so that the desired shape can be obtained.

Regardless of the fabrication technique, there are four main design points that have to be established in order to develop a mesh that will be compatible with all the techniques and requirements:

1. **Mesh hole size**

In order to not compromise the needle insertion in the biopsy step, the hole size and the spacing in between holes of the mesh needs to be optimized. On one side, the holes cannot be too small as that will increase a lot the necessary precision of the needle and limit it to one angle for entering the breast. On the other side, if the holes are quite big that may weaken the overall support provided by the mesh and at the extreme, will make the mesh have little to no effect on reducing breast deformation. The main requirement for the size is that it is large enough to fit the needle and to allow for needle steering.

To make an informed decision, this problem was discussed with a clinician who performs needle biopsy on breast cancer patients, to whom a sample of different hole sizes was presented, as it can be seen in Figure 5.2. The discussion pointed towards a hole size of 4mm and a spacing in between holes of 2mm.

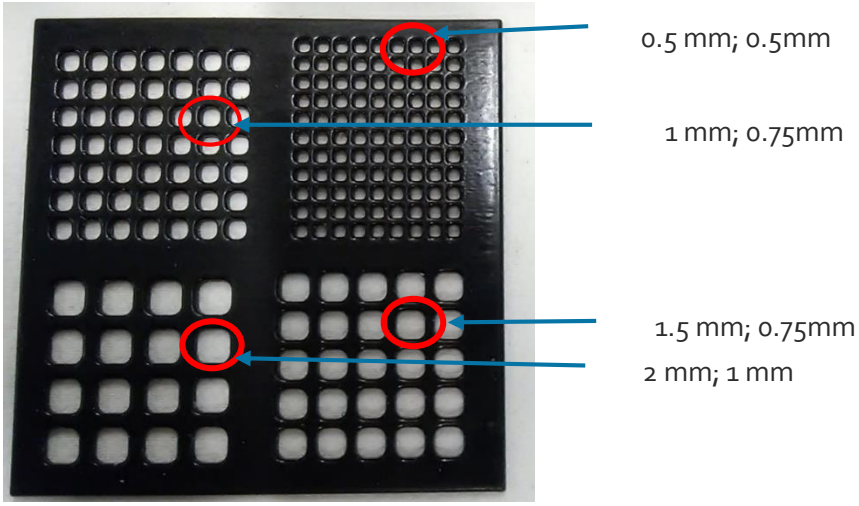

Figure 5.2 - Sample mesh with different hole sizes. Each pair of values represents: (hole size, spacing in between holes).

Nevertheless, the hole size decided upon at this stage was more of a start point to start envisioning the design as the most optimal size will still be tested in the experimental section.

2. **Mesh thickness**

As it was explained in section 2.4, the intensity of US signal decreases with how much distance it travels due to attenuation derived from the tissue and the wave's frequency. Thus, how deep the signal can penetrate the tissue is limited. By adding an external layer on top of the breast, the distance the

signal can travel inside the tissue is smaller. In order to implement this design, there is no option that can actually eliminate this problem, though it is possible to minimize it. Since the reach of a US transducer (though variable depending on the transducer) is within the range of a few centimetres, it seemed plausible to admit a thickness for the mesh of 1-5 mm, which would be adjusted considering the strength of the material used and how it performed under the tests conducted in the experiments section. Additionally, if the material has a low attenuation rate (close to zero) the thickness of the mesh can be increased. Starting from the range of thicknesses considered here, thickness is one of the properties that will be evaluated in the experimental section as well.

3. Detachable (open/close) mesh

Regardless of the fabrication process selected, it will be simpler and more cost-effective to produce this mesh structure as a flat surface in addition to allowing the breast holder not to be bound to a pre-defined shape in 3D providing more adaptability. With this in mind, the next choice is to whether or not keeping this flat surface as an open or closed structure can give the most optimal result.

Allowing the mesh structure to be able to open alongside the breast will create a better adjustment of the breast holder to the shape of the breast but also allowing for a better control of how much the breast is compressed, reducing the air that might otherwise have been trapped in between the two surfaces. This is more advantageous than a complete mesh without any separation as it will be more complicated to make it fit appropriately the breast surface.

However, having a detachable mesh means that a connecting structure will be necessary to keep the two sides together. Hence, a structure that can endure the pressure of the breast in the direction of motion of the trajectory without allowing the breast holder to break or re-open. Additionally, it will also implicate that there is a small area where needle biopsy cannot be performed and it is required that the connector occupies as least space as possible. Depending on the fabrication method of choice, different solutions for connecting structures can be contemplated. The most adequate connecting option will also be obtained through experimentation developed in the experiments section.

4. Overall mesh size

Despite the fact that the breast holder should be able to fit as many different breast sizes and shapes as possible, it is necessary to have start point in terms of what dimensions to use in order to create the design concept. The average breast dimensions are mentioned in section 2.2. However, since the research would be conducted in the breast phantoms available in the laboratory, it seemed more reasonable to use these as a start point. They are slightly larger than the average breast, though. The dimensions of the breast phantom used are visible in Figure 5.3 and the designs take these values into account.

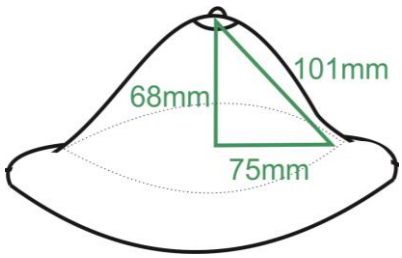

Figure 5.3 - Dimensions of the breast phantom available for the experiments

5.4 DESIGN STEPS

The goal is to be able to reach a final design from which one whole breast holder can result. However, in order to reach that level it is necessary to first complete a series of steps given the fact that it is not known whether the materials have the desired properties and what adjustments can or need to be made based on the test results. Additionally, the breast holder is a reasonably large structure to keep testing all the possibilities in the full sized designed, thus it makes more sense to start out by testing smaller portions of the mesh like structure. Nonetheless, all these intermediate steps before achieving the final design require some intermediate design themselves and that is why these intermediate steps are mentioned.

To be able to properly evaluate the materials so that the most adequate could be found, a set of tests that a material has to go through was developed, as shown by Figure 5.4. These tests are organized from a priority point of view. This is, the first tests are responsible for evaluating the most fundamental characteristics without which the material may need to be discarded. For instance, a material that is not US compatible will never be considered as viable option, regardless of having all the other ideal properties.

At the end of these steps, the breast holder is ready to be paired with the trajectory implemented in chapter 4 and face the final challenge to finally be validated (or not) as working concept for the purpose it was designed for. The validation of the breast holder as structure that can reduce breast deformation will only be tested after a final design is obtained, which means that for this testing step all the intermediate steps will have produced the optimal solution and no more design steps are executed. If this test would reveal itself fruitless, then it would be necessary to re-visit one of the previous steps, possibly involving changes to the material.

These tests should be done chronologically and will be thoroughly explained in Chapter 6.

Figure 5.4 - Sequence of tests a material should undergo until a final design can be obtained

Nevertheless, the goal of each test is simple to deduce from the name: the US compatibility test will reveal if the materials are or not US compatible by simulating an US examination; the stretch test analyses the behaviour of the material once it is stretched with a specific weight, providing insight on the kind of structural changes the material might need to suffer to become suitable (for example, thickness changes); after the design of a connecting structure that can fit with the mesh, the connector test will check whether the connector in combination with the material can handle similar forces to the ones experienced if it was holding the breast; finally, the support test is applied on a full mesh to see whether or not it can support the breast (phantom) for the necessary amount of time the procedure requires.

For the execution of all these steps, intermediate designs were developed to allow testing with smaller testing samples that would still reproduce the characteristics the material would have. Given the two fabrication methods available, some of the planned designs will be 3D printed while others will be moulded and for this reason the two design options are presented below.

- **US Compatibility Test**

In this test, a small sheet of material is tested for ultrasound compatibility. This is done by putting the sheet on a phantom and comparing the image with and without the sheet. Preferably, the sample should not be in mesh form so that it is clear whether the material is US compatible or not and if there is no influence of the presence of air in the open spaces of the mesh. In addition, it should be larger than the dimension of the transducer's surface.

- **Stretch Test**

The stretch test allows for the tuning of the main properties of the mesh, such as the thickness and the hole size and shape. This is done taking into account that this mesh should be able to support a certain force when under stretch. The force established was based on the average weight of a breast which was found to be about 500 gr [68]. This test is designed assuming that if a small portion of the breast structure can withstand such a force then, the complete structure will not only be able to hold 500 gr as it will support the weight of heavier breast.

Here, the material should be designed into a larger sample in mesh form with exactly the same structure as it would be expected in the final design. As a pre-definition, the dimensions for these meshes were settled at 94 mm x 86 mm. The 94cm length is derived from the phantom's surface dimension mentioned in Figure 5.3, 101 cm. The difference between the two comes from the fact that the nipple of the phantom will not be covered by the mesh and so the actual surface to be covered has a smaller length. The choice to use 86 cm for the width of the mesh is such so that the stretch response will not be a result of one the directions being privileged by the force distribution, thus the mesh will not respond differently if it is stretched horizontally or vertically, and 86 cm was the closest value to 94cm that allowed a symmetric structure.

If the design can be directly 3D printed, Figure 5.5 illustrates what it will be the model used. For the case of a mould, the design becomes the "negative" version of the 3D printed one, as it can be seen in Figure 5.6.

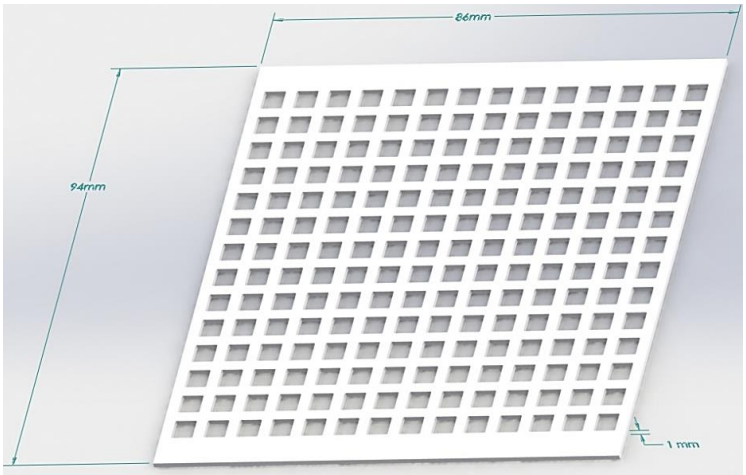

Figure 5.5 - SolidWorks rendered model of the stretch design for a 3D printed material. As a start point the thickness was set at 1 mm (the best case scenario).

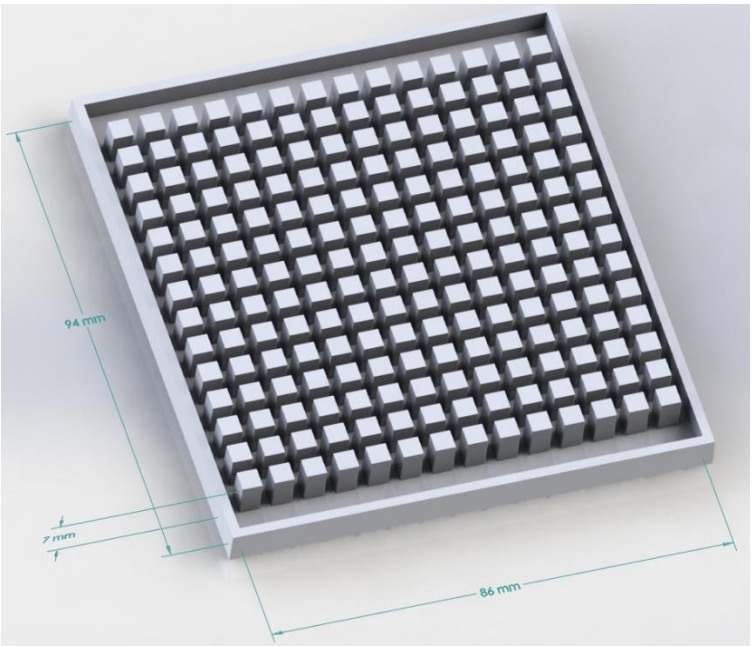

Figure 5.6 - SolidWorks rendered model of the stretch design for a mould of the mesh. It is important to note that the height of the pillars is not relevant as long as it's higher than the borders height so that it is possible to have well-defined holes. As a start point, the design was also thought so that the mesh would have 1-2 mm of thickness.

- **Connector Test**

This test is designed to evaluate whether the connector can withstand the expected forces. Not only the connector itself needs to withstand these forces, also the interface between the mesh and the connector should be strong enough to support the force. Depending on the connector that will be tested, the design will look different, though it will have the same principle. Since the connectors need to fit with the surface and provide an even stretch, the length of the structure should be the same as the mesh (94 cm). In terms of thickness, since these areas are not required to be US compatible, the requirement is that they minimize patient discomfort. For example, for the mould, the area were the connector is supposed to be inserted is 1 mm smaller on the side that will be contacting with the breast so that it can be like a continuous part of the structure.

One example of a model for each of the fabrication techniques is presented in Figure 5.7 and Figure 5.8. The mould will not be now an exact negative version of the 3D printed model since the actual connector is 3D printed in both cases, though the mesh that can fit the printed connector needs to be moulded and the mesh is the one that need to follow the principles described above, since the connector will be an external element in this case. The size of the cylindrical pillars observed in Figure 5.8 is dependent on the chosen connecting structure.

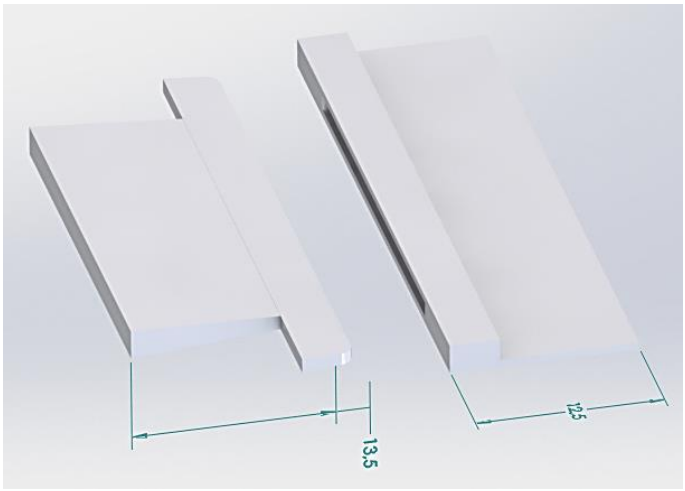

Figure 5.7 - SolidWorks model of a 3D printed connecting structure. The units are in mm and are just mentioned as an example.

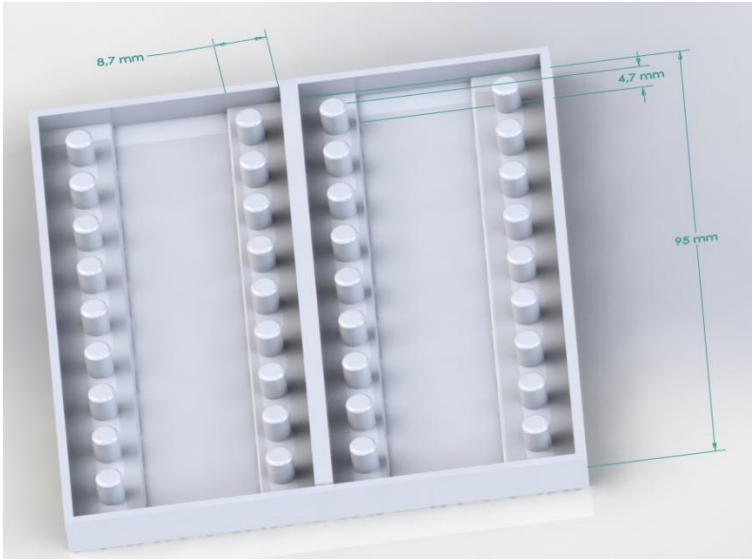

Figure 5.8 - SolidWorks model of the mould for the mesh that needs to be created in order to fit the connector. The connector itself is 3D printed separately. The distance between the central pillar and the edge of the connector area is minimized so that the connector will occupy as little space as possible of the overall mesh.

- **Support Test**

The support test can only be done once a full design is available and it can be put over the breast phantom to see whether or not it is able to support its weight. Thus, at this stage the designs are at their final stage and should already have all the ideal mechanical and acoustic properties. This test is used to confirm that the assumption made with the stretch test is valid since the breast phantom is heavier than the average breast.

In terms of design, it was decided that a flat surface would the shape presented in Figure 5.9 and Figure 5.10 and not a semi-circle, for example, as this would facilitate its assembly into a conic shape. Dimension wise, the total perimeter of the structure was based on the perimeter of the breast phantom (whose radius is 7.5 cm) and the inner incomplete circle has the perimeter of the nipple (8cm). The length

of the side is based on the surface length of the breast phantom as it was already established in previous tests.

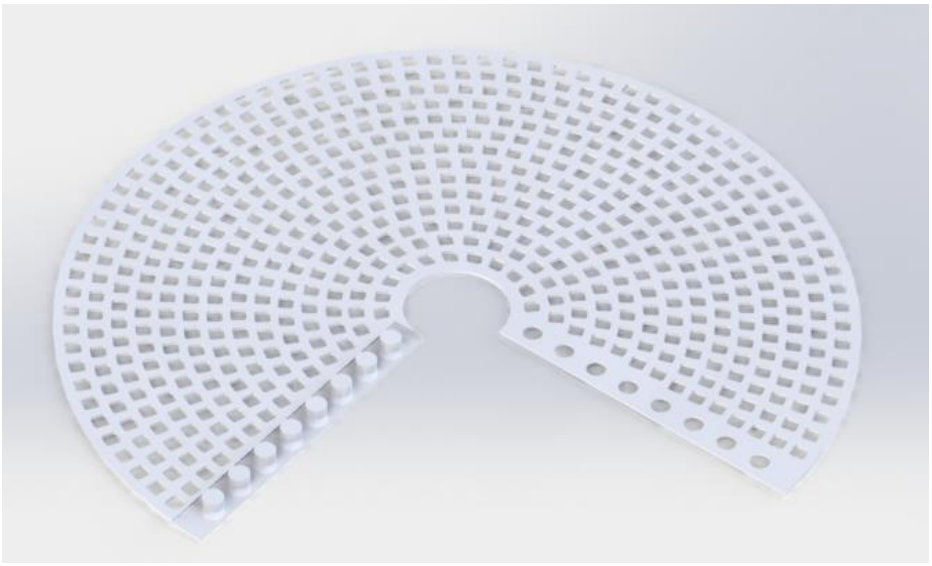

Figure 5.9 - SolidWorks model of a 3D printed functional breast holder with an example of a connecting structure.

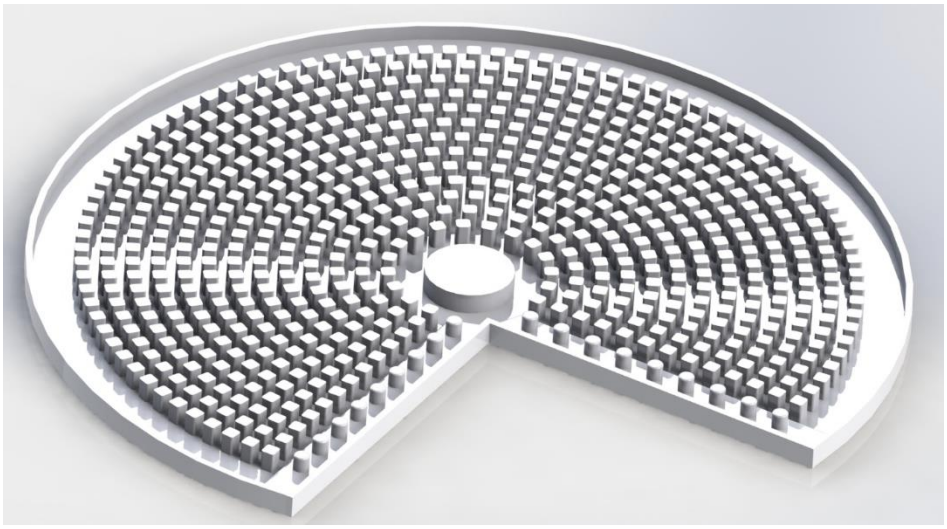

Figure 5.10 - SolidWorks mould of the breast holder structure

Assuring that all the test were successful, the breast holder is ready to be paired with the implemented trajectory to understand if the transducer and the material are compatible, i.e., if the trajectory can be conducted without any problems and the image quality is maintained (it should be, since the material is US compatible, but it is used as final confirmation step) and how does this structure influence the deformation of the breast (phantom).

6. EXPERIMENTAL RESULTS AND DISCUSSION

In the following chapter, it will be possible to encounter a description of all the experiments that were conducted, both to test the response of the robot and the adequacy of the materials for their purpose of assembling a breast holder. To each experiment set, the setup and the materials used will be presented. They are not presented initially as one whole section since the setup was very particular for each experiment. At the end of each test, results will be presented and discussed.

Experiment-wise, since the control of the robot is not implemented from a lower level and its functioning principles cannot be altered by the user, no tests were conducted to understand the robustness of the controller. Additionally, since the trajectory is pre-planned by the MATLAB simulator, the extent to which the robot executes the path that was planned is dependent only on how good the modelled system is and since that falls out of the scope of this thesis, it will not be evaluated. However, having a functional trajectory with impedance control allows for its incorporation into other experimental setups. The breast holder, on the other hand, was created from scratch and needs to be thoroughly evaluated, following all the steps described in the previous chapter, but also pairing up with trajectory to understand whether or not the presence of the breast holder does reduce breast deformation, confirm that it does not compromise image acquisition and induces changes in the force behaviour of the robot, in a comparative study between the situation without a breast holder, while the scanning of the breast is being conducted.

With each fabrication method it was necessary to tune the properties of the materials. For 3D printing, this meant adjustments to the thickness of the sample (or the mould) and, if necessary, the shape/size of the holes. However, the materials that need to be used with a mould also incorporate an extra "tuning" step involving the conditions that they are prepared in so that they can be poured into the respective moulds. For PVC and Urethane rubber, this was the case. In order to understand how this was made, the reader is referred to the Fabrication Protocols in Appendix C. Nevertheless, it is important to mention that the production of PVC suffered an extensive optimization until it could be obtained in the adequate conditions and this process will also be discussed in said appendix.

All the materials that were 3D printed for the following experiments were printed with the Connex 3 Objet 260 (Stratasys Ltd., Eden Prairie, MN, United States) printer, excepting the TPU which was printed with (Flashforge Corporation, Zhejiang, China). For the materials moulded, the urethane rubber used was from () and PVCP used LUPA Plastisol Medium (Lureparts.nl, The Netherlands) but also Plastileurre Super Rigide (Bricoleurre, France).

6.1 ULTRASOUND COMPATIBILITY TEST

The US compatibility test is conducted through the observation of a certain structure under the US without any obstacle in between the transducer and the surface to observe (control) and with the introduction of the material in the middle of the target surface and the transducer. Then, the two images are compared and how the quality of the image changes will be evaluated. It is hard to draw the line on where exactly the loss of features compromises the diagnostic and the material can be considered incompatible, so the results are prone to subjectivity of the examiner. A trained clinician could provide a more trustworthy analysis of this test.

SETUP

This experiment uses an US machine, from which one specific transducer was chosen, US gel, two controls and the materials to be tested. The apparel used had the following specifications:

- Siemens ACUSON S3000 (Siemens Healthcare, Erlangen, Germany)
- 14L5 Transducer, optimal range: 5-14MHz, used for breast examinations
- Ultrasound Transmission Gel, Aquasonic 100 (Parker Laboratories, Inc., Fairfield, NJ, USA)

Figure 6.1 - Ultrasound machine (left) [69], transducer (middle)[69] and ultrasound gel, used to improve imaging quality and reduce friction, utilized in this experiment.

As control, a cubic phantom with an identifiable mass inside was used. However, this phantom was made of PVCP (due to its acoustic properties). Since, PVCP is one of the materials that are going to be tested, it was decided to use an additional control method. Since the human body is within the detection range of the US waves, a forearm was also used as control. Thus, there were two possible setups for this experiment, as illustrated in Figure 6.2. The material would be introduced in between the transducer and the control object as mentioned previously.

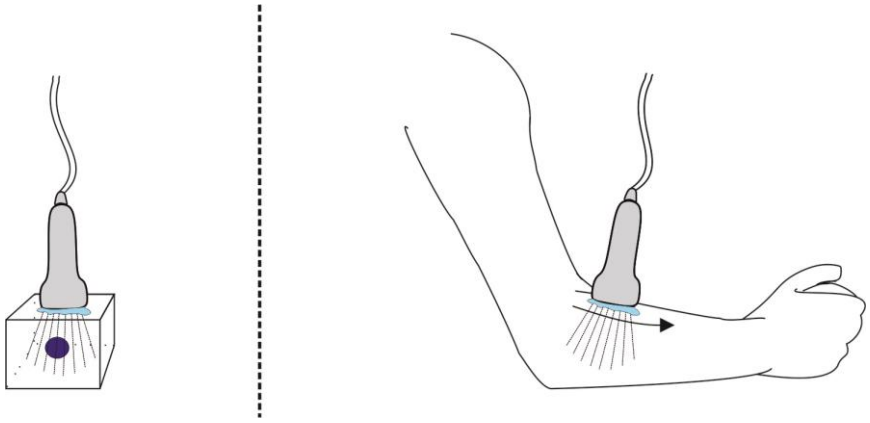

Figure 6.2 - Two possible setups for US compatibility test. On the left, there is the setup with the PVCP phantom and in dark blue there is the detectable mass. On the right, there is the setup with the human arm, the transducer has its wider face parallel to the body's frontal plane. In between the transducer and the control object it is possible to observe ultrasound gel.

RESULTS

From the 6 materials being tested here, TangoBlack, PVCP and urethane rubber will be tested in comparison with the arm, while the rest of the materials will be tested with the simpler phantom setup. TangoBlack was the first material to be printed and initially the phantom setup was not available. The urethane rubber was available as phantom with obstacles inside it, so it was tested on its own, though for the sake of comparison, a smaller piece was tested under the arm to confirm the results. Nevertheless, it was considered that there was no need to repeat the test since the arm model is actually a closer situation to the real scenario and thus, the results are equally (if not more) reliable. Since the experiments were no always conducted during the same day, the results will be presented next to its specific control.

- TangoBlack and PA2200

Control: Arm

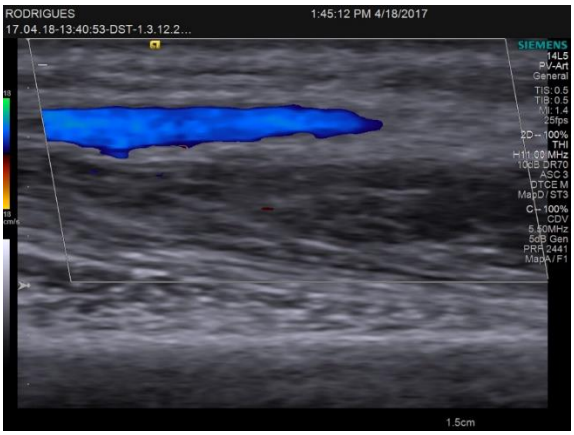

Figure 6.3 - US image on a human forearm, with the transducer perpendicular to the initial parallel direction. The blue area indicates blood flow

The presence of a vessel is used to help the re-identification of the area being observed in the control and be able to accurately compare the two images.

However, given the available sample for PA 2200 (since it was produced outside the lab), the shape did not accurately fit the setup considered initially. In order to facilitate this, the material was placed under water to remove air in the medium and the fingers were used as visible and detectable structures as it can be observed in Figure 6.6.

Material: TangoBlack (1mm and 2 mm thick)

The mesh utilized for the two measurements was very similar, with just an increase in thickness of 1mm on the second one.

Figure 6.4 - TangoBlack mesh sample with 1mm of thickness

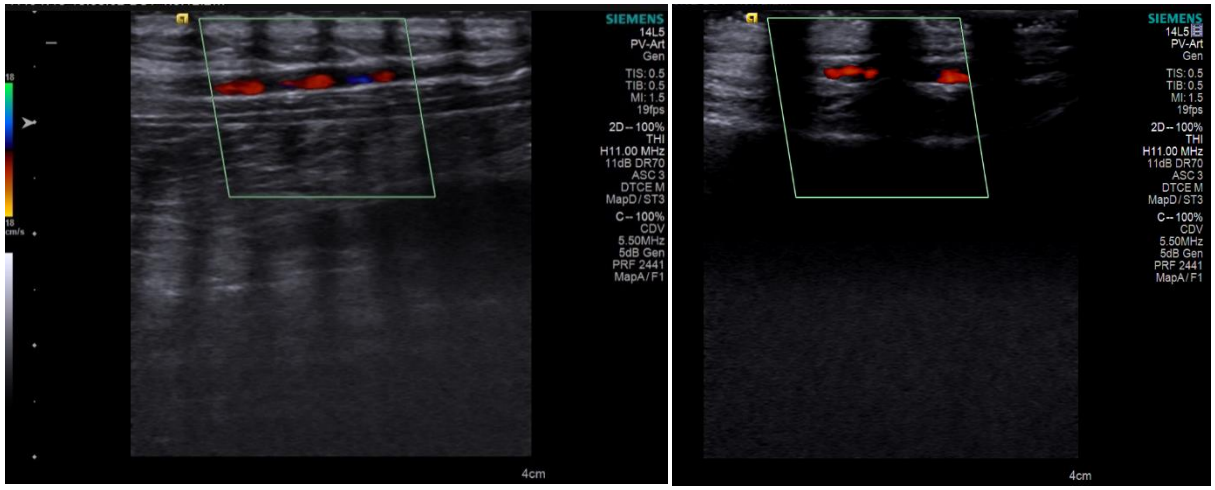

Figure 6.5 - Results of the US imaging of TangoBlack. The result with 1mm of thickness (left) and with 2mm (right). Unfortunately, the results are not at the same scale as the control.

Material: PA 2200

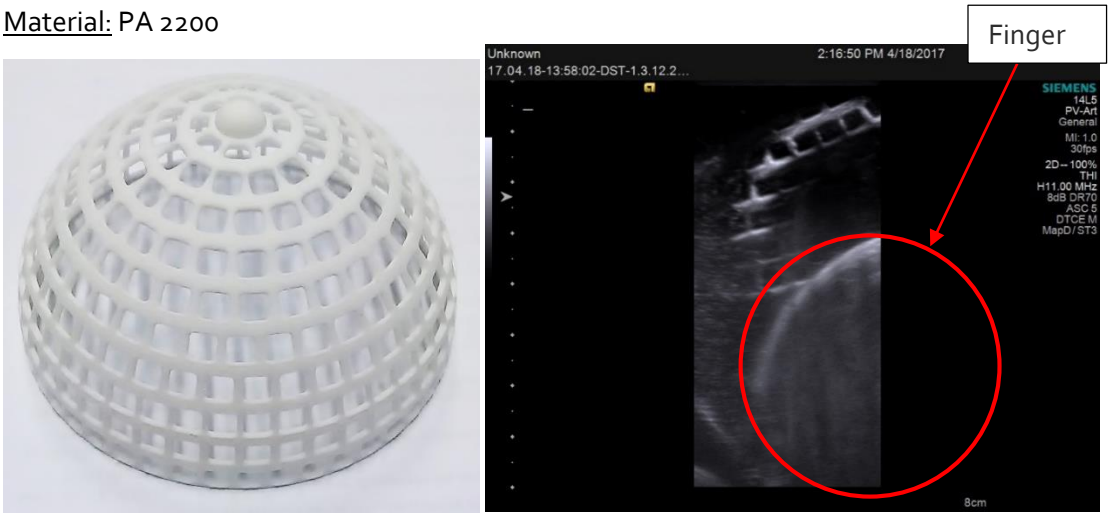

Figure 6.6 - Sample (left) and imaging response (right) of PA 2200 in aqueous medium.

In this trial, both the materials tested do not appear US compatible. TangoBlack causes a shadowing onto the tissue which is indicative that the signal is being blocked in that area given the different acoustic impedances. Additionally, this effect is worsened with the increase of thickness. Also, with a thicker mesh the attenuation effect caused by this material becomes rather clear. Despite the struggles with imaging PA 2200, it was possible to completely observe the structure of PA 2200 and, even though possible to distinguish between fingers, the image quality was rather reduced.

These two materials were, logically, discarded at this stage.

- VeroWhite (100%), VeroClear (100%), VeroClear+TangoBlack Mix, NinjaFlex 85 A and NinjaFlex 85A with a conductive material

Control: PVCP Phantom

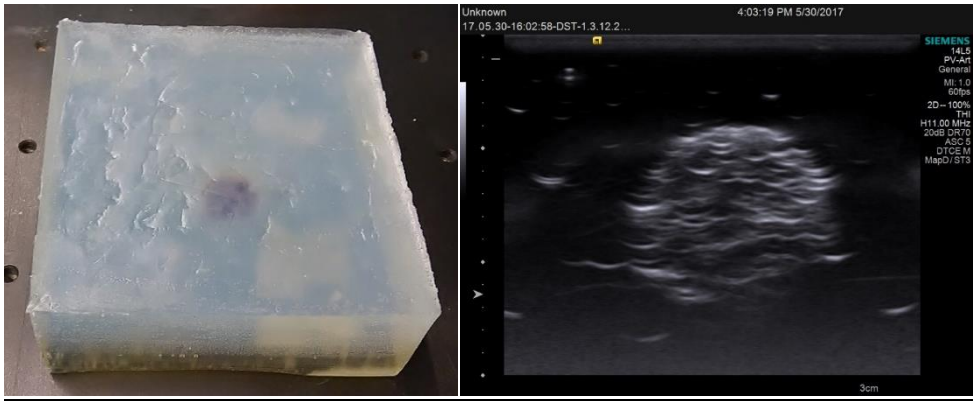

Figure 6.7 - Phantom used as control and the correspondent US image

Material: TPU

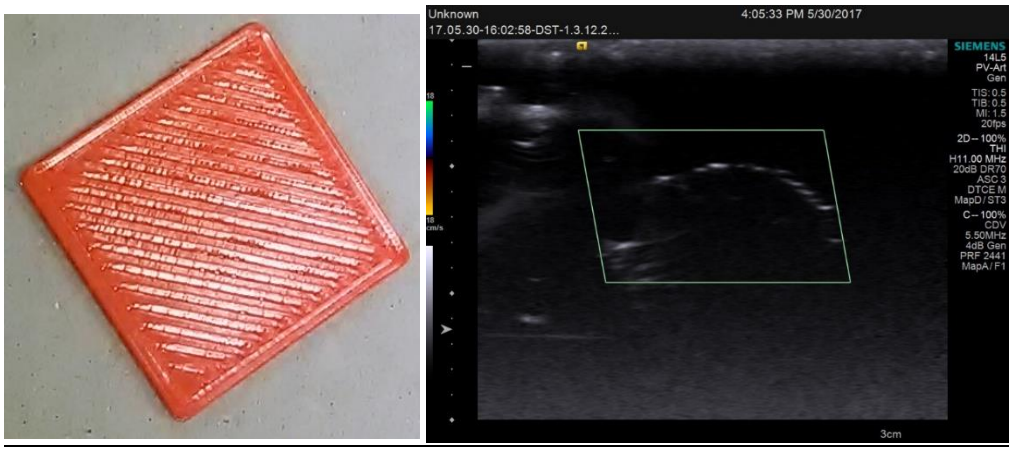

Figure 6.8 - Sample of TPU and its correspondent US image

Material: TPU with conductive material (not US compatible)

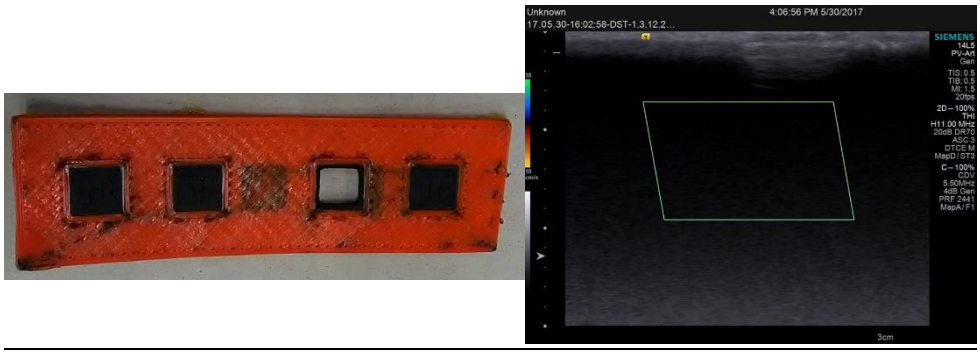

Figure 6.9 – Sample of TPU with conductive material and its correspondent US image

Material: VeroWhite (100%)

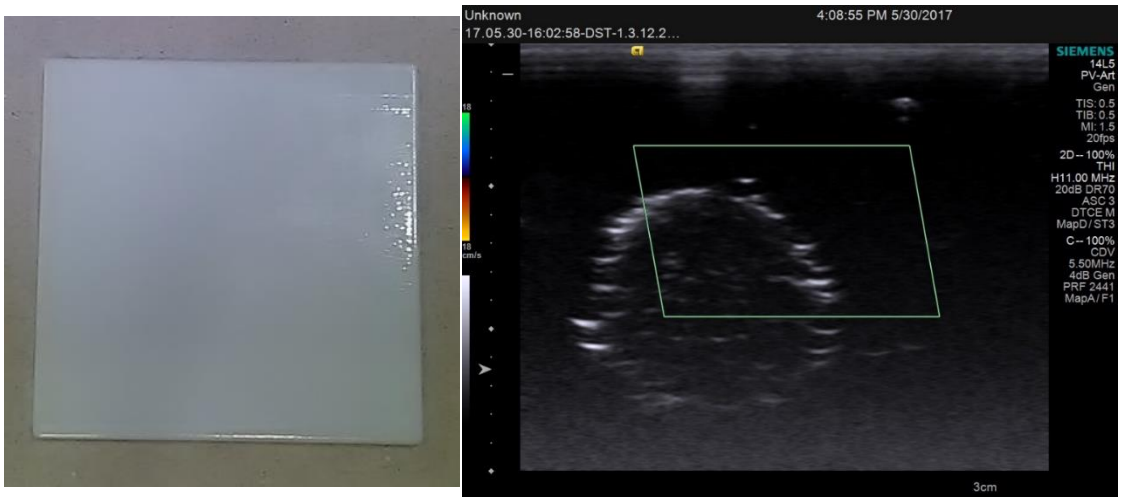

Figure 6.10 – Sample of VeroWhite (100%) and its correspondent US image.

Material: VeroClear (100%)

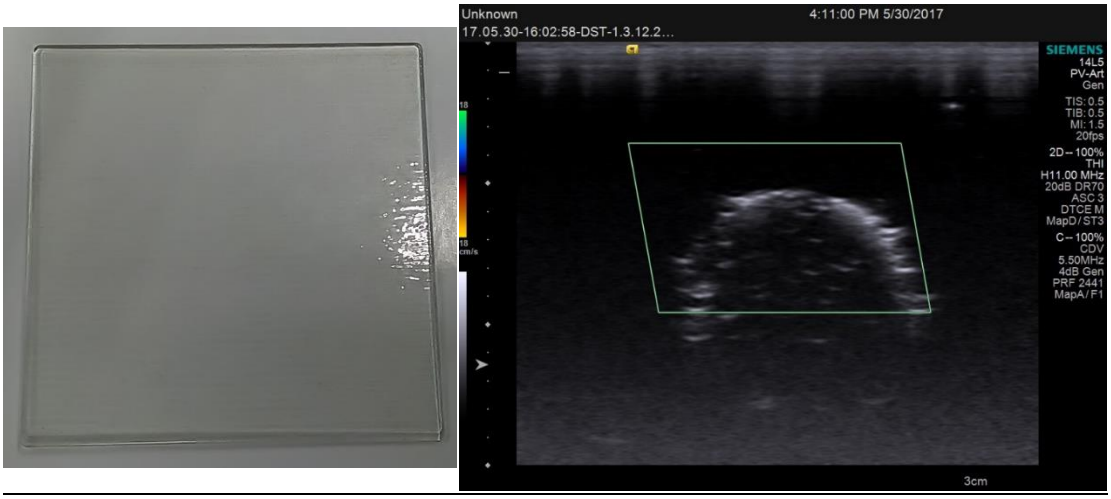

Figure 6.11 - Sample of VeroClear (100%) and its correspondent US image

In this case, both of the attempts with TPU the image quality was quite reduced and lesion cannot be completely observed, thus, TPU is not considered acoustically transparent, at least for the necessary level accuracy required in this project. Both VeroWhite and VeroClear were able to detect the edges of the lesion rather clearly and did not cause a shadowing effect. However, this lesion is rather larger than the ones expected to be encountered in MURAB and the inside of the lesion cannot be observed in both cases, thus the image quality seems to be compromised here as well.

At this stage, all the materials were considered US incompatible.

- Urethane Rubber (existent phantom, 1 cm slice and 0.35 cm mesh)

Control (for 1cm slice): Arm

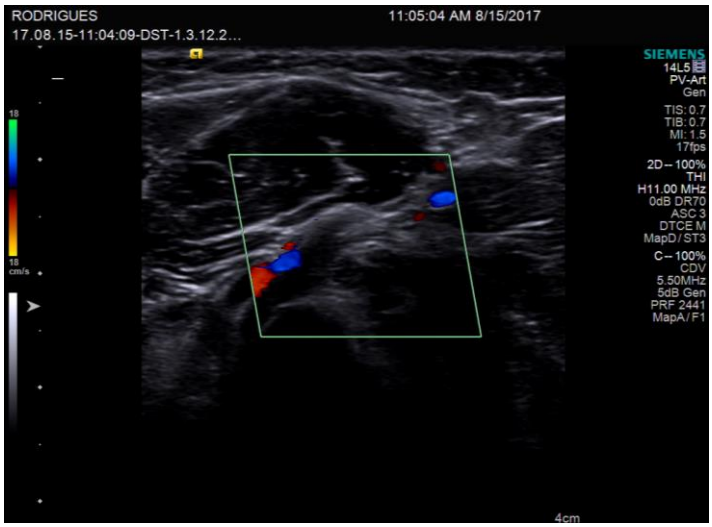

Figure 6.12 - US image of the arm (cross-sectional view) used as control for the next materials

Material: Urethane rubber phantom

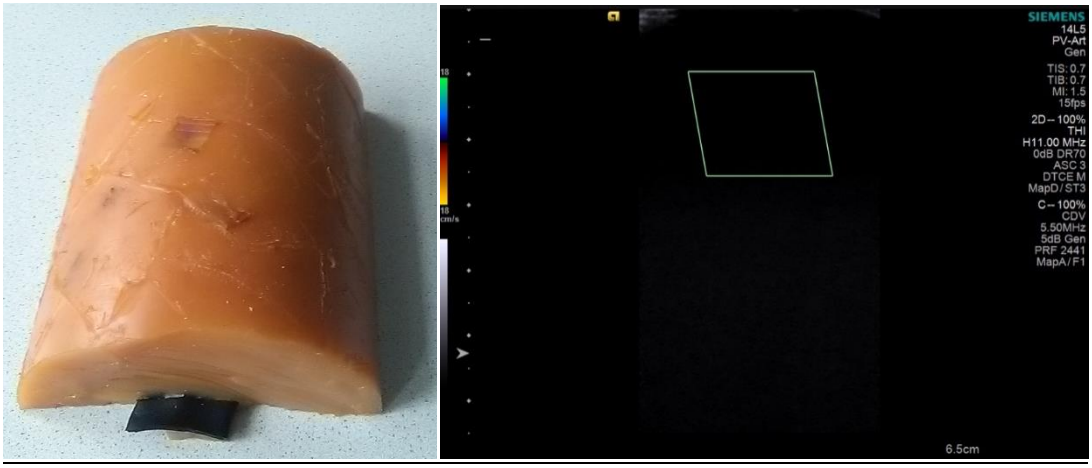

Figure 6.13 - Polyurethane rubber phantom and its correspondent US image. The dark tube and the "spots" on the surface of the phatom indicate structures that should be identifiable obtrusctions after imaging and some are also present inside but are no visible.

Material: Urethane Rubber 1 cm slice

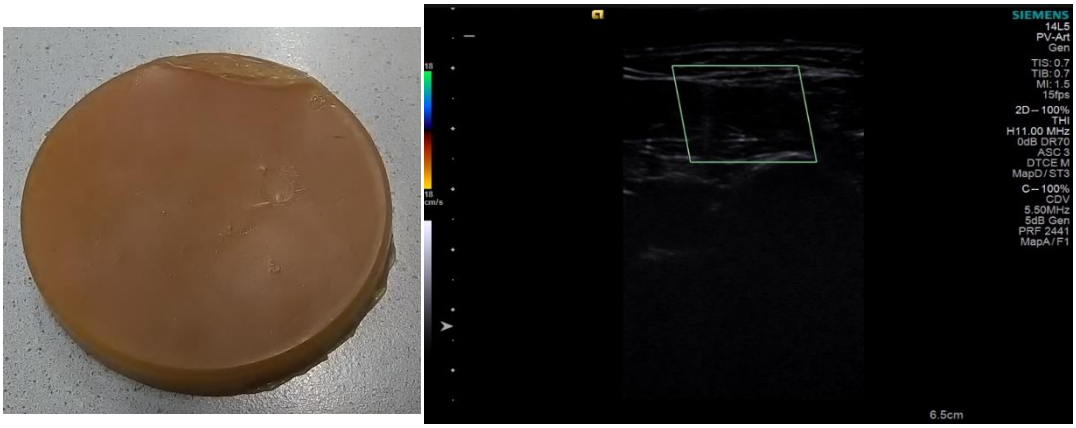

Figure 6.14 - Sample of polyurethane rubber and its correspondent US Image (when over the arm)

These images allow the discarding urethane rubber as possible candidate for further testing. However, the possibility of re-testing urethane rubber was revisited as it was wondered whether the thickness of the samples could have influenced the results. Instead of using part of pre-fabricated phantom, a new mesh was also made to clearly re-evaluate this situation (the protocol for this can be found in the Appendix C). For this case, a different phantom with several lesions was used (breast phantom) as control.

Control: Breast phantom

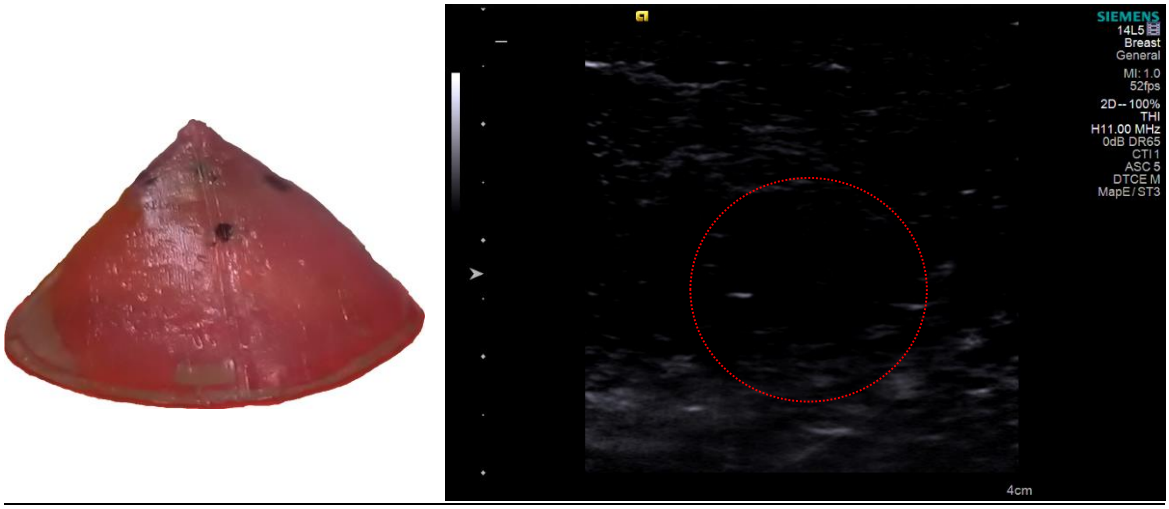

Figure 6.15 - Breast phantom with an US image of one of its lesions (red-dotter circle).

Material: Urethane rubber mesh

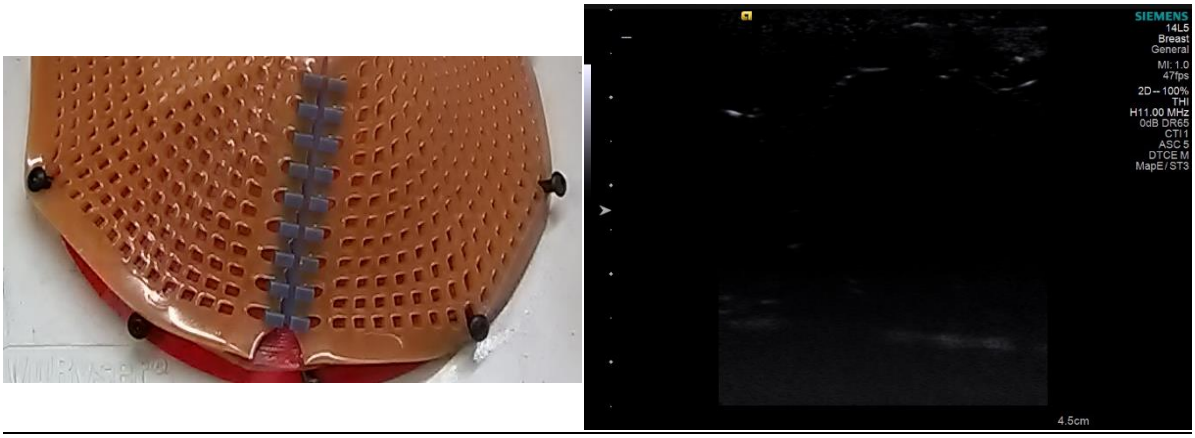

Figure 6.16 - Urethane rubber mesh and correspondent US image of the same location.

From these results it is possible to confirm that this material is not US compatible and thus it will be discarded from further analysis.

- PVCP

PVCP was compared with both the PVCP phantom and the arm, so that its compatibility could be clearly assured. PVCP was not 3D printed and thus it needed to be fabricated according to the protocol explained in the Appendix C.

Control: Phantom and arm

For the phantom, Figure 6.7 was used for comparison as the experiment was conducted in the same trial. The section of the human arm is seen in Figure 6.17.

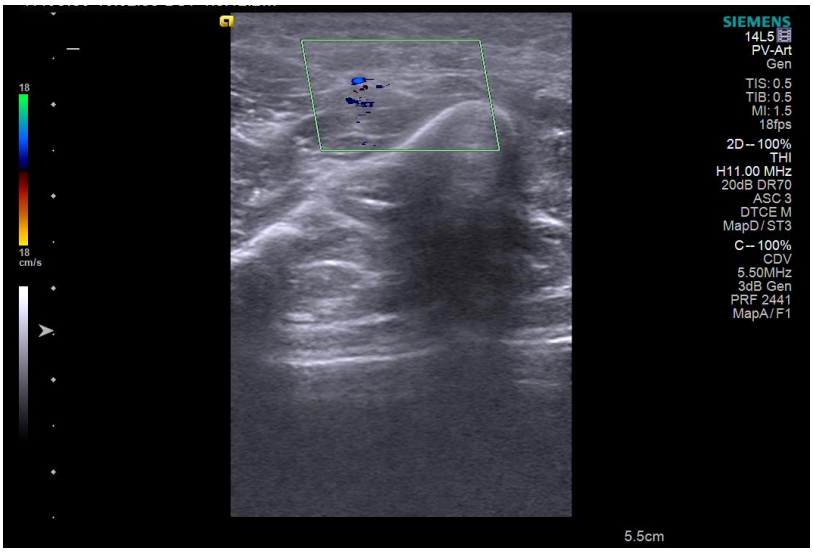

Figure 6.17 – Cross-sectional view of a human arm with an identifiable vessel.

Material: PVCP mesh with 1 mm of thickness

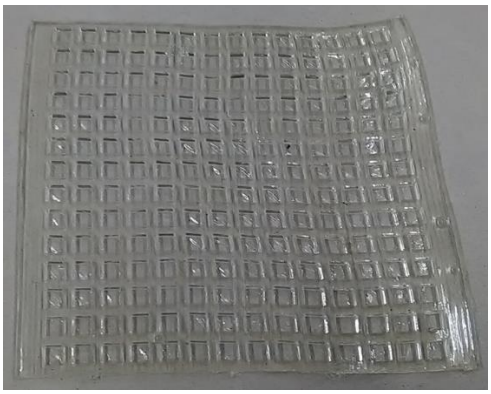

Figure 6.18 - PVCP mesh, 1 mm thick.

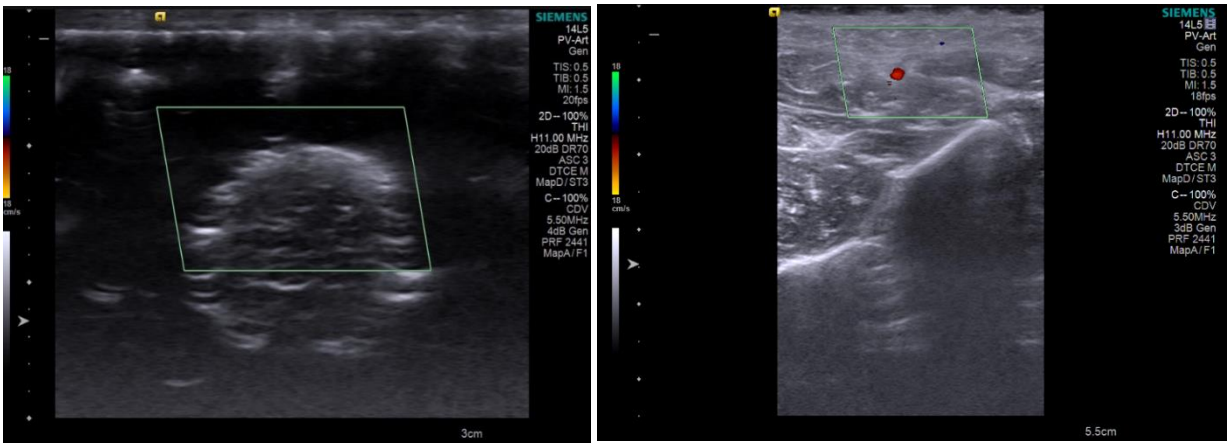

Figure 6.19 - US images respective to the both setups (left- phantom, right- arm).

The results observed in Figure 6.19 seem to prove US compatibility, as both images are very similar to the control. Nonetheless, it possible to observed a "chess"-like pattern on the top of each US image, which is the region where the mesh is located, where it seems that the mesh might not be clearly US transparent and perhaps the way PVC affects the image quality is just not shown given the thickness of the sample.

In order to understand the influence that might be caused by the mesh's thickness on the image quality and to ensure that that indeed PVC is US compatible, a few more trials were conducted, both with meshes of different thicknesses (see Figure 6.20) and with a normal squared sample of PVC (see Figure 6.21).

Figure 6.20 - PVC meshes with different thicknesses. From left to right, 3 mm, 2 mm and 3.5 mm, respectively.

Figure 6.21 - Squared sample of PVCP

Since these next trials are conducted at a different time, a control for each case is presented.

Control: Arm

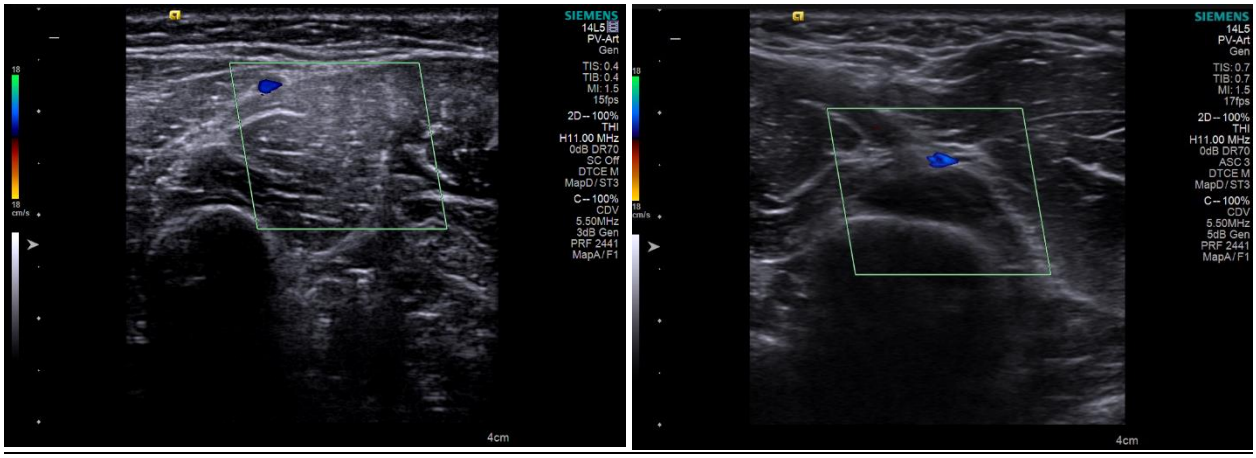

Figure 6.22 – Cross-sectional view of the arm used as control for thickness (left) and normal sample (right).

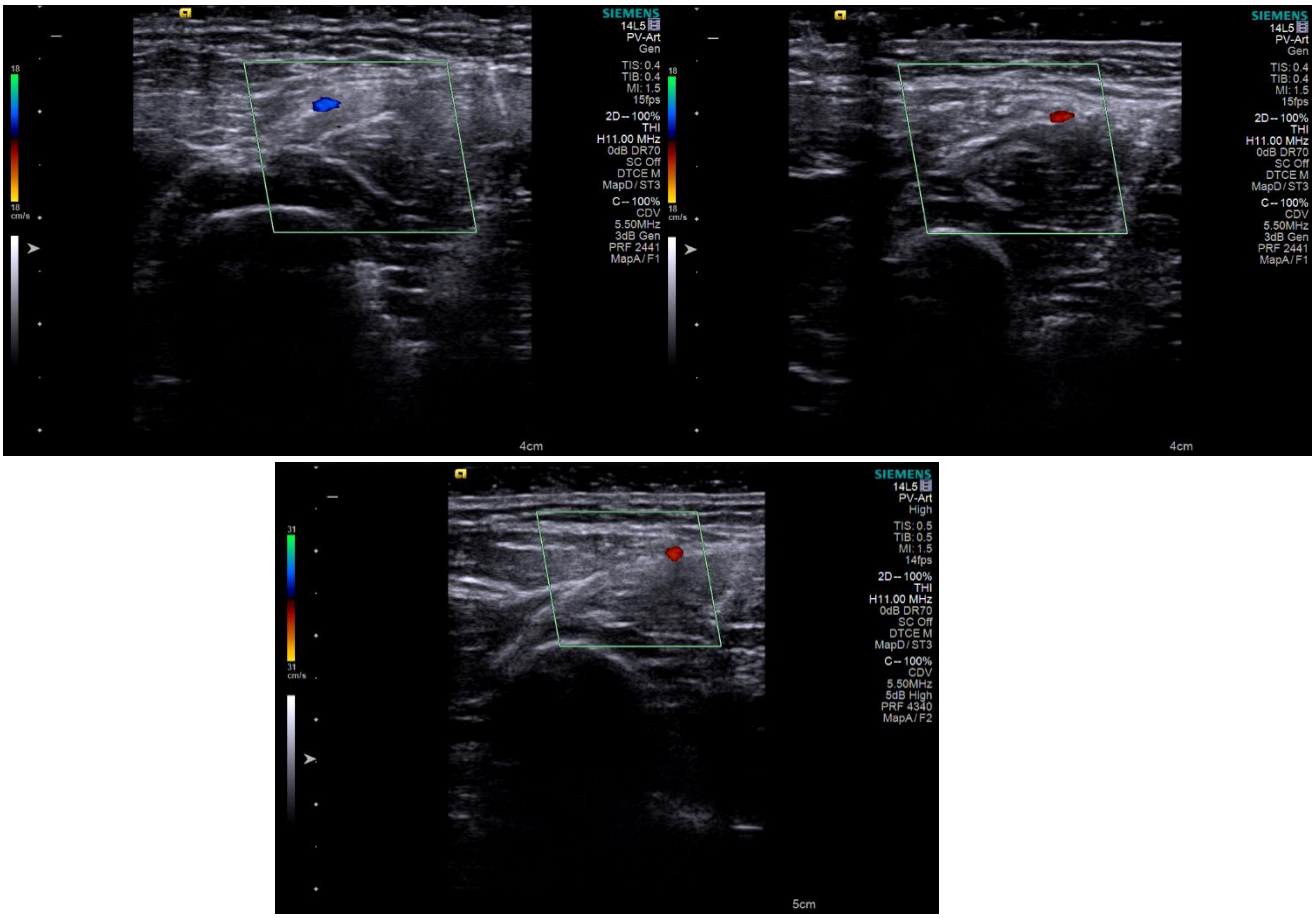

Figure 6.23 - US image of PVC meshes with different thicknesses: 0.2 cm (top left), 0.3 cm (top right), 0.35 cm (bottom)

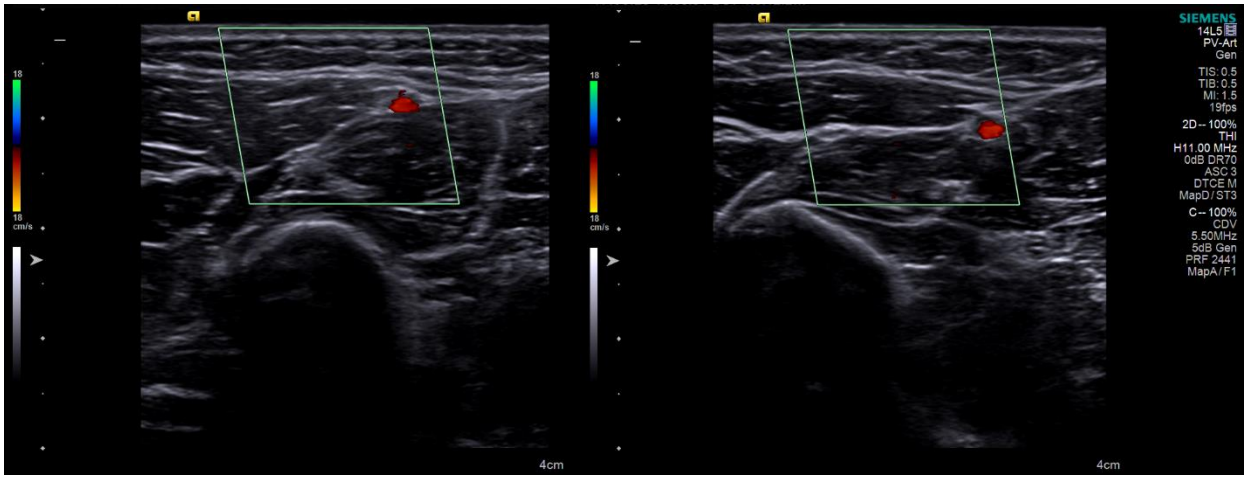

Figure 6.24 - US images of PVC squared samples, fabricated at different pressures (left - room pressure, right- 200 mbar)

Evaluating the effect of thickness, through Figure 6.23, the overall image quality is maintained, though there seems to be a slight effect of signal attenuation with tissue depth. However, the shadowing effect observed in 0.3 cm mesh occurred occasionally in all the meshes is similar to the one observed for TangoBlack, which was not helpful to validate the hypothesis of US compatibility. Nevertheless, the analysis of Figure 6.24 confirmed that PVC is US compatible as the differences between control and

sample are negligible. Here, an additional parameter (reduced pressure) was added to testing in the fabrication method, to ensure that the pressure at which the sample is created does not alter the compatibility properties of the structure. The presence of a shadowing effect was then attributed to the lack of gel inside the mesh holes which allowed for the existence of air in the medium, due to its viscous consistency that made it harder to evenly spread it throughout the mesh.

SUMMARY

After all the testing conducted above, it was only possible to ensure the US compatibility of PVCP, while all the other materials tested were not able to achieve the level of image quality required.

6.2 STRETCH TEST

The stretch test is created as a proof of concept for the support test. The goal is to examine if a smaller portion of structure can handle a larger force than the one it will have to support in the real life scenario. As mentioned in section 5.4, it was assumed that on average the weight of a breast would be approximately 500 gr though this is not valid for very larges breasts. The breast phantoms used in these experiments have a weight > 500 gr. Nevertheless, this mesh is about 3 to 4 times smaller than the actual size of the final breast holder, to if it able to support 500 gr it will seems reasonable to extrapolate that the whole mesh will be able to support heavier breasts.

Additionally, this experiment admitted only forces exerted in a vertical direction, thus assuming that the forces the breast will exert on breast holder in a horizontal direction (assuming the base of the breast in prone position as reference frame) are negligible, which is not true, though they are expected to be much smaller that the forces exerted because of gravity.

Taking Newton's second law of motion, expressed in equation 6.1, the force applied in this test was of approximately 5N in y, considering the referential in Figure 6.25.

$$\overrightarrow{|F|} = m \times \vec{a} = 0.5 \times \begin{bmatrix} 0 \\ 9.8 \end{bmatrix} = \begin{bmatrix} 0 \\ 4.9 \end{bmatrix} [N] \quad \textbf{(6.1)}$$

SETUP

To execute this test without intentional damage to the structure, the mesh was attached to a handle on both sides to which, on one of the sides, a weight of 500 gr was connected and the other was connected to the support. The test is executed for 5h (to simulate the amount of time of the procedure) during which the mesh is suspended to suffer only the effects of the weight.

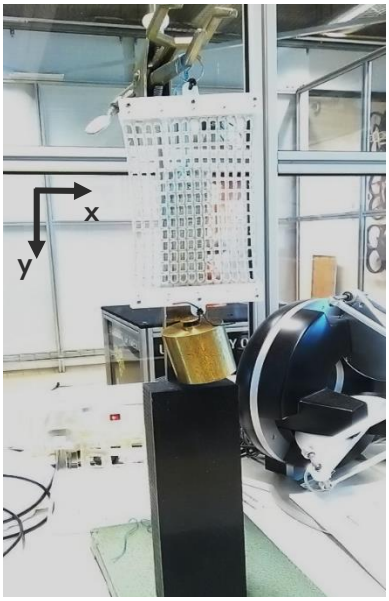

Figure 6.25 - Setup for the stretch test.

RESULTS

This procedure was executed for several types of meshes with different properties, namely, hole size and shape and thickness of the mesh, to adjust which properties provide better support, as seen in Figure 6.26, Figure 6.27, Figure 6.28, respectively. Eventually, it was understood that the material used for the production of the first set of meshes, LUPA Plastisol Medium, did not provide enough stiffness to the structure and regardless of the changes, the material kept tearing. There were two viable options at this point: increase the thickness to above 5 mm or find a version of PVC that would be more rigid.

Since the US penetration depth is reduced with the length travelled by the signal and the attenuation rate of PVC is not null, this option was discarded. PVC meshes starting being fabricated with Plastileurre Super Rigide (which was also successfully tested for US), since the previous manufacturer did not offer an adequate option. It was possible to conduct successful tests with this new material while not compromising the thickness. The minimal thickness a mesh can have is 3mm, though this is at the limit of stretch.

The attempt to change the hole shape did not seem to provide a great advantage to the structural resistance to stretch of the mesh, while it reduced significantly the area available for needle biopsy, thus this alteration was not recommended. Similarly, by increasing the size of the squares while also increasing the space between the squares to strengthen the structure while keeping the thickness at 2mm did not show significant improvement.

Ideal mesh: 0.35 cm thick with squared holes of 4x4mm

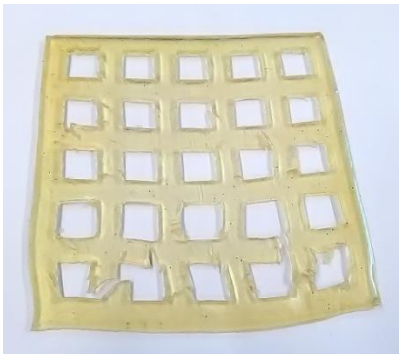

Figure 6.26 - Alternative mesh with hole size of 10x10mm and 5mm separating holes.

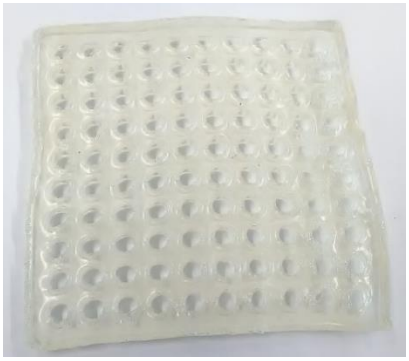

Figure 6.27 - Alternative mesh with circular holes with 2mm radius

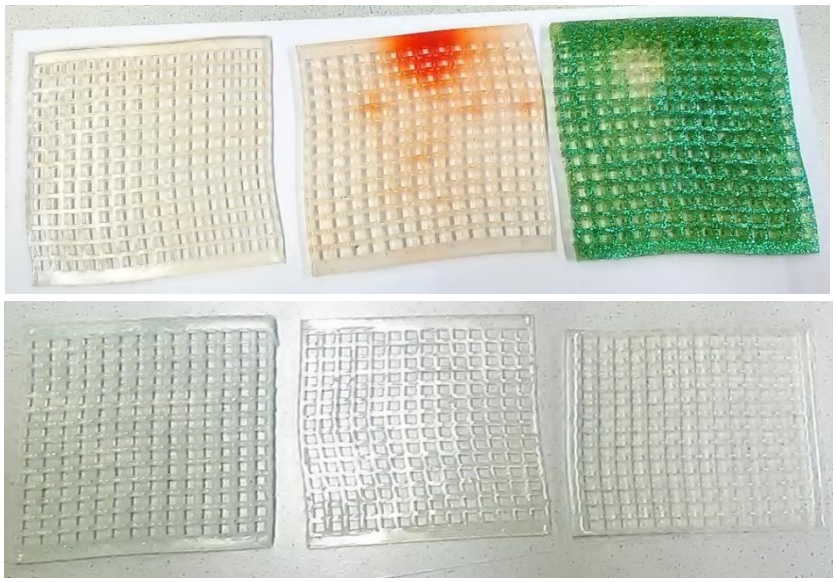

Figure 6.28 - Meshes with different thickness made out of Plastisol Medium (up) and made out of Plastileurre Super Rigide (down).

6.3 CONNECTOR TEST

The connector test uses the same principle and setup the stretch test for the structure that needs sustain the openings of the breast holder together. However, here the vertical direction where the force is being applied will actually be representative of the horizontal direction if it is applied to the same

reference as before, since the forces exerted on the connector are now on the plane of the breast surface. Again, the connector will be suspended during 5 hours only under the effect of the 4.9N force.

SETUP

Figure 6.29 - Setup used for the connector test. The connecting structure is the grey one. The referential orientation is maintained as in figure 6.25.

RESULTS

A lot of connectors were attempted, but only two of them were able to support the 500 gr weight without causing the mesh to tear. All the connectors experimented can be found in the Appendix E, including more specific details about the selected ones. The decision between the two came down to which one would be able to become a single-pillar connector instead of a double pillar, as this is seen as an advantage to be able to adjust the mesh size. This connector can be made into the shape of the mesh's holes and once used to close the breast holder on the breast, the exact place where to connect the holder can be adjustable to actual breast. The material used to make the connectors was a combination of VeroWhite and TangoBlack, RGD8530, which means that it is mainly a rigid structure though it has some flexibility to adapt to the phantom's surface.

In addition, the connector is made out of a flexible material which makes it adaptable to curvy surface of the breast (to a certain extent).

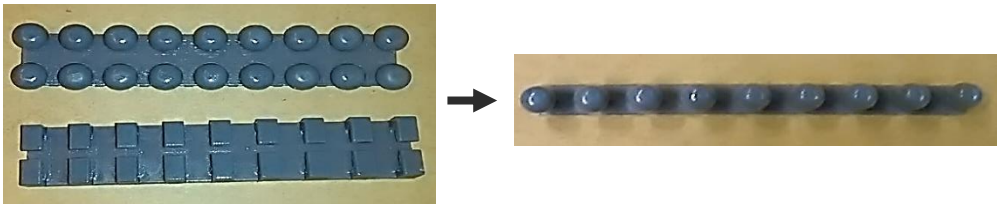

Figure 6.30 - Two successful connecting structures (left): push button and hook. On the left there is the single pillar connector idealized.

6.4 SUPPORT TEST

The goal of the support test is to ensure that the breast holder can support the weight of the breast, now applying forces on all the 3 directions, without tearing. To confirm the durability of both the mesh and the connector after a 5h period. Only complete holders can make it to this step.

SETUP

The setup involves a support that could simulate prone position of the breast was laser cut and assembled. The breast phantom with the breast holder on is put through the circular opening, while left hanging. The breast phantom used for this experiment was rather dense, thus it weight is estimated around 800 – 900 gr.

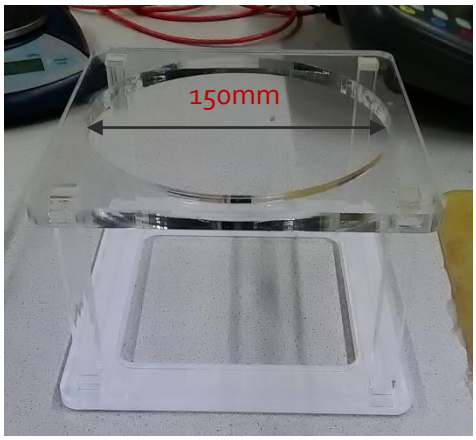

Figure 6.31 - Setup used for the support test

RESULTS

The final breast holder designed was successful in this test, since there was no observable damage to the breast holder in response to the stress applied.

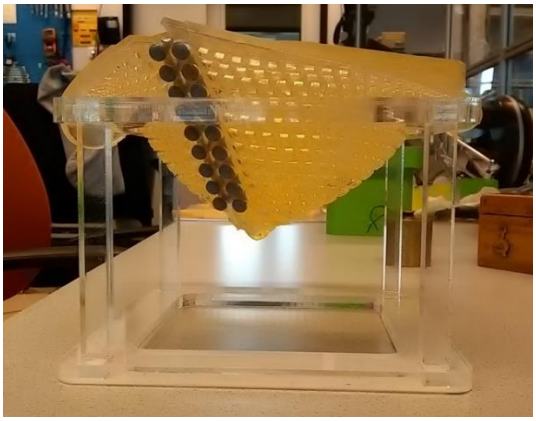

Figure 6.32 - Breast holder enduring the breast phantom's weight and distension.

The next step in the experimental process is the attempt to validate the designed conceived. In order to do this, there are some parameters that can be looked into by analysing the change it introduces to the performance of the trajectory developed in chapter 4 and by understanding its behaviour under deformation. So that the concept could be successful, it would be expected that the changes introduced to the trajectory translate into minimal differences when compared to normal trajectory and do not compromise the imaging acquisition quality. Additionally, the results of the deformation test should reveal a larger stiffness in the presence of the breast holder as this means that the breast holder is capable to counteract the effect induced by the transducer once it's deforming the tissue.

For the next experiments, the overall setup (visible in Figure 6.33 used is rather similar, though for specific types of testing some elements are introduced, namely, a webcam for tracking experiments (with the respective markers) and an US machine for the experiments that evaluate image quality (with a specifically designed 3D printed end-effector to fit the US transducer). The manipulator is the same as in Figure 4.2 and the breast phantom is the one seen in Figure 6.15. This phantom is made out PVCP and its fabrication protocol can be found in Appendix C.

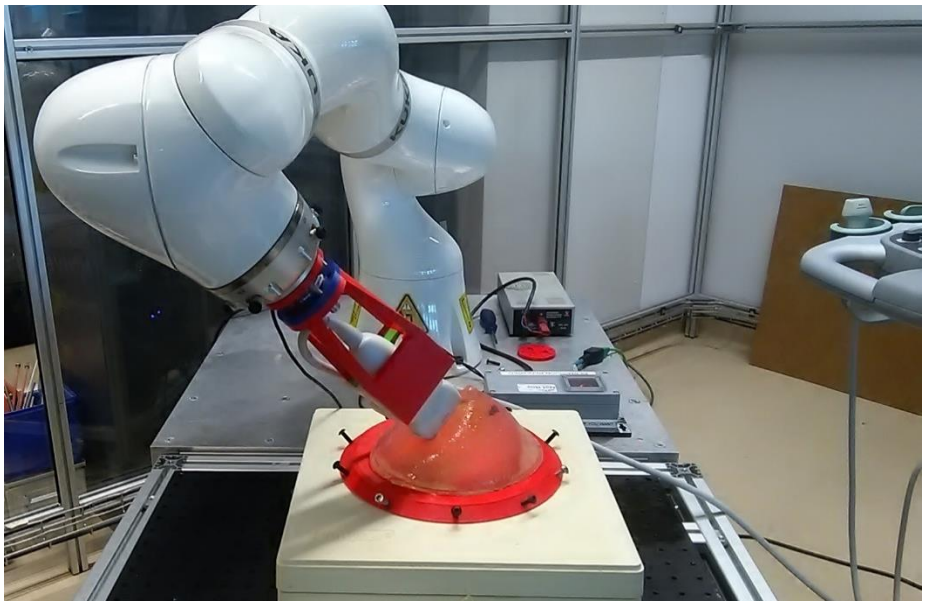

Figure 6.33 - Setup used for the ultrasound trajectory test. The external force-torque sensor is located in between the manipulator and a 3D printed end-effector.

The introduction of an external force-torque sensor was done to have a comparison term to the force sensors present in the iiwa manipulator, since the knowledge on the actual sensitivity of these sensors is not well-documented. This problem is aggravated by the fact that there is not a clear way to move the manipulator using Sunrise without having to associate it to a specific frame. The motion is always associated with position and not force, as it is not possible, to the best of the author's knowledge, to set a specific force for the robot to move with. Thus, the analysis conducted is based on the evaluation of how the forces change in specific regions of interest.

The external force used has been a part of other experiments in MURAB and so there is proof of concept that it provides accurate measurements for such a setup. Hence, the start point of the validation analysis is to understand the reliability of the LBR's sensors. Nonetheless, a previous master assignment

had to rely on an external force sensor since the sensors of the LWR4+ were not accurate enough for the required measurements [46], thus it will not be surprising if these sensors are not sensitive for the purpose of the work to be developed here.

6.5 FORCE SENSOR ANALYSIS

As mentioned, the goal of this test is understanding if the behaviour of the robot's internal sensors provide a similar response as the external force-torque sensor.

Since the forces involved in this motion will be evaluated, an external six degrees-of-freedom force-torque sensor (ATI mini 40 – ATI Industrial Automation Inc., Apex, NC, USA), seen in Figure 6.34, was introduced to the system. The force response is analysed both by using the force-torque sensors of the robot and the external force-torque sensor to be more accurate when assessing the results. The force-torque sensor is incorporated into the end-effector, in between the manipulator and the 3D printed transducer. The ATI mini40 is connected to a NetBox and a signal generator. The force-torque sensor data is recorded through an interface provided by ATI but an incorporation of the force-sensor data into the Sunrise application was not possible to be implemented during the time of this thesis. This force sensor has a resolution of 1/100 N for forces and 1/8000 Nm for torques. The sample rate of the external force-torque sensor is 20 milliseconds (50 frames per second) while the LBR force-torque sensor is collecting data at each 10 milliseconds (100 frames per second). Both sensors measure the external force-torque.

Figure 6.34 - 6 DOF force-torque sensor, ATI mini40

This experiment is the foundation for the next steps, thus it was conducted for the 3 types of trials that will be evaluated further on:

- Circular trajectory around the breast phantom's surface – impedance control
- Linear deformation of the phantom's surface – large displacement
- Linear deformation of the phantom's surface – small displacement

All these trajectories are compared against the response of the robot if the phantom is removed from the setup.

RESULTS

Each set of experiments (with phantom vs. without phantom) had 5 trials. The frame of the end-effector (where the robot's sensors are measuring) of the manipulator and the frame of the external are not correspondent, as seen in Figure 6.35 , so it was necessary to do a transformation in order to have data that would be comparable. This transformation is described in the Appendix F.

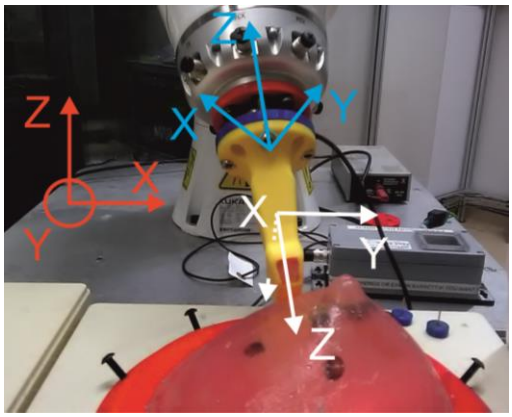

Figure 6.35 - Frame system present in this experiment. The white frame is actually located at the tip of the transducer though it was drawn like this to simplify the understanding of the figure. Red - base frame of the robot; Blue - frame of the external force-torque sensor; White - frame of the end-effector

Circular Trajectory

The end-effector used for this experiment is the one present in Figure 6.33 and not the one used during the implementation stage (Figure 4.2), to be able to encompass the US transducer. Therefore, its size changed considerably. A larger end-effector caused many constraints in the workspace which meant that the trajectory algorithm used initially no longer was able to generate joint positions able to conduct this motion. For this reason, the trajectory was set manually with 4 different frames describing almost half the trajectory. In terms of the validity of the results, nothing will be affected since the impedance controller is still the same and the trajectory described is merely a part of the complete circle but has the same properties in terms of direction changes, surface contact and transducer orientation (to some extent).

Without going into detail about the forces during the motion taking into account the direction of motion, as that analysis is more related to next test, what can be observed is that for the majority of the motion the response of the LBR sensors is different in the event where the phantom is present from the situation where it is not there. The ideal situation is that this difference is very similar to change in forces observed by the external force sensor as that means that the additional absolute force value comes from the existent noise but the change introduced by the presence of the obstacle can be accurately detected. While in Z this seems to be the case, in X and Y despite the response being different in terms of magnitude between the two scenarios, it is not coincident with the times where the force sensor actually detects force changes. Since the magnitudes of the forces in these two directions are quite smaller than the ones observed in Z, it seems to indicate that the LBR is not very sensitive in detecting changes that are smaller than 1 N. Nevertheless, these results will be investigated further with the next trajectories.

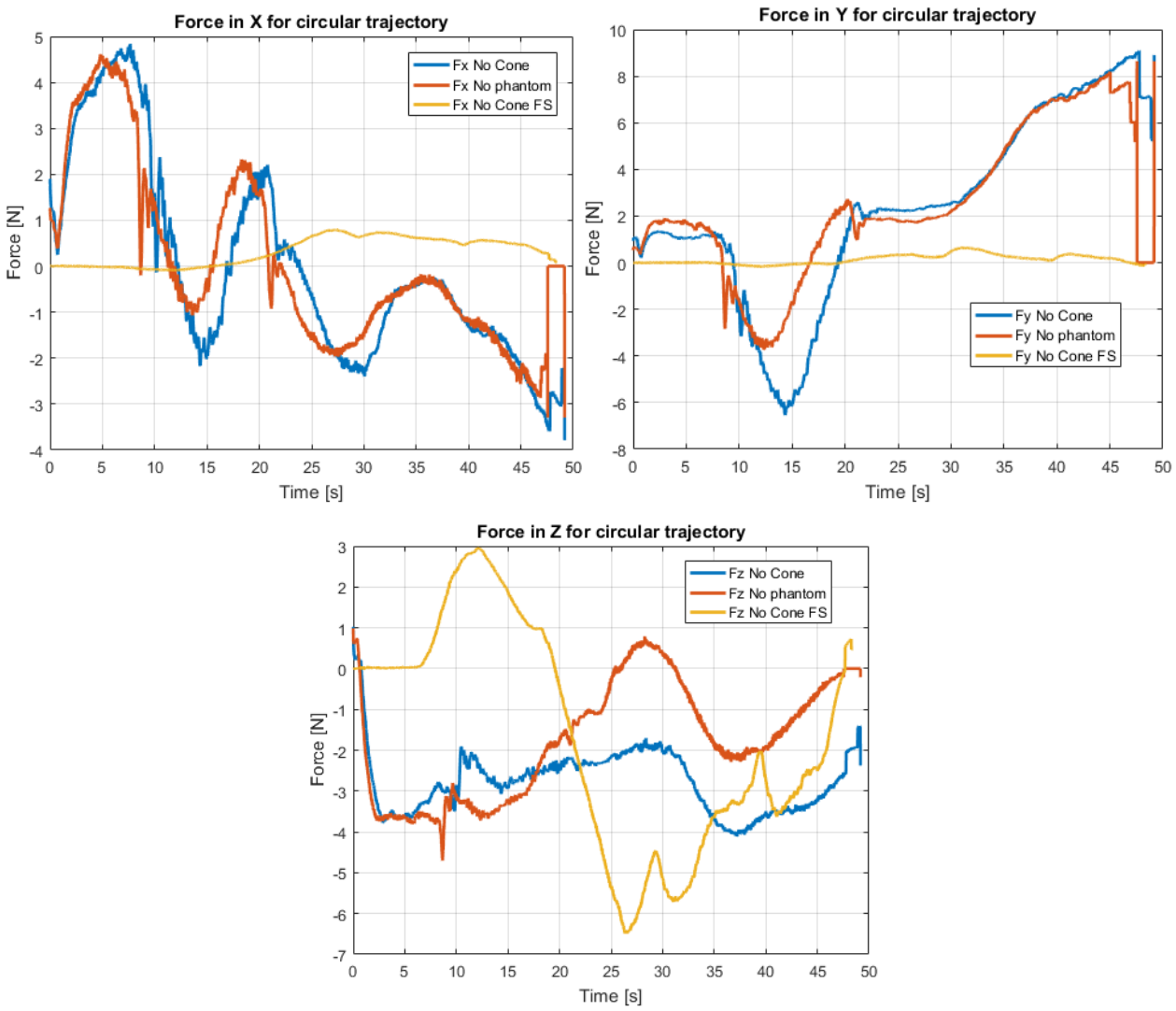

Figure 6.36 - Average force during the circular trajectory with the presence of the phantom (blue and yellow) and without it (red)

Linear Trajectory

The linear trajectory is conducted purely through position, describing a motion from a frame A to a frame B (and then back to frame A). These positions are set manually, thus, it is possible to decide on the amount of displacement desired by setting the frame B deeper into the phantom. M1 designates the trajectory with a small displacement while M2 designates the trajectory with a larger displacement. In both cases, the end effector moves in its Z (+) direction so it is expected to observe a larger force difference in this direction than all the others. For this trajectory there is a specific region of interest where the transducer is touching the marker until it reaches the point of maximum displacement (frame B). For M1, this region is defined by the interval [22, 30] s while for M2, this region is [17, 22] s approximately.

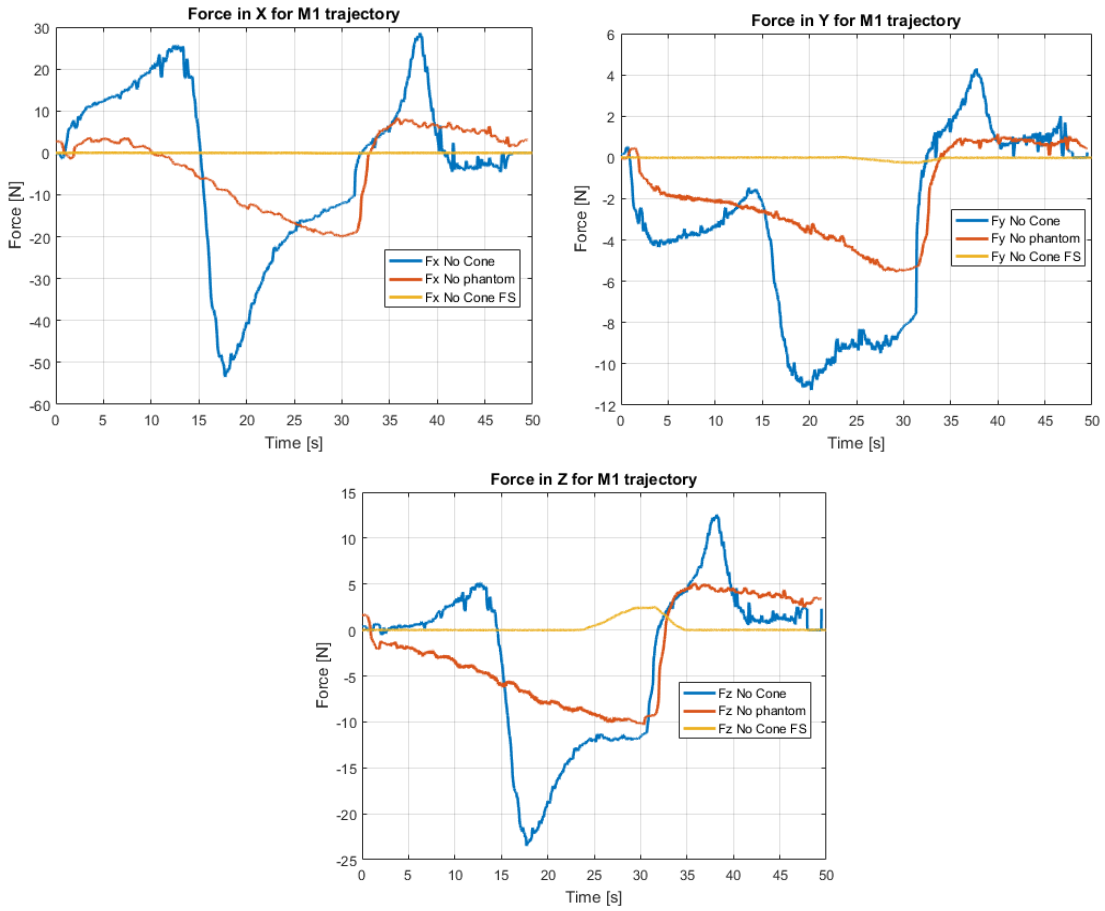

Figure 6.37 - Average force in each direction detected by the LBR (blue), by the ATI (yellow) and by the LBR without phantom (red) for M1 (small displacement).

Once more the overall response is not discussed here but the how the behaviour changed with the presence of the phantom. M1 is the motion related with a smaller displacement, thus smaller forces are involved. Despite the fact that there seems to be a mismatch between the forces detected by the force sensor, it is possible to distinguish a different response with and without the phantom, which is helpful to conclude that the response observed is not just a result of noise of the robot. Thus, once more the results seem to reinforce the idea that the LBR's sensitivity is not very good for small forces, so for M1, the analysis will be conducted taking into account the force results of the ATI sensor.

M2, on the other hand, involves a larger displacement of the phantom's surface which the robot seems to be able to detect more accurately (the exception being X direction), especially in Z which is the main direction of the motion, which can be seen in Figure 6.38. However, even if the deformation motion can be distinguished, the change added by the presence of the breast holder may not be very pronounced. For this reason, it was decided to not use the data from the LBR sensors to evaluate the deformation experiments.

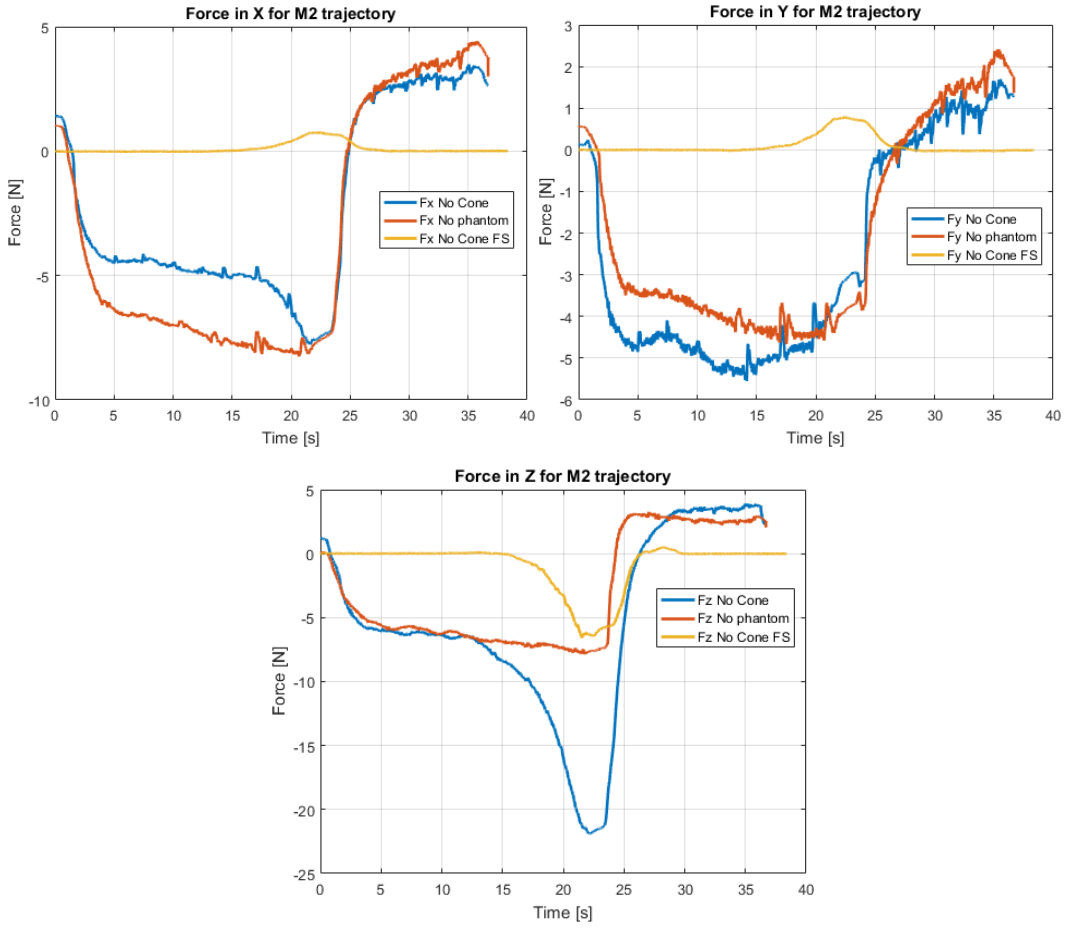

Figure 6.38 - Average force in each direction detected by the LBR (blue), by the ATI (yellow) and by the LBR without phantom (red) for M1 (small displacement).

Nevertheless, it is relevant to note that for experiments where force feedback would be required, the amount of noise introduced by the robot during motion where there is no surface contact will probably compromise the robot's response.

6.6 TRAJECTORY TEST

After obtaining a testable complete design it is necessary to test it in a setting where an US scan will be simulated, to understand if the design can handle the pressures exerted during such a scan without tearing but also to see if it causes problems to the trajectory. These could be, for example, the presence of friction to the motion so much that the transducer will not be able to conduct the scan or causing too much discomfort to the patient since friction is a result of the increase of the shear forces of the movement. The aim of pairing the KUKA with the US machine is to test whether or not the created design does not compromise the quality of the image, thus allowing for appropriate image acquisition, even if the material was already cleared as US compatible.

In order to assess this, the idea is to compare the behaviour of the transducer performing a scan with the presence of the breast holder and without it. The forces will be measured for evaluation to add to the visual feedback of the breast holder's response to pressure, on whether or not it can sustain it

without tearing. Analysing the forces allows for an understanding of their distribution throughout the trajectory and possibly identify shear forces introduced by the presence of the breast holder. In any case, the breast represents an obstacle in the goal of the impedance controller to reach the final position, thus, regardless of its stiffness, the forces should be larger. The stiffness of the impedance controller is maintained at 450N/m since changing would also introduce changes in the final position the manipulator will be able to reach at each frame. Furthermore, there is no term of comparison to know the best motion characteristics, the only possible evaluation is whether or not the stiffness used is sufficient to keep contact with the surface while providing a compliant response, which is verified.

SETUP

This experiment is conducted by placing the breast holder over the breast phantom (the same phantom as in Figure 6.15) and using the trajectory implemented in chapter 4 to simulate a US scan over the breast phantom. This trajectory was planned for a breast in supine position instead of prone so it was necessary to create a setup that allowed for the simulation of stretching of the breast holder or else it would not be able to generate the effect it was planned to have once holding the breast. Thus, the breast phantom is placed over a 3D printed base plate with screws on the lateral surface where the holes of the breast holder can be pushed into, allowing the possibility to adjust the stretching to the desired level. This plate is inserted into the base of the setup to assure that the phantom is kept in the same position throughout the motion. To conduct this experiment the US system ACUSON S3000 (in Figure 6.1) was re-used as well as the same transducer. As mentioned in section 6.5, it was necessary to design a holder for the transducer, which meant that the end-effector was changed. The planned positions had to be re-adjusted to this new addition in length.

It is important to mention that the breast phantom is made considering the possibility of US scanning its surface and so it has a small amount of detectable objects under the US.

The complete setup used for this experiment can be seen in Figure 6.33.

RESULTS

The variables tested here will be:

- Presence of the breast holder on the trajectory
- Image quality

To compare the actual breast holder behaviour it is relevant to look into the forces in each direction as if they follow the direction of the motion it can provide a more accurate interpretation of the results, especially in the presence of shear forces. In an attempt to minimize the friction, the surface of the phantom (and also the surface of the breast holder) was covered with US gel.

The end-effector starts moving in its Z(+) direction towards the breast phantom but also downwards (thus in X(+)), making contact with it and from there it starts moving mainly in Y(-), though some positions are set deeper into the breast's surface (which causes a shift in Z) and sometimes also slightly lower or upper (though causing a shift in X). Figure 6.42 gives a clearer picture of what the trajectory looks like facilitating the interpretation of the results. The contact with the breast phantom is achieved roughly 5 seconds after the start. For the sake of simplicity the breast holder is referred to as "cone" in the legend of the plots.

Observing the data in Figure 6.39, the response of the average forces measured by the LBR sensors seems to follow a very similar pattern for both the scenarios in study, though the forces between the "cone" vs "no cone" never seem to vary more than 2 N from each other. This is also the case for the external force sensors, except when it comes for the forces exerted in Z, where there is a very big difference between the two situations being tested.

To make sure that this big difference was not being introduced by the analysis being conducted only taking into account the average force of the 5 trials, Figure 6.40 shows what is the difference between the maximum force obtained and the average force so that it can be understood if there was a big error in only observing the average response. It was possible to conclude that the deviations were not large enough to make a difference and thus it was decided to base the conclusions for this trajectory taking only into account the response of the ATI mini40 force sensor, since its sensitivity is reliable.

Given the fact that the motion is conducted with impedance control, by adding another obstacle into the motion (even if the stiffness was exactly the same), it would be expected that the forces would increase since now it will be more difficult to reach the final position, though not a lot given the compliance of the robot and the small thickness of the breast holder. However, the effect of the thickness should be only considered in the Z direction where this increase occurs and the robot is compliant. This seems to be the explanation for the first 22.5 s of the motion (after the contact has been made). Nevertheless, after this instant an increase in the forces is verified in all the directions, particularly in Z. A reason for this large increase could be because the frame the manipulator is trying to reach is located deeper into the phantom which will require now a larger force to reach. In any case this increase is already present in the "no cone" result. So, other options will be considered.

In X, the increase should be the result of shear forces created by the breast holder since it is the direction perpendicular to the direction of motion that is along the phantom's surface. Additionally, this area of the trajectory represents a significant rotation around the X axis of the transducer to continue perpendicular to the surface, meaning that the increase of the force can also be justified by the torque created here.

In Y, the response should also be a result of shear forces as well since there is also motion in Z direction that is now more pronounced. Z seems to be direction that feels the effect of the breast holder the most and it should be because of the resistance to motion that was observed around this time of the trajectory to the transducer and prevents it from moving smoothly and the breast holder is "dragged" by the transducer. However, this does seem to provide some insight to the amount of forces that this breast holder is able to handle as it appears that a force increase of around 7N (registered in the motion without the breast holder around [20,25] s) in the Z direction will cause a significant shear stress in Y, increasing the friction between the two surfaces and causing this "dragging" effect. At this stage, it was also verified that the transducer was slightly slowed by this dragging effect. There are some things that could help minimize this effect that do not need to be necessarily related with the breast holder's presence itself: usage of more US gel to smoothen the trajectory and applying it every time between trials, or increase the stretch of the breast holder, as whenever the breast holder is not stretched sufficiently, it will just be pulled by transducer with its motion.

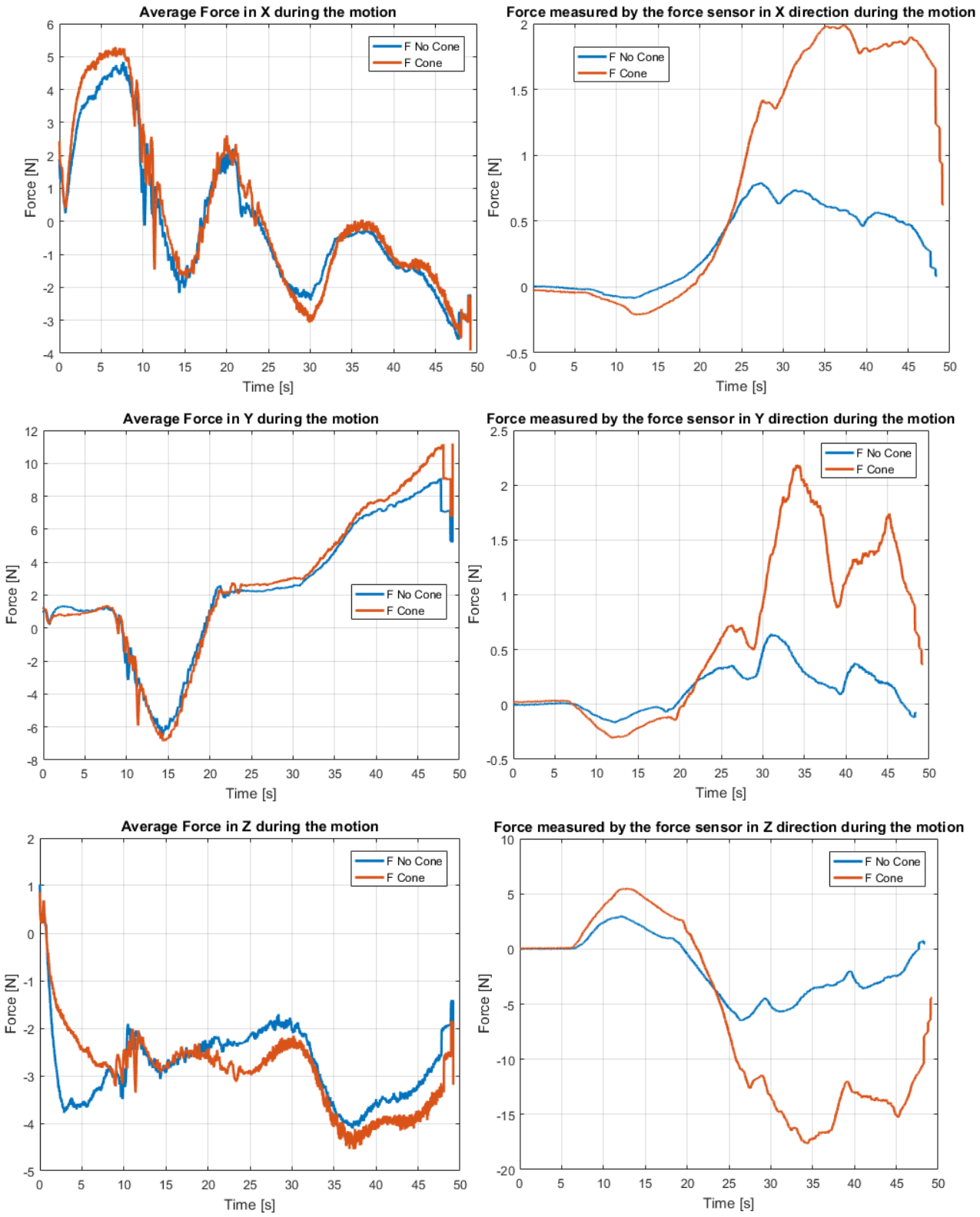

Figure 6.39 – Average force measurements during the described motion in each of the 3 directions. The plots on the left column represent the sensors from the LBR iiwa, while the ones on the right come from the external force sensor.

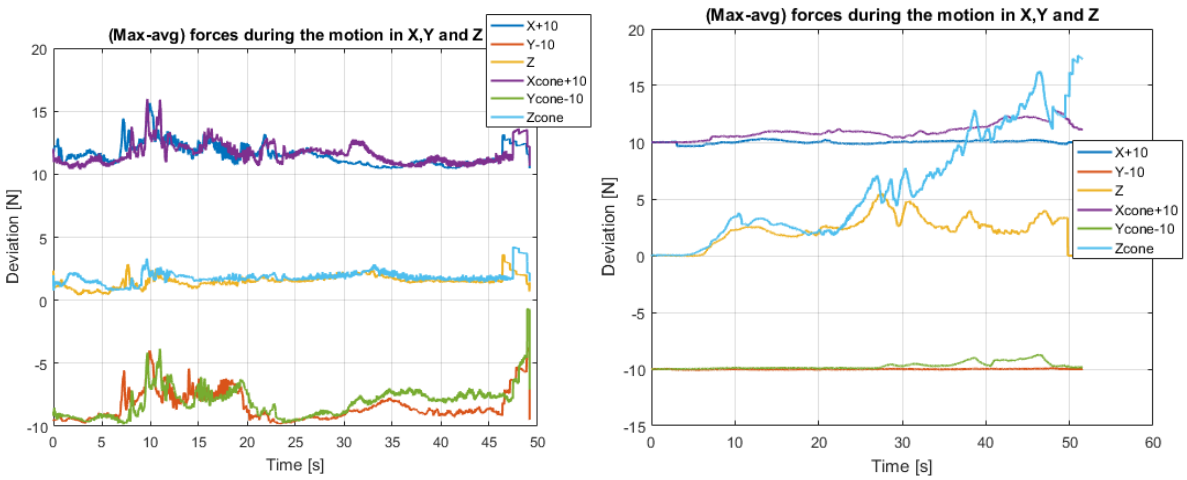

Figure 6.40 - Difference between the maximum and the average value to understand if there is a considerable error in focusing the analysis in the average response. The X and Y data are shifter by +10 and -10 units, respectively so that all the plots can be observed simultaneously.

Nevertheless, the magnitude of these forces is worrying as they would cause patient discomfort, thus despite the breast holder not preventing the motion from being conducted, the force response is not yet ideal. These forces were so intense that in certain areas, the breast holder suffered localized tearing, though this did not compromise the integrity of the whole structure and it only happened after the motion had been conducted more than once.

This could be tackled by adjusting the parameters mentioned in the previous paragraph or the frames should be set differently: not very deep into the surface but enough to assure contact. Additionally, Sunrise has class type called "Force Condition" which allows to add a specific motion the possibility of breaking or stopping completely if this condition is verified, so this could be an option to add a "ceiling" to the maximum force that can be exerted, though this was not done here as the goal was to find out exactly if these sensors can fit the purposes of MURAB or if it would be better to incorporate other alternatives so there were no force restrictions.

As for the US results, the control is an image of the breast phantom without the breast holder. Despite the fact that the whole motion is conducted, since the only way to evaluate this test is through visual comparison of two variables (with vs. without breast holder), the results presented are judged based on images collected during this motion where it was possible to analyse the lesions.

Nonetheless, these phantoms are made with an external layer that is supposed to mimic the skin which can become detached from the inner surface if it under a reasonable amount of pressure. This means that there is the possibility of encountering air space in between these two layers, which can contribute as artifacts and also made it more difficult to clearly localize the obstructions.

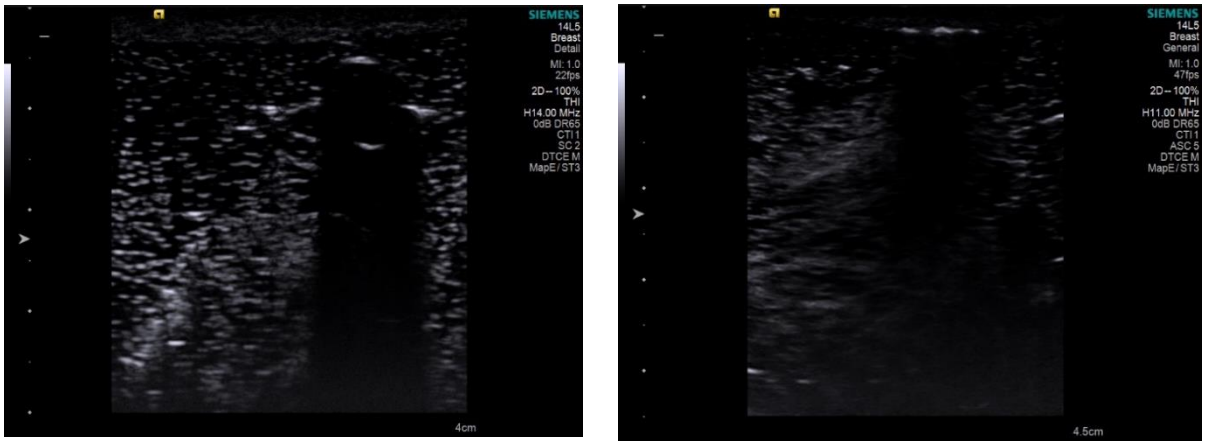

Figure 6.41 -US image of one of the breast phantom's lesions without (left) and with (right) the breast holder.

In both cases it is still possible to identify the lesion, though the presence of the breast holder does generate an image that is darker, diminishing the overall quality of the US. Nevertheless, it is important to mention that detecting a lesion even without the breast holder was a rather difficult task, so a breast phantom with more lesions or without the skin layer could perhaps facilitate this task. Additionally, comparing this image to Figure 6.16 obtained for polyurethane, the quality is much better.

To confirm that, not only that trajectory is as expected and that having a smaller trajectory is still valid for such a study, Figure 6.42 presents the trajectory conducted by the end-effector on both cases.

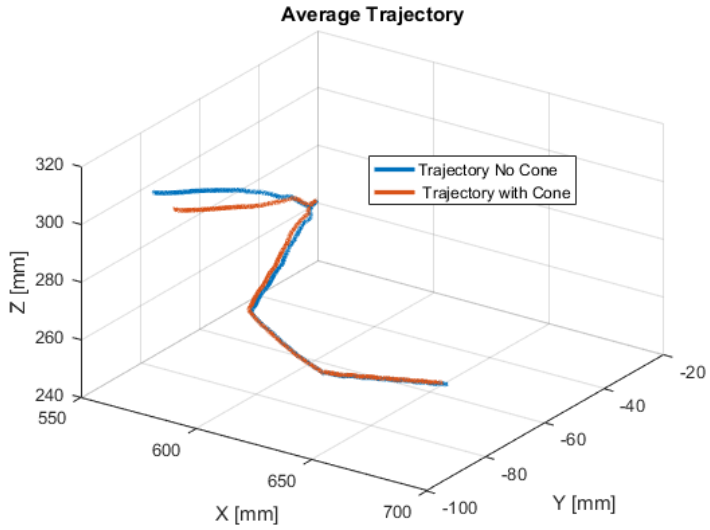

Figure 6.42 - Trajectory conducted by the end-effector to conduct this test. The trajectory starts on the highest values of Z and lowest of X.

6.7 DEFORMATION TEST

The breast holder aims to reduce the deformation suffered by the breast during US scan caused by the transducer's motion. However, evaluating this during an ongoing trajectory is rather complicated as the local deformation at every instant is hard to identify given the continuity of the motion. Thus, in order to clearly observe the effect of the breast holder in the deformation of the breast, the experiment was simplified: a linear motion, parallel to the contacting surface, with and without the breast holder. Since initiating a force controlled motion is not available with Sunrise, the motion evaluated here is purely position based with a high stiffness in all the directions. The results are evaluated through force changes.

With a position motion, since the position is kept exactly the same, if the forces are larger (i.e. more force is required to reach the desired position) when the breast holder is present that means that the overall stiffness of the system has increased and that it is opposing the motion. Thus, on a motion where the forces would be constant (as expected for MURAB), the transducer would penetrate less into the surface of the actual breast and the deformation would be reduced.

It is important to note that the position information is measured in relation to the base frame of the robot.

SETUP

In order to perform this experiment, the following materials were added, slightly changing the setup to what can be seen in Figure 6.44:

- 3D Printed Markers seen in Figure 6.43
- Webcam, Logitech HD Pro Webcam C920 (Logitech Europe S.A, Switzerland) seen in Figure 6.43

The linear motion is executed in between two manually set frames such that the end-effector moves only its (+) Z direction (on its own frame), from a start point A, away from the phantom but parallel to the breast surface, to a point B, also parallel to the breast surface, located a few centimetres inside the breast phantom. In relation to the base frame of the robot, the motion is conducted in the (+) X and (-) Z directions. Two different locations of the breast phantom were selected to evaluate the behaviour of different regions and exclude the possibility of the deformation behaviour analysed being only a consequence of the location, so for each location the behaviour of the two markers is taken into account. Only two locations were selected given the similarities of the breast phantom surface's shape and the size of the transducer used being too large, not being able to conduct the motions without touching one of the other markers.

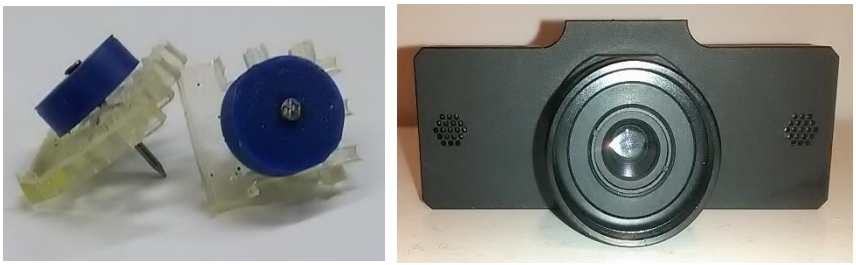

Figure 6.43 - New materials added to the setup. From left to right: Markers and Webcam.

The position response is evaluated by both the position sensors of the robot and a Webcam responsible for tracking the position of the markers seen in Figure 6.43. In order to detect the markers, a MATLAB algorithm was implemented and the code behind it can be found in the Appendix B. The usage of the Webcam was introduced to be able to evaluate how the two markers affect each other, as the robot's sensors can only provide the position of the end-effector.

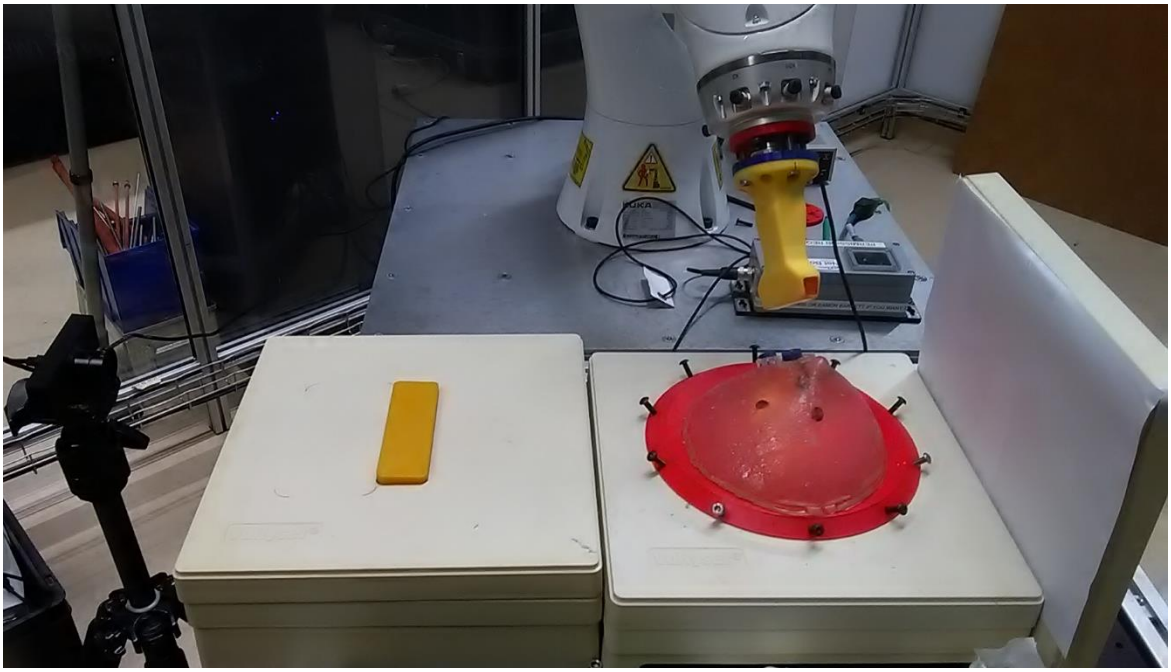

Figure 6.44 - Setup used for the deformation test. The white paper behind the breast phantom is used to enhance image acquisition with the webcam.

RESULTS

For the deformation, the following main variables were created:

- Marker 1 (M1) without cone
- M1 with cone
- Marker 2 (M2) without cone
- M2 with cone

Where M1 is the marker located next to the nipple of the breast phantom and M2 is the marker located closer to the base of the breast phantom. Each trial (where one of the variables above is tested) is conducted 5 times and the results presented are the average response for each type of variable. The regions of interest are the same as defined in section 6.5. The markers have a layer of PVC in between themselves and the phantom, approximately the same size as the breast holder's thickness, which can be seen in Figure 6.43. This was added so that the position difference could not be a factor contributing to changes in the forces detected. The sampling rates of both sensors are maintained also in this experiment.

For a position based motion, the expectation would be that final position would be very similar for both cases, which is verified by the position sensor of the robot. Thus, it would be expected that a similar

displacement would be detected by the image detection algorithm but that is not what is observed in Table VIII.

Table VIII – Changes in position with and without the breast holder. The position (x, y, z) is obtained from the manipulator's sensors and the displacement comes from the markers position change detected by the webcam.

		M1			**Elongation (Δ) M1**		**Elongation (Δ) M2**	
		X (mm)	Y (mm)	Z (mm)	X (mm)	Z (mm)	X (mm)	Z (mm)
M1	No Cone	132.4986	-3.4399	35.1401	31.1061	25.2174	3.5419	0.0855
	Cone	132.4987	-3.4354	35.1558	24.0940	17.0237	3.3144	0.1571
		M2						
		X (mm)	Y (mm)	Z (mm)				
M2	No Cone	121.6914	-5.1935	26.7758	2.2955	0.0140	26.0362	7.8174
	Cone	121.5618	-5.1964	26.8439	1.4731	0.0839	11.0841	8.0863

It is necessary take into account the conditions that generated the results. The algorithm designed struggled to detect both markers during the whole motion, this was caused by shadowing effects due to the transducer's motion in addition to the transparency of the breast holder which reflected more light than the phantom's surface. Also the added thickness of the breast holder causes the marker to be "covered" from the perspective of the webcam during most of the time the transducer is pressing on it and it goes undetected. Therefore, what can be seen as small deformation from the results will most likely be a result of the low visibility of the marker when there is a larger change in position. This phenomenon is observed in the plots when there is a "plateau" region, which can be found in Appendix B.

As consequence of this, it was possible to determine that the sensitivity of the data acquired with this algorithm is not enough to get the desired precision in results and draw accurate conclusions regarding the response of the breast holder. It seems a better option to disregard the data collected through this method. The figures that depict the measured position differences will be shown only in the Appendix B as they do not add value to the conclusions.

Looking at the response of the position difference of the marker that was not under stress, where the previous effects are minimized, the evidence points to a smaller change in position. This can mean that locally the breast holder is not very effective in reducing deformation but for the overall breast, the deformation reaction triggered by the US transducer will be reduced. However, it could just be a result of a high stiffness of the breast phantom causing its response to be small in both scenarios.

In terms of force analysis, given the predominant motion direction being Z, it seemed reasonable to focus mainly on the results obtained in this direction. Due to the results of section 6.5, only the force sensor results are presented. To observe a more complete analysis in all the directions, the reader is referred to Appendix G. If the breast holder does have a positive effect in reducing deformation, it is expected that there is a force increase from the situation without the breast holder present and when it is added to the setup, as this will implicate that this structure is indeed stiffer than the breast phantom.

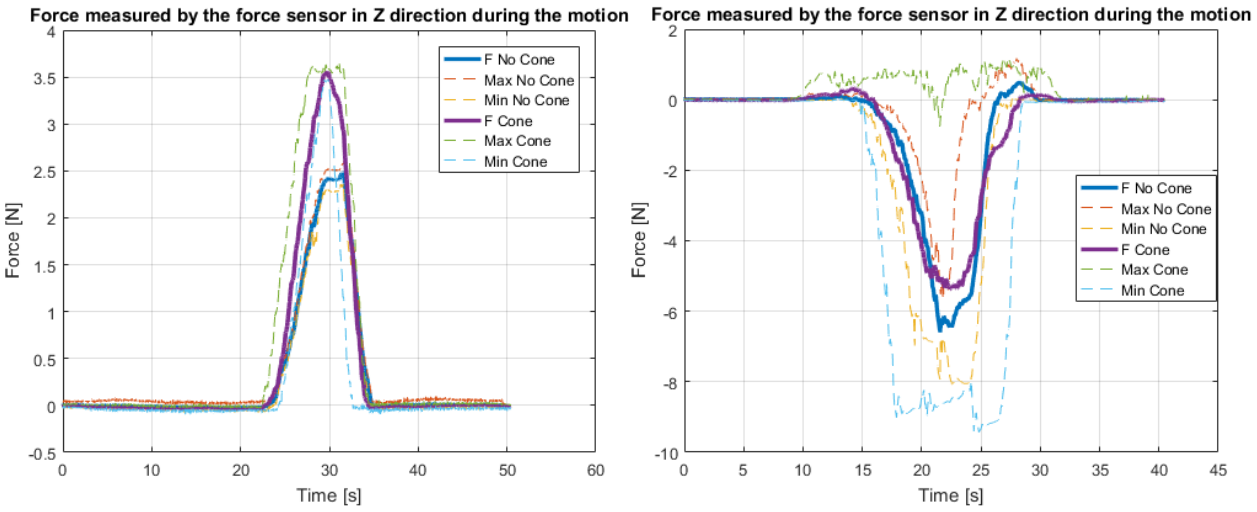

Figure 6.45 – Average force response in Z direction for M1 (left) and for M2 (right) with maximum and minimum deviations.

Observing the force sensor response for M1, it is possible to realize that the result is as expected, despite the small changes in force, the force increases in the presence of the breast holder by 1N, and actually. On the other hand, for M2 the response is contradictory. The average response indicates that the presence of the breast actually involves less forces than without it. However, observing the maximum and minimum deviations in Figure 6.45, both the responses are far from the average. The same signals for the "No cone" also experience some variations, though not so extreme. With such a response, the results are inconclusive as the repeatability of this test can be questioned. In order to draw solid conclusions, this test should be conducted more times.

To corroborate the evidence encountered through the analysis of the forces, it was also decided to evaluate the relationship between the forces and the position. However, in order to use the data from the external force sensor, the data had to be aligned with the position data from the LBR sensors since it cannot collect its own position information.

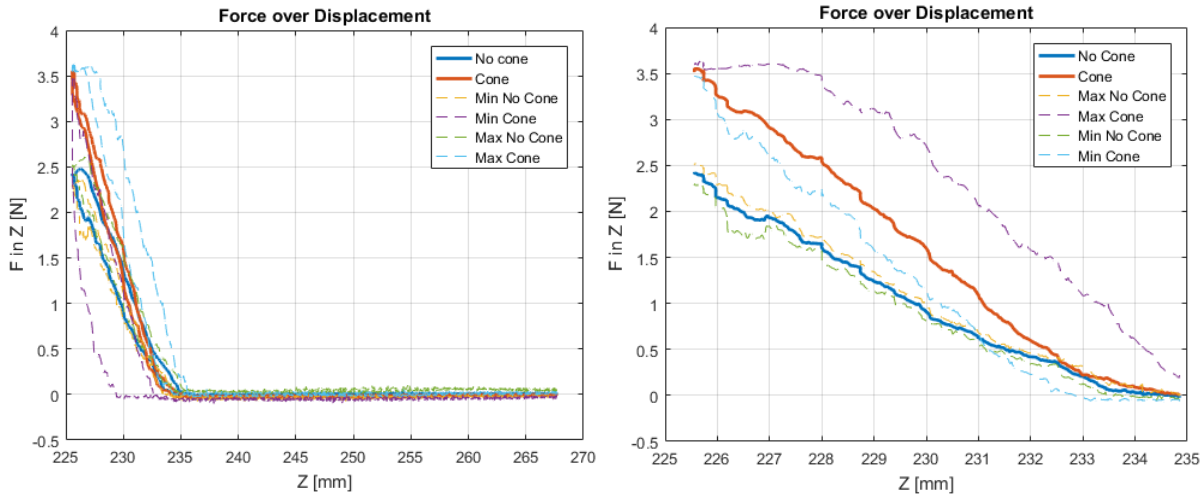

Figure 6.46 - Force distribution over the displacement generated for M1. The plot on the right represents the response in the region of interest defined previously.

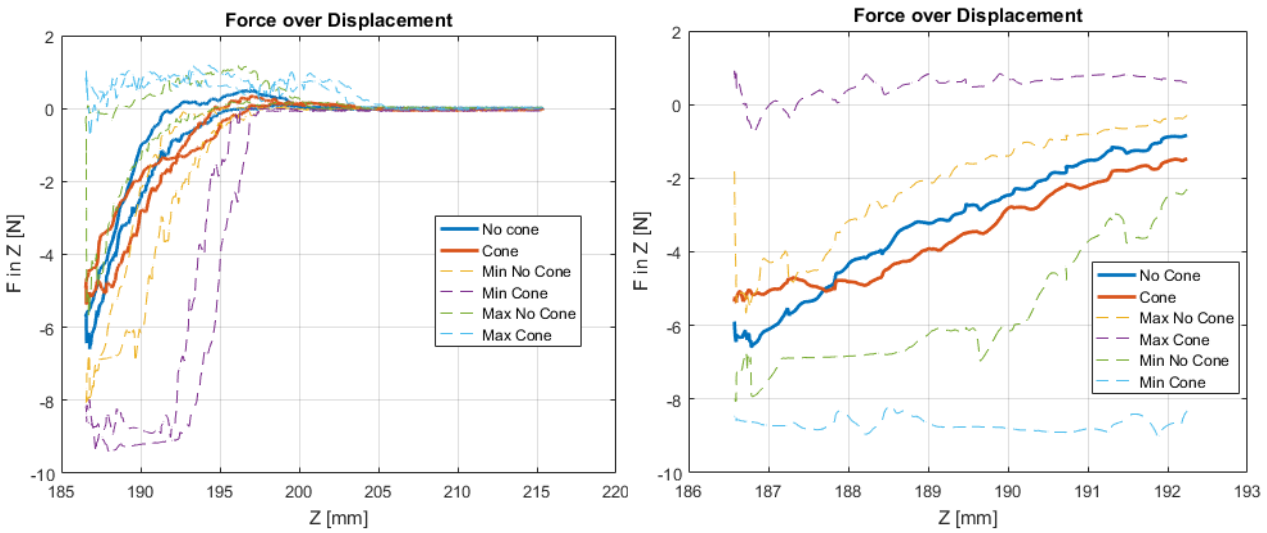

Figure 6.47 - Force distribution over the displacement generated for M2. The plot on the right represents the response in the region of interest defined previously.

The results observed in Figure 6.46 and Figure 6.47 are consistent with had been observed in the previous figures relative to the force. Pointing again towards a larger stiffness associated to the presence of the breast holder for M1. Thus, it does seem reasonable to admit that the breast holder will have an effect on reducing the breast deformation, even if this effect is not very prominent for small displacements. Additionally, the external force sensor the response is almost linear, which is what would be expected of a linear deformation experiment as well as the hysteresis behaviour expected from an elastic deformation.

For M2, the average response indicates that the presence of the breast holder can increase deformation. However, taking into account the actual motion conducted by the manipulator it seems unlikely that this material induces force changes very close to zero, as it happens in the maximum response (which is in reality the minimum). Nevertheless, given the data that was obtained, it is not possible to say that the breast holder is effective for larger displacements.

It is possible to notice that for the initial region of displacement, the increase of stiffness is not very noticeable for both markers as it is very similar to the stiffness registered without the breast holder. This could mean that the breast holder only starts providing an effective response for deformations of more than 2-3mm and a force change of at least 0.5N. This information, if verified, could implicate that there is specific range of displacement where the breast holder behaves as expected, though it is complicated to be certain without repeating the experiment for M2.

In spite of appearing to reduce deformation for small displacements, when paired with the trajectory developed, the breast holder did not have the most ideal response. Additionally, the small amount of trials conducted is not enough to be confident in the response, as it was not possible to conduct any kind of statistics and obtain confidence intervals. It is not very clear whether the LBR can provide a very repeatable response which makes the outcome obtained for the trajectories tested harder to interpret.

7. CONCLUSIONS AND FUTURE RECOMMENDATIONS

At the start of this master thesis, it was proposed to handle two subtopics of the MURAB project, namely, the US automated trajectory and the breast holder. For the first topic, the goal was to improve the already existent trajectory, introducing the requirements that had not been fulfilled yet while implementing this trajectory into a new platform (Sunrise Workbench). For the second topic, the goal was to design a structure that would be able to support the breast throughout the procedure while being able to reduce deformation caused by the US trajectory. Since the second subtopic is dependent on the trajectory and how it is performed, the last goal of this master assignment was to make sure that two topics are functional together.

7.1 TRAJECTORY DESIGN AND IMPLEMENTATION

At the end of this master thesis, it is possible to encounter a functional trajectory in Sunrise that is able to move around the surface of the breast phantom always perpendicular and in contact with this surface, while assuring a compliant interaction. This can be ensured provided that there is a way to obtain the 3D model of the structure being imaged. However, there is still one requirement that was not able to be implemented: the manipulator cannot re-adjust its position after the motion has been started, so in the event of sudden movements, contact will be lost.

The main setback encountered in order to build the desired trajectory was the software chosen to programme the robot. Sunrise is not a widely used Workbench. Despite using Java as a language, the amount of information available regarding the robot specific classes and functions is quite limited. With the knowledge that it was possible to build, the solution provided incorporates the best features of this software, i.e., its inbuilt impedance controller and its own mechanism to compute forwards kinematics. The disadvantage of this trajectory is indeed that it cannot be adaptable to the environment but, given the force sensors readouts that were evaluated in the results section it does not seem likely that these sensors could be used for accurate force feedback even if the software would allow it. It is important to take into account that the experiments used to test the force sensor activity are somewhat more complex than what it is generally done to have complete certainty in a sensor's response. The data obtained for the LBR's sensors showed that its sensitivity for small deviations is low as the behaviour with and without obstacle are the same. In addition, it indicated that for any given motion the noise levels are rather elevated and cannot be completely understood. However, provided that the LBR can detect the changes, it is possible to conduct an analysis based on the relative behaviour of the parameter being evaluated.

Moreover, when it was attempted to use this trajectory with a different end-effector (which will ultimately be the case for MURAB), the workspace selected was also responsible for a lot of constraints which resulted from the setup used being in supine position.

An existent simulator used for the iiwa manipulators was encountered online, the KUKA PRC. This software is capable of planning the positions the user wants the robot to move into and generates a text file that can be given to the Workbench. This would allow for an easier implementation of the desired trajectories being less dependent on the Matlab algorithm used, though it would not be enough to completely discard the pre-planned trajectory. However, this software is not available alone and requires the install of Rhino(ceros 3D), which requires purchase, so this simulator was never used.

- **Recommendations**

Despite the existent trajectory being functional and effective, it is still considered that adaptability is a very important requirement that cannot be overlooked. Therefore, if there is a way to implement the initial plan described in chapter 4 using Sunrise it would be the most advantageous outcome for MURAB. Nonetheless, for now this does not seem possible. It is recommended to wonder about whether or not there will be more benefit in using ROS instead of continuing with Sunrise Workbench, as ROS allows for more control over the parameters that create the controller, while having extensive libraries available and specific nodes for different types of parameters that want to be tested.

If Sunrise is maintained, it is highly recommended that an introductory course to the software is conducted before using it. Additionally, given the situation encountered with the force sensors, the LBR sensors are not reliable. It seems more reasonable to keep the external force sensor as part of the end-effector and incorporate its online response into the control loop developed assuring that the response is more accurate. The communication of the external force sensor with Java has to be developed at a lower-level to be able to communicate with a few Java functions provided by ATI. Afterwards, it would still be necessary to incorporate this into the application of the trajectory to have a constant readout of the forces and this would still not assure the possibility of being able to move the robot with a constant force. On the other hand, ROS already has a node especially developed to communicate with the external force sensor which means this task would be easily accomplished using this operating system instead. Additionally, since force control is necessary to implement the desired strategy, it would be preferable to use ROS, as the two previous master thesis were able to successfully incorporate force control. Adding to it, instead of using a pre-defined force to keep surface contact, the force of the motion can be determined by the initial contact between the two surfaces.

The other challenge encountered were the workspace constraints, due to the trajectory being planned for supine position instead of prone. Therefore, using a prone setup in the future will provide more accurate results relatable to the real situation in addition to allowing a more flexible workspace. Moreover, a prone setup provides the situation where it is possible to test if the counterforce generated by the breast holder is sufficient to reduce patient discomfort when the scanning takes place. This step should be one of the next steps to focus on in the future as it would be beneficial to learn more about the breast holders' properties as well as to incorporate the trajectory in a more feasible manner and understand if these two can still work well together.

Finally, after discussing with one of the partners from MURAB of RadBoudUMC, it seems that it might be easier to reconstruct an US image if the trajectory is conducted radially instead of circularly. However, little proof of concept was provided to support this argument. Nevertheless, it could be interesting to investigate this further and attempt to implement a radial trajectory. Using the pre-planning algorithm, this would not be a very big challenge and it would quickly be possible to verify whether or not there is actual improvement in the image acquisition step.

7.2 BREAST HOLDING STRUCTURE

Adding to the trajectory design, a finalized design of a breast holding structure is also presented. With this design it was possible to investigate different materials and their properties looking for the optimal solution. From the tests conducted, PVC was the only material that could be considered US

compatible. PVC is also a very cost-effective solution as it is quite affordable and easy to obtain with minimal environmental impact, when compared to other polymers [70]. Based on the properties of this material, the final design is a flat mesh surface obtained through moulding, where the holes are 4x4 mm squares and its thickness is approximately 35mm. In order to make this design more adaptable to the breast shape, even if the material itself is already flexible, the surface will be an open structure so that it can be closed at the appropriate size. Given this design choice, the holder incorporates a connecting structure made with one column of several pillars with a "mushroom" shape.

With the process developed for testing PVC, it was not only possible to develop a fabrication protocol optimal for the purpose, as it was possible to design a whole set of steps that a material should be able to follow in order to achieve the final breast holder if another material should be used for this purpose later in MURAB. However, one of the disadvantages of using PVC is actually its fabrication process, as it requires heating to very high temperatures to achieve the desired elastic properties causing it to release very toxic gases in that process. Even though it was possible to appropriately ventilate the working environment, the situation was not ideal and it would be beneficial to avoid it.

To validate this design, two different experiments were conducted, one using a scanning trajectory while the other used a linear deformation. It was possible to conclude that the final structure was compatible with the US and allowed for the planned trajectory to be conducted. However, this resulted in an inadequate force response due to excessive friction between the two surfaces. The deformation experiment revealed an increase in stiffness, through the increase of forces, for the marker that suffered a small displacement. For larger displacements, the data was inconclusive, though it is expected that motion that involves higher forces in principle should allow for a more clear response in a deformation experiment. However, perhaps these larger force changes are what make the response more unstable.

Despite the results obtained for the breast holder's validation, it is still possible to wonder whether or not these results would've been the same if an actual breast would be used instead of a breast phantom. This because the phantoms used are much stiffer than an actual breast which could point for a much prominent response in the increases observed in the presence of the cone and hence, a clearer effect on deformation reduction.

- **Recommendations**

Nevertheless, there are some steps that could be implemented in the future to provide improve the results obtained. For example, the lack of an appropriate measurement tool did not allow for the execution of a more elaborate support test. If there had been an accurate distance measurement from the start position to final position of the breast phantom (vertically and laterally) more variables could be introduced to this test, such as how much it actually feels the effects of gravity and small motions to simulate the displacement induced by patient sudden movements or the patient being carried from room to room to finish the procedure. This would allow for a more accurate validation of the breast holder for the events where the breast is moved as a result of external causes.

Another way to improve the testing steps would be to test the breast holder in a clinical setting. This recommendation comes more logically for the breast holder but it could also be very helpful to experiment with the transducers and contact forces while conducting an ultrasound scan on an actual patient and evaluate the required force to have a clear image.

Material wise, given the fabrication protocol of PVC leading to the production of toxic gases, if an alternative material that fulfils the requirements can be found, then preference should be given if the fabrication method is less harmful. Additionally, a hardener material was encountered which could have been paired with the super rigide PVC to increase the stiffness of the structure, which is one of the areas that could be enhanced. An experiment like this would need a lot of testing to find out the optimal concentrations of both substances to provide adequate support, deformation reduction and good image quality. The amount of PVC available in the lab was not sufficient for conducting so many tests and more PVC could not be delivered in time, thus this experiment would be the next step to attempt.

From the analysis of scanning experiment where the two parts of the project were brought together it was possible to suggest some alterations, so that this process could be improved. The simpler method is to adjust the US gel and the stretch and re-do the testing. The magnitude of the forces causing the friction should be reduced. However, if this is not sufficient, then the trajectory can introduce force conditions to limit the maximum force. If this step fails, then the suggestion is to look into improvements for the material properties.

Lastly, for both scenarios where a trajectory was used to evaluate the breast holder's response, it was not clear from the measurements if this response will be always the same, which also prevented a complete understanding of the results. It is, therefore, highly recommended that more trials will be conducted, so that some kind of statistical test can be performed and there is more confidence in the type of response provided.

8. APPENDIX

A. JAVA ALGORITHM

The trajectory that simulates an US scan over the breast phantom was implemented in java. Even though the pseudo code was already presented in chapter 4, the full implementation is shown below. In order to run this Sunrise Application it is necessary to have the version of the Workbench 1.13.

```
package application;


import java.util.ArrayList;
import java.util.Date;

import javax.inject.Inject;

import kuka.murab.grpc.RobotServer;

import spline.ReadFile;
import spline.SpiralTrajectory;

import com.kuka.common.ThreadUtil;
import com.kuka.roboticsAPI.RoboticsAPIContext;
import com.kuka.roboticsAPI.applicationModel.RoboticsAPIApplication;
import static com.kuka.roboticsAPI.motionModel.BasicMotions.*;

import com.kuka.roboticsAPI.conditionModel.ICondition;
import com.kuka.roboticsAPI.conditionModel.MotionPathCondition;
import com.kuka.roboticsAPI.deviceModel.LBR;
import com.kuka.roboticsAPI.geometricModel.AbstractFrame;
import com.kuka.roboticsAPI.geometricModel.CartDOF;
import com.kuka.roboticsAPI.geometricModel.Frame;
import com.kuka.roboticsAPI.geometricModel.Tool;
import com.kuka.roboticsAPI.geometricModel.World;
import com.kuka.roboticsAPI.geometricModel.math.CoordinateAxis;
import com.kuka.roboticsAPI.motionModel.MotionBatch;
import com.kuka.roboticsAPI.motionModel.PTP;
import
com.kuka.roboticsAPI.motionModel.controlModeModel.CartesianSineImpedanceContr
olMode;
import com.kuka.roboticsAPI.sensorModel.DataRecorder;
import com.kuka.roboticsAPI.sensorModel.StartRecordingAction;
import java.io.BufferedReader;
import java.io.FileNotFoundException;
import java.io.FileReader;
import java.util.ArrayList;
import java.util.Scanner;
/**
 * Implementation of a robot application.
 * <p>
 * The application provides a {@link RoboticsAPITask#initialize()} and a
 * {@link RoboticsAPITask#run()} method, which will be called successively in
 * the application lifecycle. The application will terminate automatically
after
```

```
 * the {@link RoboticsAPITask#run()} method has finished or after stopping
the
 * task. The {@link RoboticsAPITask#dispose()} method will be called, even if
an
 * exception is thrown during initialization or run.
 * <p>
 * <b>It is imperative to call <code>super.dispose()</code> when overriding
the
 * {@link RoboticsAPITask#dispose()} method.</b>
 *
 * @see UseRoboticsAPIContext
 * @see #initialize()
 * @see #run()
 * @see #dispose()
 */
public class ScanningApplication extends RoboticsAPIApplication {

	ScanningApplication()
	{
		super();
	}

	ScanningApplication(RoboticsAPIContext context)
	{
		super(context);
	}

	@Inject
	private LBR _lbr;
	private Tool _tool;
	private ReadFile _rf;
	Double[][] _array;
	static String filename;
	private SpiralTrajectory trajectory;
	double distance;
	double minFrameDist = 5.0;
	static CartesianImpedanceControlMode _ctrlMode;
	static DataRecorder _rec;
	static StartRecordingAction _startAction;
	static MotionPathCondition _pathCondition;
	static ForceCondition _forceCond;


	@Override
	public void initialize() {
		_lbr = getContext().getDefaultController().getDevice(LBR.class);
		_tool = getApplicationData().createFromTemplate("tool");
		_tool.attachTo(_lbr.getFlange());
		_rf = new ReadFile();
		filename = "D:\\Twente3.txt";

		trajectory = new SpiralTrajectory();
		_ctrlMode = new CartesianImpedanceControlMode();
_ctrlMode.parametrize(CartDOF.Z).setStiffness(450.0);
		_rec = new DataRecorder();
		_rec.addCartesianForce(_tool.getDefaultMotionFrame(),
_tool.getDefaultMotionFrame());
```

```
            _startAction = new StartRecordingAction(_rec);
            _pathCondition = new MotionPathCondition(ReferenceType.START,
0.0, 0);

      }
      public ArrayList<PTP> distanceFilter(ArrayList<PTP> pathPTPtmp){
            // Take unfiltered ArrayList with PTP and filter the distances
            ArrayList<PTP> allMotions = new ArrayList<PTP>();
            PTP pre = pathPTPtmp.get(0);

            for(int i = 1; i < pathPTPtmp.size(); i++){
                  PTP currPos =  pathPTPtmp.get(i);
                  Frame preframe =
_lbr.getForwardKinematic(pre.getDestination());
                  Frame currframe =
_lbr.getForwardKinematic(currPos.getDestination());
                  distance = preframe.distanceTo(currframe);

                  if(Math.abs(distance) <= minFrameDist){
                        continue;
                  }
                  else if(Math.abs(distance) > minFrameDist){
                        allMotions.add(pathPTPtmp.get(i));
                        pre = currPos;
                  }
            }
            return allMotions;
      }

      @Override
      public void run() {

            // Import file, filter it and build motion batch
            _rf.importFile(filename);
            ArrayList<PTP> pathPTPFiltered =
this.distanceFilter(_rf.getPathPTP());
            MotionBatch batch = trajectory.getMotionBatch(pathPTPFiltered);

            // Move LBR
      _tool.move(ptp(getFrame("/StartPos")).setJointVelocityRel(0.2));

      _tool.move(batch.setJointVelocityRel(.1).setBlendingRel(0.1).setMode(_c
trlMode).triggerWhen(_pathCondition, _startAction));
      _tool.move(lin(getFrame("/EndPos")).setJointVelocityRel(0.2));

      }
```

B. IMAGE ACQUISITION ALGORITHM

As described in section 6.6, an image acquisition algorithm for position tracking was developed. This algorithm is based on colour detection and is implemented to track the centroid position of two blue markers. In order to establish a position detection function, the application "colour thresholder" available in Matlab was used to filter all the colours out of the image leaving only the markers to be detected. Given the composition of the image, it was decided to use the RGB colour space to isolate the blue markers. The function generated is called "createMaskSmallmarker()".

It was decided to collect 2 frames per second (fps). The Matlab code for this algorithm is presented below. Additionally, the pixel value in millimetres was calculated using a snapshot of the setup with a ruler to have a clear picture of how many pixels correspond to 1mm. Using Figure 8.1 , it was calculated that 1mm is equal to 3.2 pixels (or 1 pixel equals 0.31 mm).

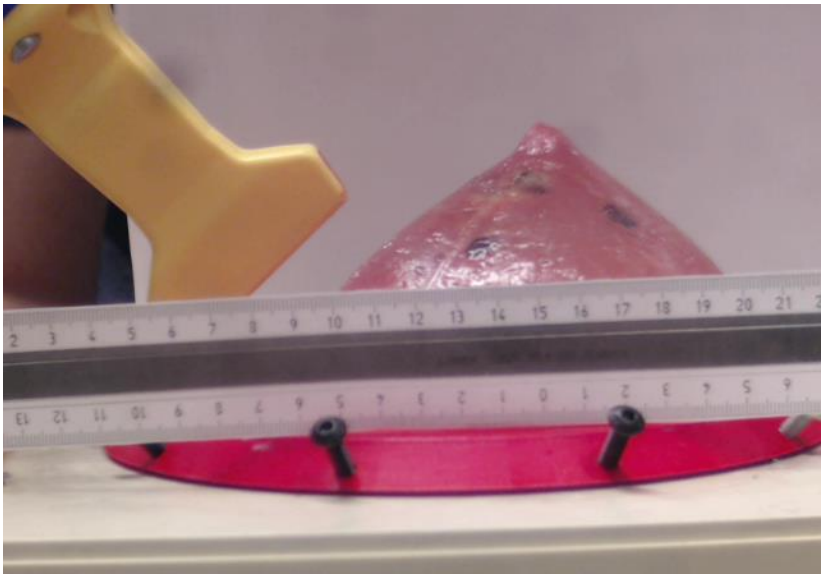

Figure 8.1 - Image with ruler to determine the pixel space in mm.

Matlab algorithm:

```
clear all; close all; clc;
cam = webcam(1);
cam.Resolution = '640x480';
preview(cam)
pause(2);
fps = 2;
Mtemp = [];

for i=1:300;
    tic
    x = snapshot(cam);

    rect5 = [130 80 220 230];
    I2 = imcrop(x,rect5);

    [BW,~] = createMaskSmallmarker(I2); % Filtering Mask
```

```
    se = strel('disk',4);
    BW = imfill(BW,'holes');
    BW = imerode(BW,se);
    se = strel('disk',10);
    BW =  imdilate(BW,se);
    BW =  imfill(BW,'holes');

    stats = regionprops(BW,'Centroid','Area');
    temp = [stats.Centroid];
    if size(temp,2)<3

        temp = [Mtemp(i-1,1:2) Mtemp(i-1,3:4)];
    else
        temp = [stats.Centroid];
    end
    Mtemp = [Mtemp; temp];
    subplot(121); imshow(BW)
    subplot(122); imshow(I2)
    t = toc;
    pause((1/fps)-t);
    i

end
closePreview(cam);
%%
% SEPERATE TWO MARKERS INTO M1 AND M2
M2 = Mtemp(:,3:4);
M1 = Mtemp(:,1:2);

pixelSpa = 0.31 xmax = 300; ymax = 12; ymin = -5;
```

The plots of the results showing the difference in elongation of the phantom with and without the presence of the breast holder will be shown in Figure 8.2. These plots were obtained before the whole measurement was considered neglectful, which was only decided upon once comparing with the data from the position sensors. Unfortunately, the collection of the data was very dependent on the lightning conditions of the environment that introduced a very large error to the values of maximum deformation. Nevertheless, to confirm that this data is not in line with was obtained with the force sensors, it still was worth presenting the obtained figures.

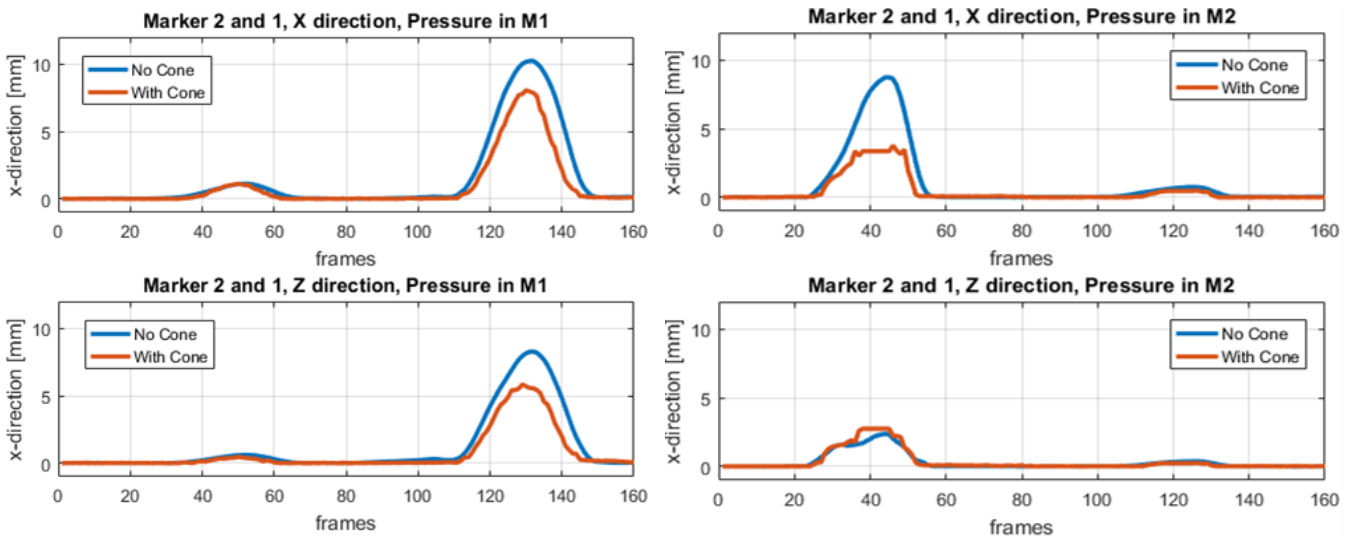

Figure 8.2 - Position change of the markers once the motion is pressuring M1 (left) and when it is pressuring M2 (right). The marker with higher signal is always the one who is under pressure, as it would be expected.

As already observed in chapter 6, the only case where it seems as the breast holder will not be useful in reducing deformation is in the impedance motion when there is pressure put on M1. Though these results might have been encouraging for the validation of the breast holder's performance, as explained in chapter 6, the conditions that lead to obtaining this data provide very unreliable data, whose values did not add up to the information collected by the position sensors.

C. FABRICATION PROTOCOLS

PCVP PHANTOM

PVC is a material that has a set of properties that can be changed with temperature. To make a new breast phantom, a breast mould with the average size of the breast needs to designed and printed (in such a way that it can sustain high temperatures. To approximate the characteristics of breast tissue, the breast phantom is actually a mixture of PVC with plasticiser, hence PVCP. Depending on the concentration of both it is possible to achieve phantoms with different E.

Using then a pot and a heating plate, the material (approximately 500mL, depending on the breast shape) is poured into to the pot to be heated until its colour turns transparent, which is generally after 200ºC. It is necessary to be careful not to overheat the material as it can cause it to burn and it cannot be utilized then. Once cool enough to handle, the material will be put inside the mould and let to cool down (only then will the phantom keep one single position. Optionally, when it starts cooling down but not completely it is possible to add detectable objects than are visible under US. If there are air bubbles in the sample, it can be put in the oven at 200 mbar so that the air bubbles are released from this viscous material with the decrease of pressure.

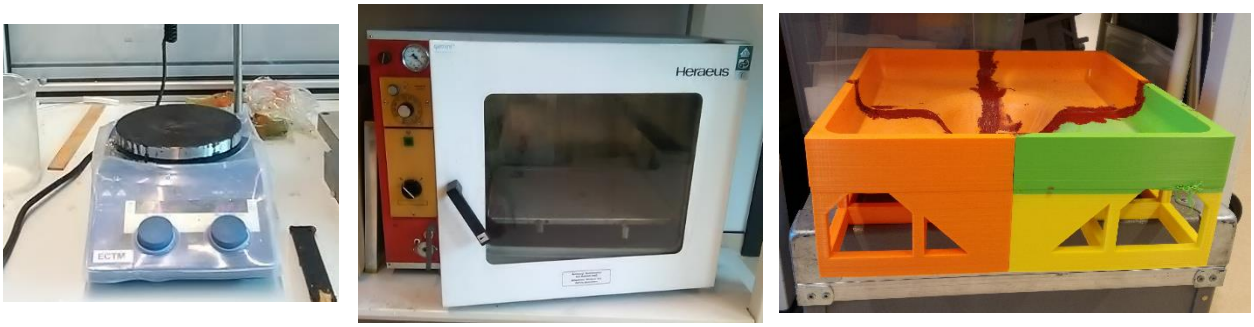

Figure 8.3 - Equipment used for the production of the breast phantoms. From left to right: Heat plate, Oven and Breast Mould

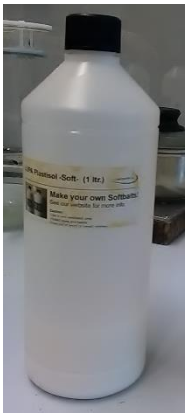

Figure 8.4 - LUPA Plastisol Soft version (Lureparts.nl, The Netherlands)

PVC BREAST HOLDER

The fabrication of the PVC meshes, and later the breast holder, started out with a similar fabrication procedure as the breast phantom. However, since the mould use for this purpose is much smaller and has a lot of extrusion features, it was hard to get an even result once pouring the heated form

of the PVC (which is rather viscous) onto the mesh. Thus, the whole procedure was conducted in the oven instead.

Since this technique had not been used before, it was necessary to determine how long the PVC could stay in the oven so that it would not burn. Additionally, just heating in the oven did not prevent the appearing of bubbles in the final structure and solving this situation is crucial to have a material that is ultrasound compatible. It is known that reducing the pressure of the environment of the material can help in the removal of air bubbles from the sample, however, the same procedure as for the phantom was attempted and it was not successful.

In order to remove the breast holder from the mould with ease, it is necessary to apply a coating layer with a coating agent to the mould's surface a let it actuate for at least 5 minutes before pouring the material.

After conducting several tests changing the time the material was kept in the oven interchanging with the time it would be exposed to a smaller pressure (also done in the oven) it was possible to come to a production protocol that optimizes the result to have minimal to no air bubbles:

- Pour the liquid PVC into the (coated) mould at room temperature
- Turn on the oven to 200ºC and put the mould inside it
- Set the pressure at 200mbar for approximately 20 min
- Set the pressure at 1000mbar again and wait around 45-55 min, depending on the transparency of the PVC
- When the PVC is clearly transparent, the mould should be removed from the oven and left to cool in the fume hood until it has become completely hard and it's possible to remove the mesh from the mould.

In addition to the equipment seen in Figure 8.3, given the stiffness requirements that were necessary for the production of a viable breast holder, the type of PVC used here changed and two different types were used, LUPA Plastisol Medium (Lureparts.nl, The Netherlands) and Plastileurre Super Rigide (Bricoleurre, France).

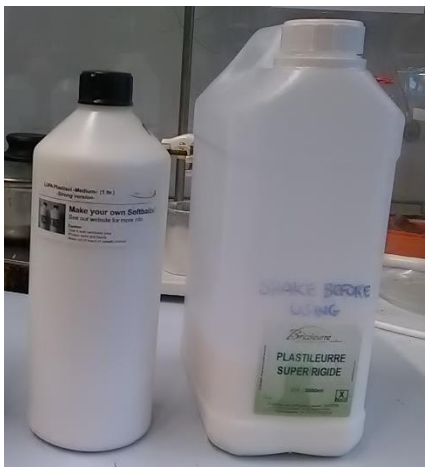

Figure 8.5 - LUPA Plastisol Medium (Lureparts.nl, The Netherlands) and Plastileurre Super Rigide (Bricoleurre, France)

WARNING: Breathing PVC fumes that are released during the heating process is quite toxic to humans and possibly carcinogenic, thus a very good ventilation is mandatory to conduct this experiment. If available, wearing a mask is also recommended. Read the safety sheet provided by the manufacturer before using.

POLYURETHANE RUBBER

In addition to PVC, a polyurethane rubber mesh was also fabricated in the lab. The advantage of this material is that the technique is much simpler and the whole procedure can be conducted at room temperature, though it is more time consuming. The material used was VytaFlex 10 (Smooth-On, Inc., Macungie, PA, USA) and it is constituted of two separate parts (Part A and Part B). The protocol followed is the one described by the manufacturer and is mentioned below:

- Apply a coating agent very thoroughly and let it actuate for at least 5 min
- Mix part A and part B before using
- Pour equal amounts of part A and part B into a mixing container (in this case, approximately 100mL of each were used)
- Mix carefully for 3 minutes, ensuring the bottom and sides are scrapped during that process
- Pour slowly onto the mould. Given the thickness and viscosity of this material, it might be possible that the mix will slightly overflow or that some of it will fall over the extrusions of the mould (which is not desired to obtain clear shaped holes in the mesh shape), so the amount being poured at each time should not be very much and it should be done slowly.
- After an even pouring of the material in the mesh, let it sit for at least 24h at room temperature (23°C).
- Remove from the mould

Figure 8.6 - VytaFlex 10 used for making polyurethane rubber

D. ALTERNATIVE DESIGN

Finding an US compatible proved itself to be very complicate task, adding to the already challenging job of finding a material that would have the ideal properties for purpose of supporting the breast and reducing deformation. At a certain stage of the master project, it seemed reasonable to work on an additional design, in the event that such a material could not be encountered.

Since the main challenge was that the material would be US compatible, the open design was considered as a good alternative since the scan here is conducted in direct contact with the skin. However, the conceived idea was just a plan B so its properties were not adequately tuned to fit the purposed, but a mere start point to work from if necessary. The material used was TangoBlack to assure flexibility of the structure, though the thickness was much larger (1cm) since the support necessary would have to be provided by a fewer areas. The connecting area of the structure is not closed here as it required a special glue on the extrusion that would be inserted in the hole designed in the opposite pillar. The height of the pillars was established at 95 mm given the size of the breast phantom. The inner and the outer rings (if the structure is being looked at from above) are also set to fit the phantom available (8 cm of perimeter for the inner ring and 15 cm of diameter for the outer ring).

Figure 8.7 - Open design concept.

E. CONNECTOR STRUCTURES

Though only the successful connectors were presented in the chapter 6, there were a few other options that were attempted (unsuccessfully) before a result that gathered the conditions required was obtained. It was decided to present this information to help build up the knowledge for this specific problem.

Figure 8.8 - First connector concept. The outer cylinders have 2mm diameter and the inner circles have 1mm. The total height of the combined structure is 5 mm.

The initial concept considered was thought to take up the minimum space necessary, so it was designed to be 10 mm wide, seen in Figure 8.8. The overall idea was to have two separate parts (one top and one bottom), each one with cylindrical extrusions. One of them will have an opening inside and the other one should have a smaller pillar of the approximate size of the corresponding opening. To adjust the fit between these two parts, the open cylinder will have an inner layer made out of Tango Black (which is very flexible). The rest of the structure is made out of RGD8530. Unfortunately, the connection between the two parts was not strong enough to keep them together as expected, so the first solution was to try out the best inner diameter, which was settled at 1.8mm. However, the mesh was too weak to comply with the dimensions of the structure without tearing. Thus, different sizes (cylinder and width), materials and ways to close the two pieces were evaluated, though the final height of the combined structures was maintained at 5mm.

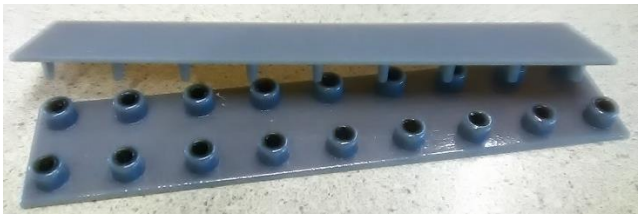

Figure 8.9 - Similar concept as the initial but with an outer cylinder of 3.80 mm diameter and angled insertion pillars.

Figure 8.10 - Same concept but only composed of TangoBlack to increase flexibility.

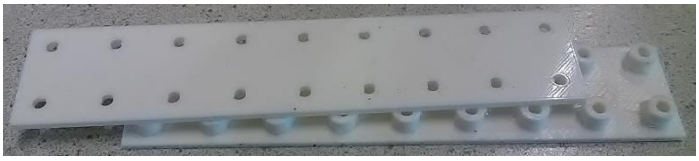

Figure 8.11 - Similar concept but connection between the two parts is assured with screws. This connector is made out of PLA and is stiffer than the previous two.

The designs attempted in Figure 8.9, Figure 8.10 and Figure 8.11 all failed to achieve their purpose of supporting the 500 gr weight. However, if on one side the two first ones were not strong enough to keep the structure closed, the last one provided enough strength but the mesh part that fall outside the connecting structure would not support the exerted pressure and ended up tearing. All of these were about 17 mm wide.

The working concepts differ from what was tested up until now by incorporating the materials' ability to stretch more evenly and as much as it needs to support the induced force of 5N. The two designs seen in Figure 6.30 are made of only one part (instead of two) of 15 mm width. The "mushroom" shaped pillars of the selected connector is 3.8 mm diameter and the height of the pillar without the "head" is of about 4mm to fit with the meshes' height, though the overall height is about 7mm. The hook connector is only 5.5 mm in height, with 4mm pillar height to have enough space for the mesh as well.

F. FRAME TRANSFORMATION

Due to the way the external force sensor was attached to the flange of the robot, the frame of the end-effector and this force sensor were not coincident. Thus, it was necessary to compute the rotation matrix that allowed for an accurate comparison of the force values collected by the two sensors.

With the SolidWorks model of the 3D printed attachment, with as possible to approximate the angles between the two frames to compute the rotation. For a purpose of simplification, it was admitted that the angle between Y_1 and Y_2 is 60º and the angle between X_1 and X_2 is 240º (60º+180º) about Z_1 (+).

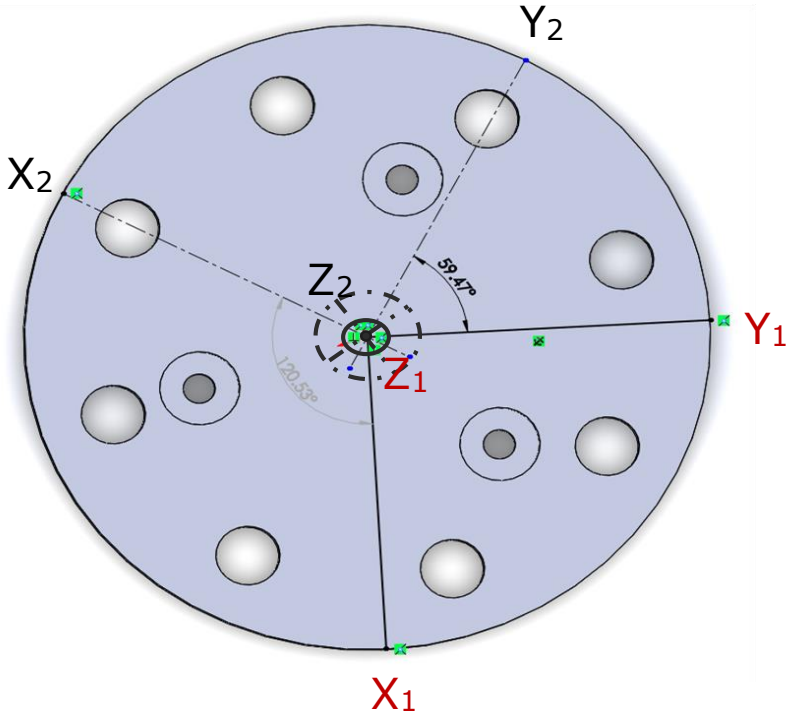

Figure 8.12 - Angular relation between frame 1 (end-effector) and frame 2 (external sensor). The dashed lines represent frame 2 while the continuous lines represent frame 1.

The typical rotational matrix above Z can be obtained by using the formula in equation 8.1. However, since the two frames are not oriented in the same direction, it is also necessary to change Z_2. Thus, the transformation used can be found in equation 8.2.

$$R_z = \begin{bmatrix} \widehat{X_2}\cdot\widehat{X_1} & \widehat{X_2}\cdot\widehat{Y_1} & 0 \\ \widehat{Y_2}\cdot\widehat{X_1} & \widehat{Y_2}\cdot\widehat{Y_1} & 0 \\ 0 & 0 & 1 \end{bmatrix} \tag{8.1}$$

$$T = \begin{bmatrix} \cos(\theta+\pi) & \cos(\theta+\frac{\pi}{2}) & 0 \\ \cos(\theta+\frac{\pi}{2}) & \cos(\theta) & 0 \\ 0 & 0 & -1 \end{bmatrix} = \begin{bmatrix} -\cos(\frac{\pi}{3}) & -\sin(\frac{\pi}{3}) & 0 \\ -\sin(\frac{\pi}{3}) & \cos(\frac{\pi}{3}) & 0 \\ 0 & 0 & -1 \end{bmatrix} \tag{8.2}$$

G. ADDITIONAL DATA OF DEFORMATION TEST

So that is possible for the reader to have a more complete overview of the results of the deformation test in the other directions they will be mentioned here. Despite not adding value to the final conclusion, it is expected that the response in these directions is rather low in terms of forces and that there are no significant differences between the presence of the breast holder and without it.

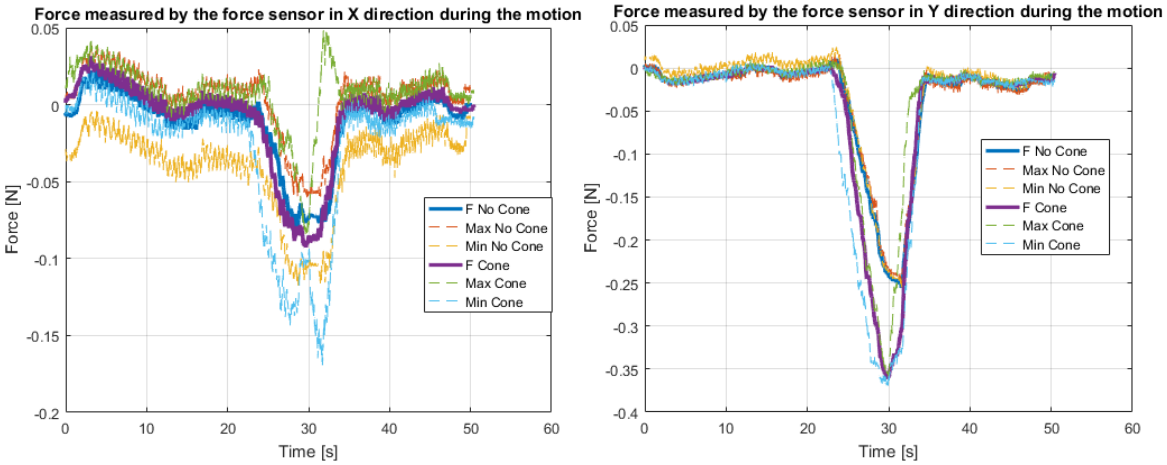

Figure 8.13 - Average force response in X (left) and Y (right) directions registered by the ATI sensor for the M1 motion, with maximum and minimum deviations.

As expected, the response is always very small and very similar between the "cone" vs. "no cone", which means that the deformation was indeed taking place in the in Z as it was planned. However, for M2, a very instable response is again verified for the response in the presence of the breast holder.

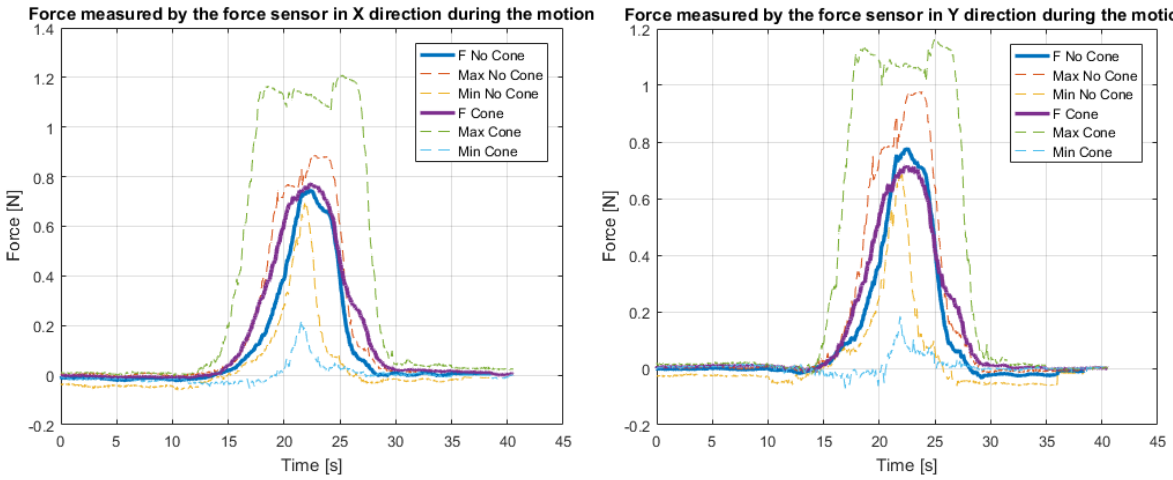

Figure 8.14 - Average force response in X (left) and Y (right) directions registered by ATI sensor for the M2 motion, with maximum and minimum deviations.

9. REFERENCES

[1] E. de Rinaldis, A. Tutt, and G. Dontu, "Breast Cancer," *Breast Pathol.*, vol. 47, no. 5 Suppl, pp. 352–359, 2011.

[2] C. Desantis, J. Ma, L. Bryan, and A. Jemal, "Breast Cancer Statistics , 2013," *CA Cancer J. Clin.*, vol. 64, no. 1, pp. 52–62, 2013.

[3] E. M. Ward *et al.*, "Cancer statistics: Breast cancer in situ.," *CA. Cancer J. Clin.*, vol. 65, no. 6, pp. 481–95, 2015.

[4] "Breast-Cancer-Statistics @ Www.Wcrf.Org." .

[5] B. C. I. Flowers, B. P. Mooney, and J. S. Drukteinis, "Breast Cancer Diagnosis," vol. 5481, no. July, pp. 59–64, 2012.

[6] L. E. M. Duijm, J. H. Groenewoud, F. H. Jansen, J. Fracheboud, M. van Beek, and H. J. de Koning, "Mammography screening in the Netherlands: delay in the diagnosis of breast cancer after breast cancer screening.," *Br. J. Cancer*, vol. 91, no. 10, pp. 1795–9, 2004.

[7] M. Tsukune, Y. Kobayashi, T. Miyashita, and G. M. Fujie, "Automated palpation for breast tissue discrimination based on viscoelastic biomechanical properties," *Int. J. Comput. Assist. Radiol. Surg.*, vol. 10, no. 5, pp. 593–601, 2015.

[8] N. G. Ramião, P. S. Martins, R. Rynkevic, A. A. Fernandes, M. Barroso, and D. C. Santos, "Biomechanical properties of breast tissue, a state-of-the-art review," *Biomech. Model. Mechanobiol.*, vol. 15, no. 5, pp. 1307–1323, 2016.

[9] A. M. Smelser, J. C. Macosko, A. P. O'Dell, S. Smyre, K. Bonin, and G. Holzwarth, "Mechanical properties of normal versus cancerous breast cells," *Biomech. Model. Mechanobiol.*, vol. 14, no. 6, pp. 1335–1347, 2015.

[10] M. S. T. A.-T. T.- Sabel, "Essentials of breast surgery." Mosby/Elsevier, Philadelphia, PA :, 2009.

[11] "1a5f0016609197b2b1c03ce098f26051ff793f30 @ blog.shescience.com.au." .

[12] A. D. Koch, J. P. A. Nicolai, and J. de Vries, "Breast cancer and the role of breast size as a contributory factor," *Breast*, vol. 13, no. 4, pp. 272–275, 2004.

[13] B. S. Garra, "Imaging and estimation of tissue elasticity by ultrasound.," *Ultrasound Q.*, vol. 23, no. 4, pp. 255–268, 2007.

[14] P. N. T. Wells and H.-D. Liang, "Medical ultrasound: imaging of soft tissue strain and elasticity," *J. R. Soc. Interface*, vol. 8, no. 64, pp. 1521–1549, 2011.

[15] I. Katz-Hanani, T. Rothstein, D. Gaitini, Z. Gallimidi, and H. Azhari, "Age-Related Ultrasonic Properties of Breast Tissue In vivo," *Ultrasound Med. Biol.*, vol. 40, no. 9, pp. 2265–2271, 2014.

[16] M. Golatta *et al.*, "Normal breast tissue stiffness measured by a new ultrasound technique: Virtual touch tissue imaging quantification (VTIQ)," *Eur. J. Radiol.*, vol. 82, no. 11, pp. e676–e679, 2013.

[17] D. Weishaupt, V. D. Köchli, and B. Marincek, *How does MRI work?* 2008.

[18] M. D. Schnall and S. G. Orel, "Breast MRI," *Breast Dis*, vol. 10, no. 3–4, pp. 97–111, 1998.

[19] M. O. F. Cervical and I. Neoplasia, "Clinical Investigation," vol. 40, no. 4, pp. 881–887, 1998.

[20] S. Ramella *et al.*, "Whole-breast irradiation: A subgroup analysis of criteria to stratify for prone position treatment," *Med. Dosim.*, vol. 37, no. 2, pp. 186–191, 2012.

[21] A. M. Kirby, P. M. Evans, E. M. Donovan, H. M. Convery, J. S. Haviland, and J. R. Yarnold, "Prone versus supine positioning for whole and partial-breast radiotherapy: A comparison of non-target tissue dosimetry," *Radiother. Oncol.*, vol. 96, no. 2, pp. 178–184, 2010.

[22] H. Azhari, *Basics of Biomedical Ultrasound for Engineers*. 2010.

[23] S. N. Narouze, "Atlas of ultrasound-guided procedures in interventional pain management," *Atlas Ultrasound-Guided Proced. Interv. Pain Manag.*, pp. 1–372, 2011.

[24] S. Cochran, "Piezoelectricity and basic configurations for piezoelectric ultrasonic transducers," *Ultrason. Transducers*, pp. 3–35, 2012.

[25] T. L. Szabo and T. L. Szabo, "4 – ATTENUATION," in *Diagnostic Ultrasound Imaging*, 2004, pp. 71–95.
[26] N. M. Tole, "Basic Physics of Ultrasonographic Imaging," pp. 1–5, 2005.
[27] M. O. Culjat, D. Goldenberg, P. Tewari, and R. S. Singh, "A review of tissue substitutes for ultrasound imaging," *Ultrasound Med. Biol.*, vol. 36, no. 6, pp. 861–873, 2010.
[28] F. A. Duck, "Acoustic Properties of Tissue at Ultrasonic Frequencies," *Phys. Prop. Tissues*, pp. 73–135, 1990.
[29] T. Y. Fang, H. K. Zhang, R. Finocchi, R. H. Taylor, and E. M. Boctor, "Force-assisted ultrasound imaging system through dual force sensing and admittance robot control," *Int. J. Comput. Assist. Radiol. Surg.*, vol. 12, no. 6, pp. 983–991, 2017.
[30] H. I. Vargas, R. V Agbunag, and I. Khaikhali, "State of the art of minimally invasive breast biopsy: principles and practice.," *Breast cancer*, vol. 7, no. 4, pp. 370–379, 2000.
[31] B. D. Florentine, C. J. Cobb, K. Frankel, T. Greaves, and S. E. Martin, "Core needle biopsy: A useful adjunct to fine-needle aspiration in select patients with palpable breast lesions," *Cancer*, vol. 81, no. 1, pp. 33–39, 1997.
[32] D. David Dershaw, "Imaging guided biopsy: An alternative to surgical biopsy," *Breast J.*, vol. 6, no. 5, pp. 294–298, 2000.
[33] M. S. Soo, S. Ghate, and D. Delong, "Stereotactic biopsy of noncalcified breast lesions: Utility of vacuum-assisted technique compared to multipass automated gun technique," *Clin. Imaging*, vol. 23, no. 6, pp. 347–352, 1999.
[34] N. H. G. M. Peters *et al.*, "Feasibility of MRI-guided large-core-needle biopsy of suspiscious breast lesions at 3T," *Eur. Radiol.*, vol. 19, no. 7, pp. 1639–1644, 2009.
[35] J. Ophir *et al.*, "Elastography," *Comptes Rendus l'Academie des Sci. - Ser. IV - Phys.*, vol. 2, no. 8, pp. 1193–1212, 2001.
[36] G. Rizzatto, "Ultrasound Elastography," *Breast Cancer Res.*, vol. 10, no. Suppl 3, p. P4, 2011.
[37] B. S. Garra, "Elastography: current status, future prospects, and making it work for you," *Ultrasound Q*, vol. 27, no. 3, pp. 177–186, 2011.
[38] I. Acoustique, E. T. Optique, and D. E. S. Milieux, "Imagerie acoustique et optique des milieux biologiques," *Media*, vol. 2147, no. 1, pp. 1193–1212, 2001.
[39] L. Beales, S. Wolstenhulme, J. A. Evans, R. West, and D. J. A. Scott, "Reproducibility of ultrasound measurement of the abdominal aorta," *Br. J. Surg.*, vol. 98, no. 11, pp. 1517–1525, 2011.
[40] K. M. Kelly and G. A. Richwald, "Automated Whole-Breast Ultrasound: Advancing the Performance of Breast Cancer Screening," *Semin. Ultrasound, CT MRI*, 2011.
[41] S. Tovar-Arriaga, R. Tita, J. C. Pedraza-Ortega, E. Gorrostieta, and W. A. Kalender, "Development of a robotic FD-CT-guided navigation system for needle placement-preliminary accuracy tests," *Int. J. Med. Robot. Comput. Assist. Surg.*, vol. 7, no. 2, pp. 225–236, 2011.
[42] C. Hennersperger *et al.*, "Towards MRI-Based Autonomous Robotic US Acquisitions: A First Feasibility Study," *IEEE Trans. Med. Imaging*, vol. 36, no. 2, pp. 538–548, 2017.
[43] "MRI of the BREAST @ www.med.unc.edu." .
[44] "Quantitative Shear Wave Ultrasound Elastography: Initial Experience in Solid Breast Masses @ Www.Medscape.Com." .
[45] G. Tarantino, "Design and Implementation of automated breast scanning with force feedback control," 2017.
[46] J. S. Uiterkamp, "Design and implementation of autonomous robotic scanning of the breast .," 2016.
[47] K. M. Kelly and G. A. Richwald, "Automated Whole-Breast Ultrasound: Advancing the Performance of Breast Cancer Screening," *Semin. Ultrasound, CT MRI*, vol. 32, no. 4, pp. 273–280, Aug. 2011.

[48] M. R. Burcher, J. A. Noble, L. Han, and M. Gooding, "A system for simultaneously measuring contact force, ultrasound, and position information for use in force-based correction of freehand scanning," *IEEE Trans. Ultrason. Ferroelectr. Freq. Control*, vol. 52, no. 8, pp. 1330–1342, 2005.

[49] R. P. Goldberg, M. Dumitru, R. H. Taylor, and D. Stoianovici, "A modular robotic system for ultrasound image acquisition," *Lect. Notes Comput. Sci. (including Subser. Lect. Notes Artif. Intell. Lect. Notes Bioinformatics)*, vol. 2208, pp. 1430–1432, 2001.

[50] A. Cerussi *et al.*, "Effect of contact force on breast tissue optical property measurements using a broadband diffuse optical spectroscopy handheld probe.," *Appl. Opt.*, vol. 48, no. 21, pp. 4270–7, 2009.

[51] R. X. Xu, D. C. Young, J. J. Mao, and S. P. Povoski, "A prospective pilot clinical trial evaluating the utility of a dynamic near-infrared imaging device for characterizing suspicious breast lesions.," *Breast Cancer Res.*, vol. 9, no. 6, p. R88, 2007.

[52] S. Jlassi, S. Tliba, and Y. Chitour, "An Online Trajectory generator-Based Impedance control for co-manipulation tasks," *IEEE Haptics Symp. HAPTICS*, pp. 391–396, 2014.

[53] N. Hogan and S. P. Buerger, "Impedance and Interaction Control," *Robot. Autom. Handb.*, pp. 19–1, 2005.

[54] M. Kawamura *et al.*, "Development of the breast immobilization system in prone setup: The effect of bra in prone position to improve the breast setup error," *J. Appl. Clin. Med. Phys.*, vol. 18, no. 4, pp. 155–160, 2017.

[55] Y. S. Y. Mike Q. Zheng, "Method and device for immobilization of the human breast in a prone position for radiotherapy @ www.google.com," US7597104 B2, 2009.

[56] "LBR iiwa Collaborative Robot @ www.aetlabs.com." .

[57] KUKA, "KUKA Sunrise.OS 1.11 KUKA Sunrise.Workbench 1.11," 2016.

[58] A. Holton, E. Walsh, A. Anayiotos, G. Pohost, and R. Venugopalan, "Comparative MRI Compatibility of 316L Stainless Steel Alloy and Nickel???Titanium Alloy Stents," *J. Cardiovasc. Magn. Reson.*, vol. 4, no. 4, pp. 423–430, 2003.

[59] L. C. Cabrelli, P. I. B. G. B. Pelissari, A. M. Deana, A. A. O. Carneiro, and T. Z. Pavan, "Stable phantom materials for ultrasound and optical imaging," *Phys. Med. Biol.*, 2017.

[60] L. C. Cabrelli, P. I. B. G. B. Pelissari, A. M. Deana, A. A. O. Carneiro, and T. Z. Pavan, "Stable phantom materials for ultrasound and optical imaging," *Phys. Med. Biol.*, vol. 62, no. 2, pp. 432–447, 2017.

[61] W. Li, B. Belmont, and A. Shih, "Design and Manufacture of Polyvinyl Chloride (PVC) Tissue Mimicking Material for Needle Insertion," *Procedia Manuf.*, vol. 1, pp. 866–878, 2015.

[62] S. L. Vieira, T. Z. Pavan, J. E. Junior, and A. A. O. Carneiro, "Paraffin-Gel Tissue-Mimicking Material for Ultrasound-Guided Needle Biopsy Phantom," *Ultrasound Med. Biol.*, vol. 39, no. 12, pp. 2477–2484, 2013.

[63] E. L. Madsen *et al.*, "Anthropomorphic breast phantoms for testing elastography systems," *Ultrasound Med. Biol.*, vol. 32, no. 6, pp. 857–874, 2006.

[64] G. Cortela, N. Benech, W. C. A. Pereira, and C. Negreira, "Characterization of acoustical properties of a phantom for soft tissues (PVCP and Graphite Powder) in the range 20-45??C," *Phys. Procedia*, vol. 70, pp. 179–182, 2015.

[65] P. Formiga, "Material data sheet PA 2200."

[66] NinjaTek, "NinjaFlex ® 3D Printing Filament: Flexible Polyurethane Material for FDM Printers," 2016.

[67] R. O. Materials, "Digital Materials (DMs) Data Sheet," 2000.

[68] V. L. Katch, B. Campaigne, P. Freedson, S. Sady, F. I. Katch, and A. R. Behnke, "Contribution of breast volume and weight to body fat distribution in females," *Am. J. Phys. Anthropol.*, vol. 53, no. 1, pp. 93–100, 1980.

[69] P. August, "ACUSON S3000 ™ Ultrasound System," 2012.
[70] "Polyvinyl Chrolide @ www.chemicalsafetyfacts.org." .